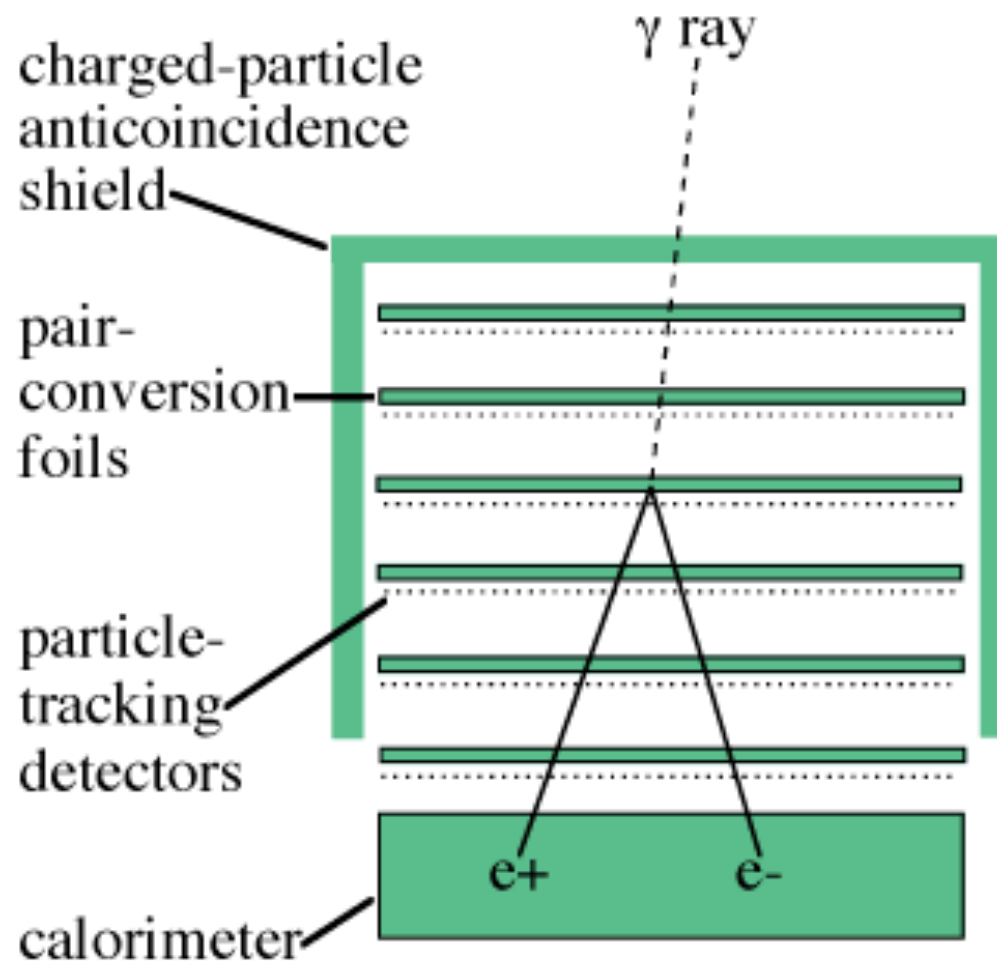


Astrofisica Nucleare e Subnucleare
GeV Astrophysics

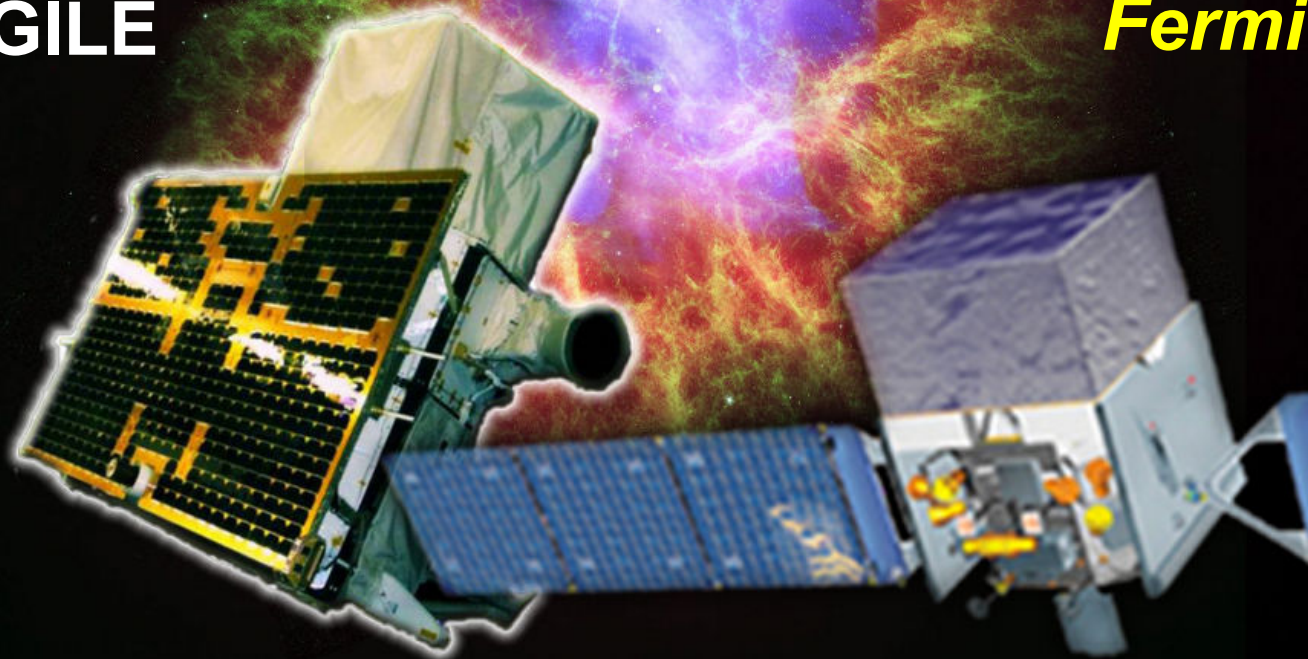
Detector Project



Gamma-ray astrophysics above 100 MeV

AGILE

Fermi



Picture of the day, Feb. 28, 2011, NASA-HEASARC[®]

Exercise on GeV gamma-rays

- Find the web sites of AGILE and Fermi/LAT
- Check the status of “new” gamma-ray detectors (CALET, DAMPE, Gamma-400, HERD, other?)

AGILE

RECENT DETECTIONS

Gamma-ray flare from Cygnus X-3
detected by AGILE
ATel # 13458

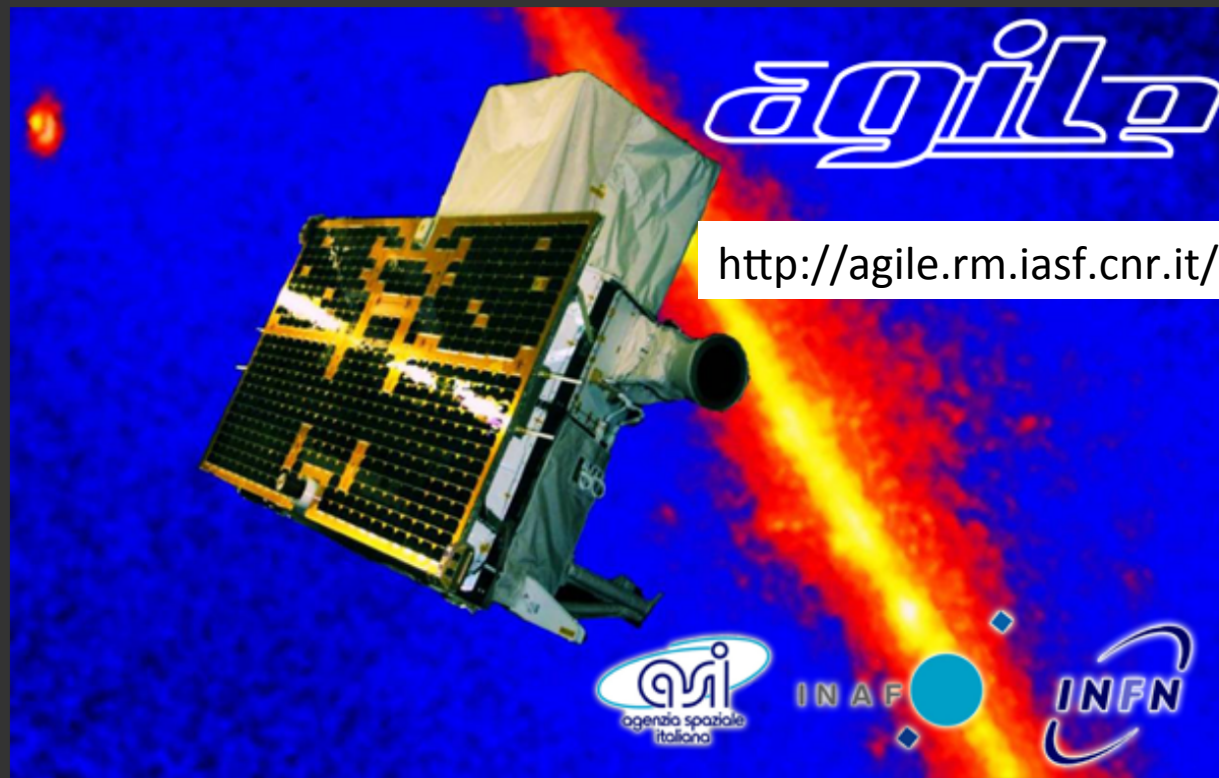
Swift X-ray Observations of the
Repeating FRB 180916.J0158+65
ATel # 13446

AGILE gamma-ray observations of
Cygnus X-3 during the current
quenched/hypersoft state
ATel # 13423

AGILE detection of enhanced
gamma-ray activity from the FSRQ
PKS 0208-512
ATel # 13352

Enhanced gamma-ray activity from
Eta Carinae
ATel # 13329

AGILE confirmation of the gamma-
ray flaring activity from the narrow-
line Seyfert1 Galaxy PKS 2004-447
ATel # 13244



<http://agile.rm.iasf.cnr.it/>



[Home](#) [AGILE Team](#) [AGILE in ASI](#) [AGILE Data Center](#) [Contacts](#) [AT reserved](#)

AGILE Launch

AGILE Principal Investigator
and ASI Directors

Time elapsed since the AGILE launch on April 23, 2007 at 10:00 GMT

Days Hours Mins Secs
62 15:22:04:13

AGILE



SSDC SPACE SCIENCE DATA CENTER

ASI Agenzia Spaziale Italiana

Space Science Data Center

Home About SSDC News and Communication Quick Look Missions Multimission Archive Catalogs Tools Links Bibliographic services Helpdesk Privacy

AGILE Science Data Center

<https://agile.asdc.asi.it/>

AGILE Home About AGILE ASI HQ AGILE AGILE News AGILE Data Archive Public Software AGILE Pointings AGILE Catalogs Restricted Area Guest Observer Program User Feedback Form AGILE Workshops Agile Helpdesk

Welcome to the AGILE Data Center Home Page at SSDC

These pages provide updated information and services in support to the general scientific community for the mission AGILE, which is a small Scientific Mission of the Italian Space Agency (ASI) with participation of INFN, IASF/INAF and CIFS .

AGILE is devoted to gamma-ray astrophysics and it is a first and unique combination of a gamma-ray (AGILE-GRID) and a hard X-ray (SuperAGILE) instrument, for the simultaneous detection and imaging of photons in the 30 MeV - 50 GeV and in the 18 - 60 keV energy ranges. AGILE has been operating nominally for more than 16 years, providing valuable data and important scientific results.

AGILE operations:

Launch date: 23 April, 2007 - Re-entry date: 14 February, 2024

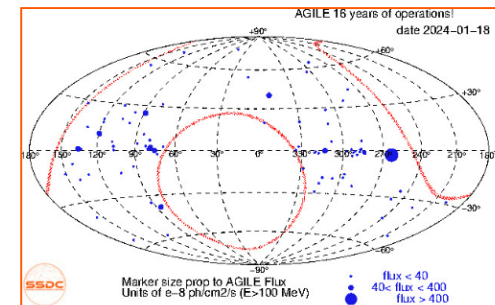
Science observations ended on 18 January, 2024

Planned Nominal Phase: 2 + 2 extended years

Elapsed: 16 years and 10 months in orbit (6.141 days)

AGILE spinning sky view

[\(Click here for previous pointing details\)](#)



[Click here to access the AGILE Spinning FOV plotter](#)

[Click here to access the AGILE Real Data FOV Plotter](#)

Fermi LAT

Stanford | The Fermi Large Area Telescope

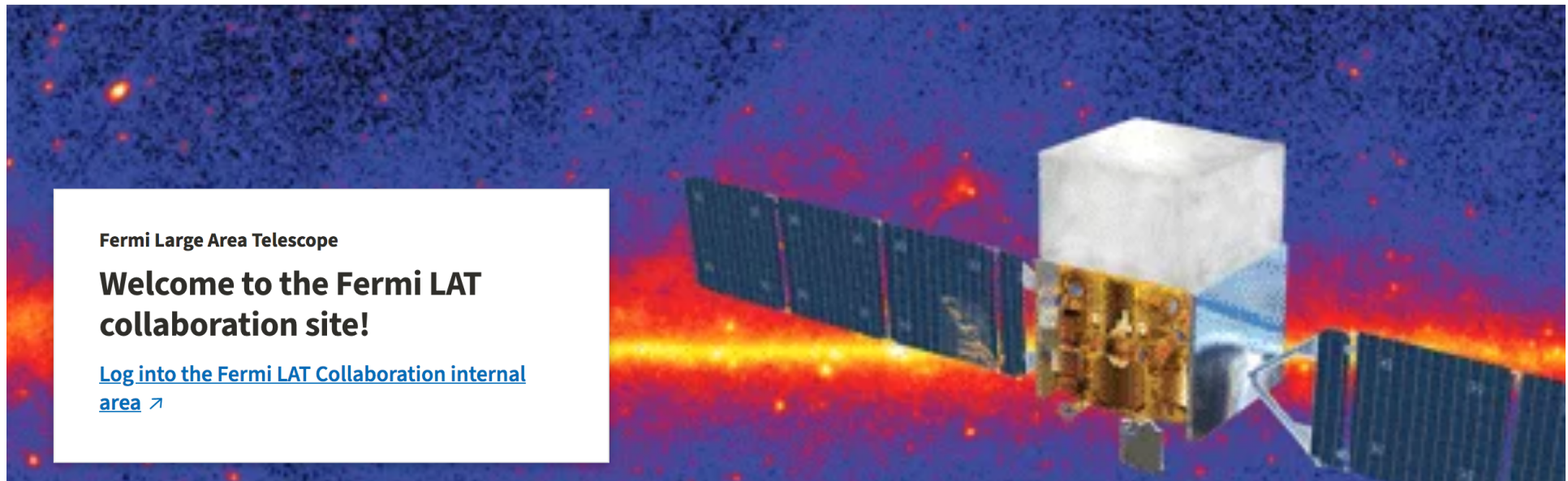
Search this site



[Home](#) [About](#) [News](#) [Opportunity Board](#) [Add an Opportunity](#) [Fermi LAT Mentoring Program](#) [Fermi LAT CMs](#)

[Events](#) [Past Events](#) [LAT Pictures](#) [LAT documents](#) [LAT Rapid Publications](#) [LAT Publications](#)

[Fermi LAT GW Table](#) [Fermi Overview Presentation](#) [Resources](#) [Latest Results](#)



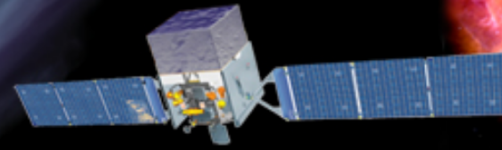
<https://glast.sites.stanford.edu/>

Fermi LAT

Fermi

<https://fermi.gsfc.nasa.gov/>

Gamma-ray Space Telescope



Home

What is Fermi

Science

Conferences

Support Center

Mission Page

Students/Teachers

Eleventh International Fermi Symposium

SEPTEMBER 9-13, 2024
COLLEGE PARK, MARYLAND, USA

11TH INTERNATIONAL FERMI SYMPOSIUM

Topics include Gamma-ray Studies of:

- Supernova Remnants and Pulsar Wind Nebulae
- Gamma-ray Bursts and Other Transients
- Blazars and Other Galaxies
- Future Missions and Instruments
- Multimessenger Sources
 - Other Galactic Sources
 - Diffuse Emission
 - Solar System
 - Dark Matter
 - Pulsars

Important Dates

- Abstracts Due – May 1, 2024
- Registration Deadline – August 1, 2024

fermi.gsfc.nasa.gov/science/mtgs/symposia/eleventh/

Latest News

Apr 23, 2024

Explore the Universe with the First E-Book from NASA's Fermi

To commemorate a milestone anniversary for NASA's Fermi spacecraft, the mission team has published an e-book called "Our High-Energy Universe: 15 Years with the Fermi Gamma-ray Space Telescope."

[+ Read More](#)

Apr 16, 2024

NASA's Fermi Mission Sees No Gamma Rays from Nearby Supernova

A nearby supernova in 2023 offered astrophysicists an excellent opportunity to test ideas about how these types of explosions boost particles, called cosmic rays, to near light-speed. But surprisingly, NASA's Fermi Gamma-ray Space Telescope detected none of the high-energy gamma-ray light those particles should produce.

[+ Read More](#)

Apr 5, 2024

11th International Fermi Symposium

Please join us in College Park, Maryland, USA on

Astrofisica Nucleare e Subnucleare

Electromagnetic Showers

ELECTROMAGNETIC SHOWERS

SCIAMI ELETTROMAGNETICI

$$-\frac{dE}{dX} \approx \frac{E}{X_0}$$

SIA e^\pm CHE γ

$$E = E_0 e^{-\frac{X}{X_0}}$$



ΔX DOPO UNA LUNGHEZZA DI RADIAZIONE $= X_0$
(AFTER ONE RADIATION LENGTH)

$$-dE = \frac{E dX}{X_0}$$

$$\Delta E \approx E \frac{\Delta X}{X_0} \approx E$$

RADIAZIONE
(RADIATION)

$$e^\pm \rightarrow e^\pm \gamma$$

BREMSSTRAHLUNG

CONVERSIONE
(CONVERSION)

$$\gamma \rightarrow e^+ e^-$$

CREAZIONE COPPIE
(PAIR CREATION)

$$1 \rightarrow 2$$

$$E_i \rightarrow 2 \left(\frac{E_i}{2} \right)$$

DOPO TANTE LUNGHEZZE DI RADIAZIONE
(AFTER MANY RADIATION LENGTHS)

$$X = t X_0$$

$$t = \frac{X}{X_0}$$

$$1 \rightarrow 2^t \equiv N$$

$$E_i \rightarrow 2^t \left(\frac{E_i}{2^t} \right) = N \left(\frac{E_i}{N} \right) = N E(t)$$

$$E(t) = \frac{E_i}{N} = \frac{E_i}{2^t}$$

QUANDO (WHEN) $E(E)$ ARRIVA (REACHES) A E_c
DIVENTANO (BECOME) DOMINANTI (DOMINANT) : $(E = \frac{E_i}{N} = E_c)$
PER α : IONIZZAZIONE

PER γ : COMPTON E FOTOELETTRICO

N SMETTE LA CRESCITA ESPONENZIALE

N RAGGIUNGE IL MASSIMO

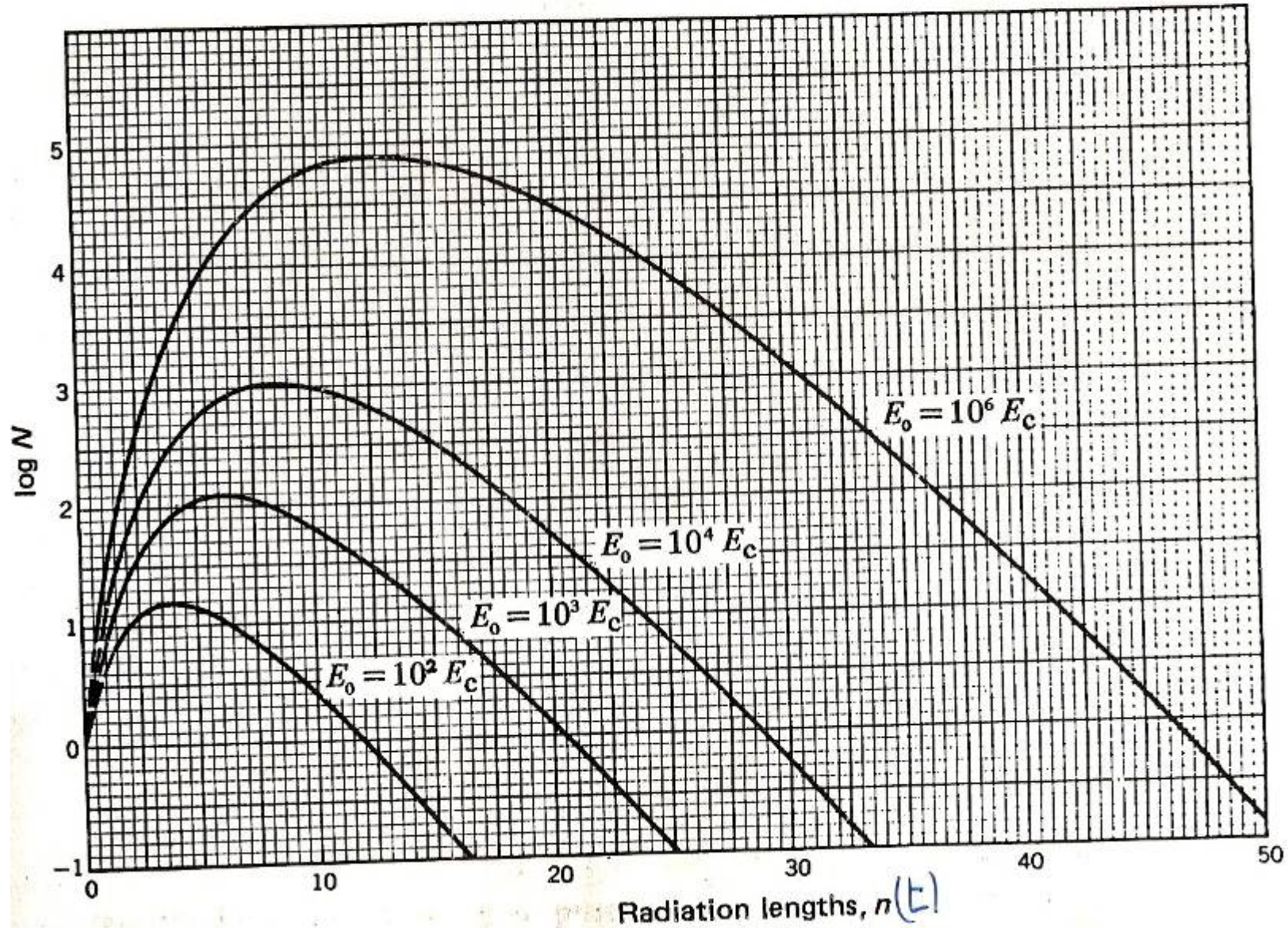
$$N_{MAX} = \frac{E_i}{E_c}$$

$$N_{MAX} = 2^{t_{MAX}} = \frac{E_i}{E_c}$$

$$t_{MAX} = \ln \frac{E_i}{E_c} \cdot \frac{1}{\ln 2}$$

N POI DECRESCHE PER
PROGRESSIVA PERDITA DELLE
ENERGIE RESIDUE

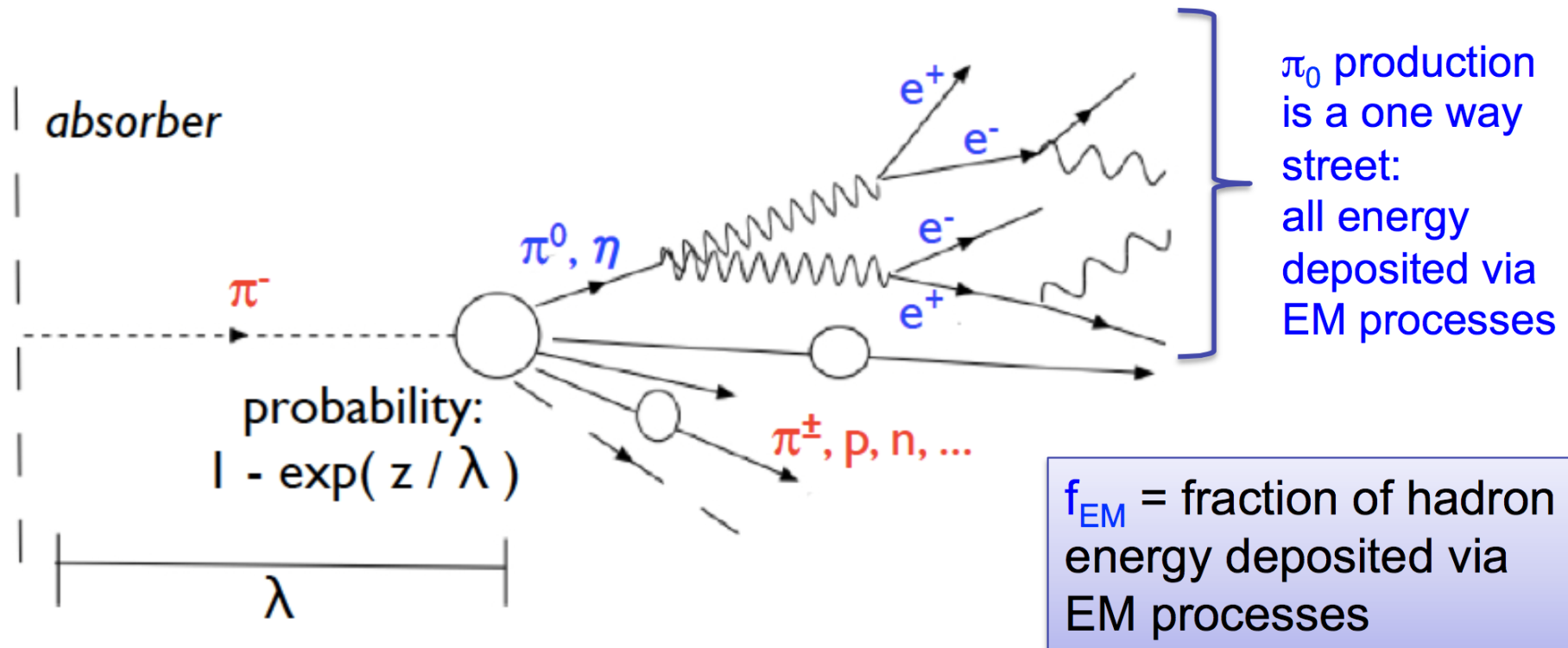
Fig. 4.6. The total number of particles N in a shower initiated by an electron of energy E_0 , as a function of depth n , measured in radiation lengths; E_c is the critical energy of the material. (From Leighton, 1959, p. 693, after Rossi & Greisen, 1941.)



Astrofisica Nucleare e Subnucleare

Hadronic showers

Hadronic showers



Electromagnetic → ionization, excitation (e^\pm)
→ photo effect, scattering (γ)

Hadronic → ionization (π^\pm, ρ)
→ invisible energy (binding, recoil)

Hadronic shower

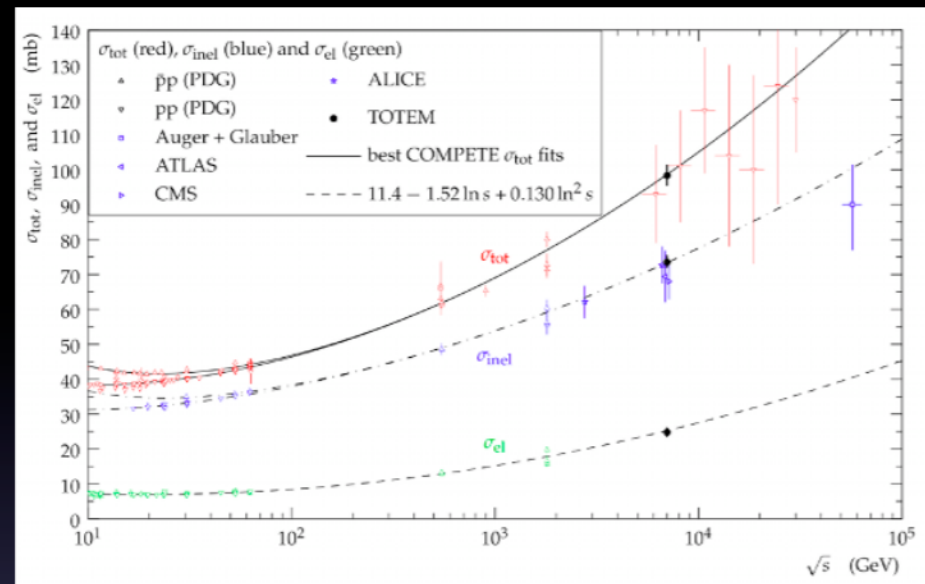
■ Hadronic interaction Cross section

$$\sigma_{Tot} = \sigma_{el} + \sigma_{inel}$$

$$\sigma_{el} \approx 10mb \quad \sigma_{inel} \approx A^{2/3}$$

$$\sigma_{Tot} = \sigma_{tot}(pp)A^{2/3}$$

where: $\sigma_{tot}(pp)$ increases with \sqrt{s}



■ Hadronic interaction length

$$\lambda_{int} = \frac{1}{\sigma_{tot} \cdot n} = \frac{A\rho}{\sigma_{pp} A^{2/3} N_A} \approx (35g/cm^2) A^{1/3}$$

$$N(x) = N(0)e^{-x/\lambda_{int}}$$

■ λ_{int} characterizes both longitudinal and transverse shower profile

Rule of thumb argument: the geometric cross section goes as the square of the size of the nucleus, a_N^2 , and since the nuclear radius scales as $a_N \sim A^{1/3}$, the nuclear mean free path in gm/cm^2 units scales as $A^{1/3}$.

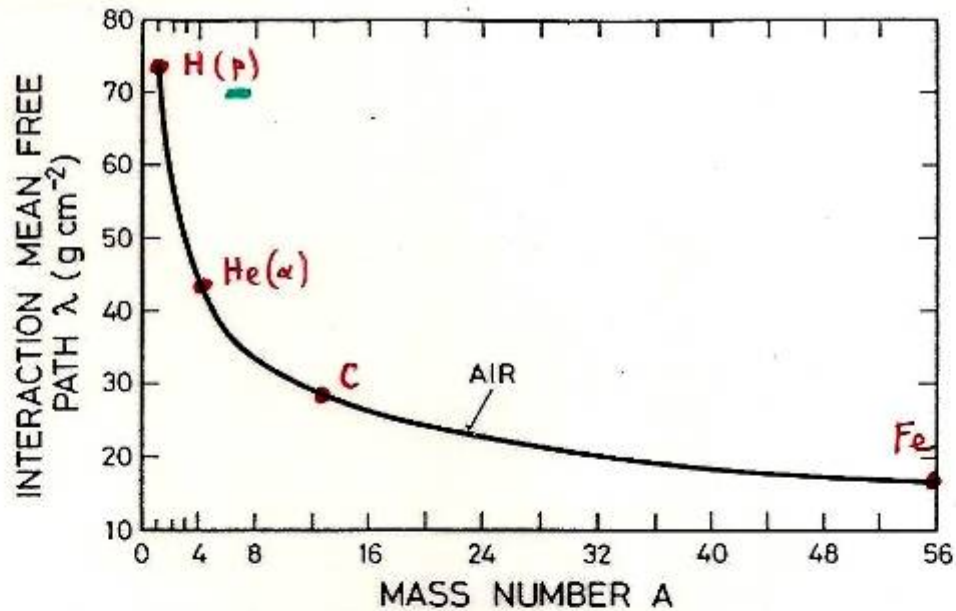


Fig. 1.1.1: Interaction mean free path for high energy nuclear interactions in air versus projectile mass.

$$X_{\text{INT. NUCL.}} \rightarrow \lambda_I$$

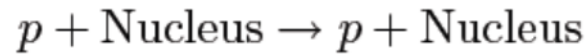
Table 5. Radiation length X_0 , critical energy E_c and hadronic absorption length λ_{had} for some materials

Material	X_0 (g/cm ²)	K_0 /m ²	E_c (MeV)	λ_{had} (g/cm ²)
H ₂	63	630	340	52.4
Al	24	240	47	106.4
Ar	20	200	35	119.7
Fe	13.8	138	24	131.9
Pb	6.3	63	6.9	193.7
Lead glass SF-5	9.6	96	~11.8	
Plexiglas	40.5	405	80	83.6
H ₂ O	36	360	93	84.9
NaI(Tl)	9.5	95	12.5	152.0
Bi ₄ Ge ₃ O ₁₂	8.0	80	10.5	164

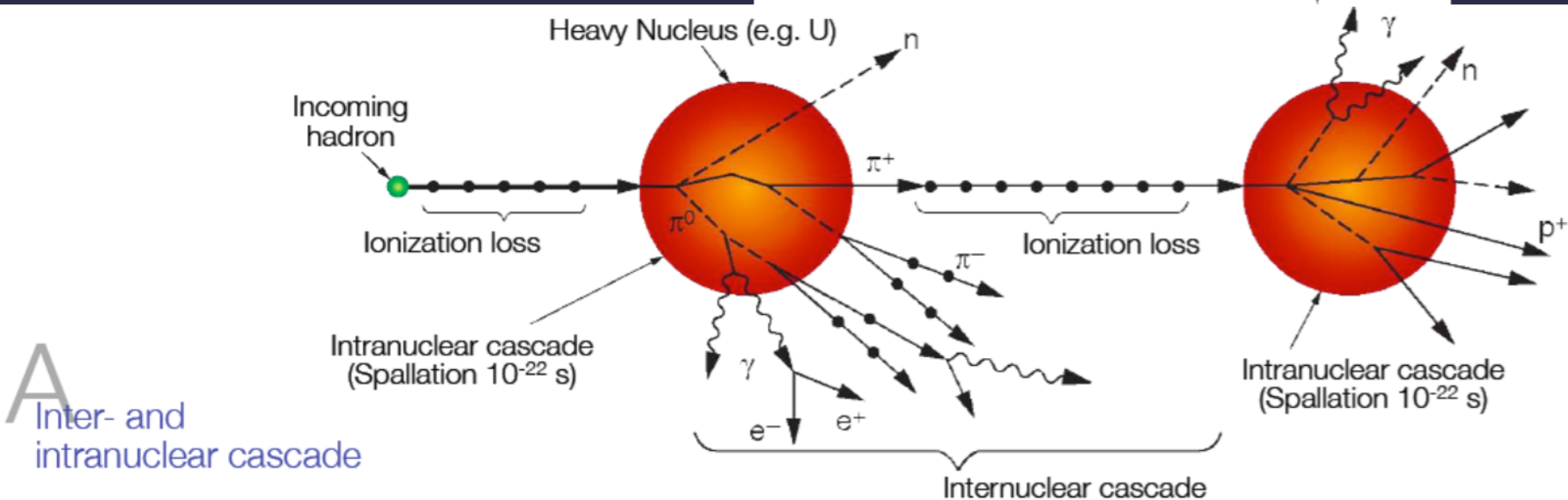
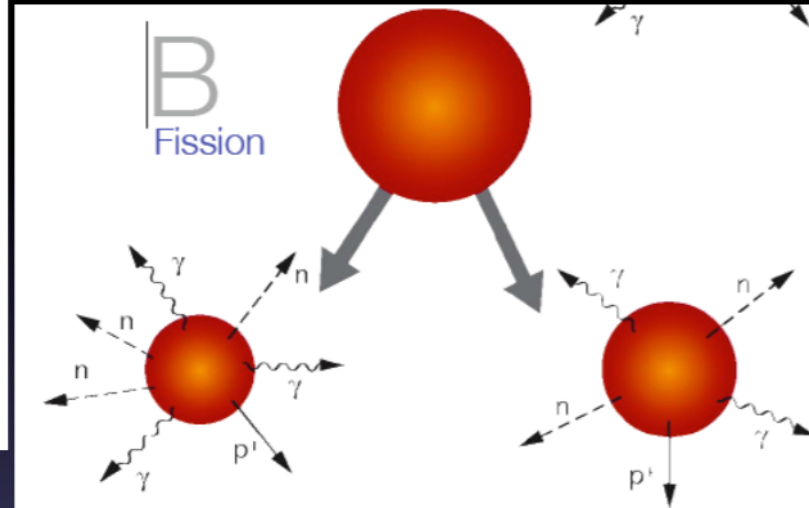
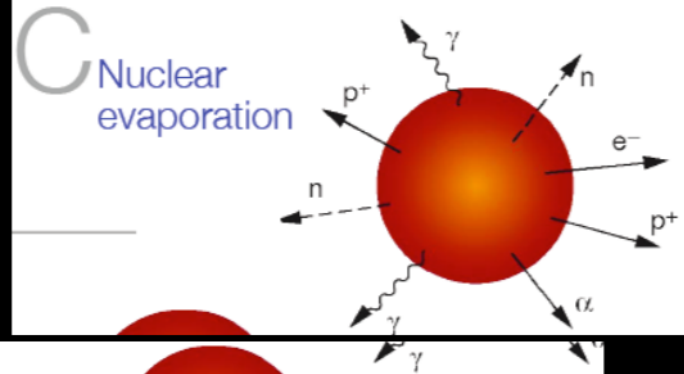
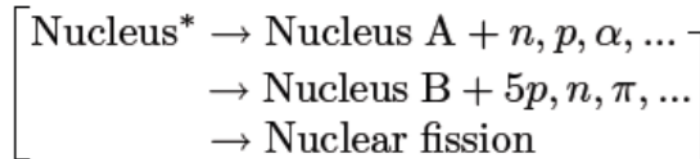
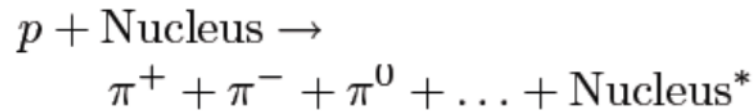
Hadronic shower

Hadronic interaction:

Elastic:

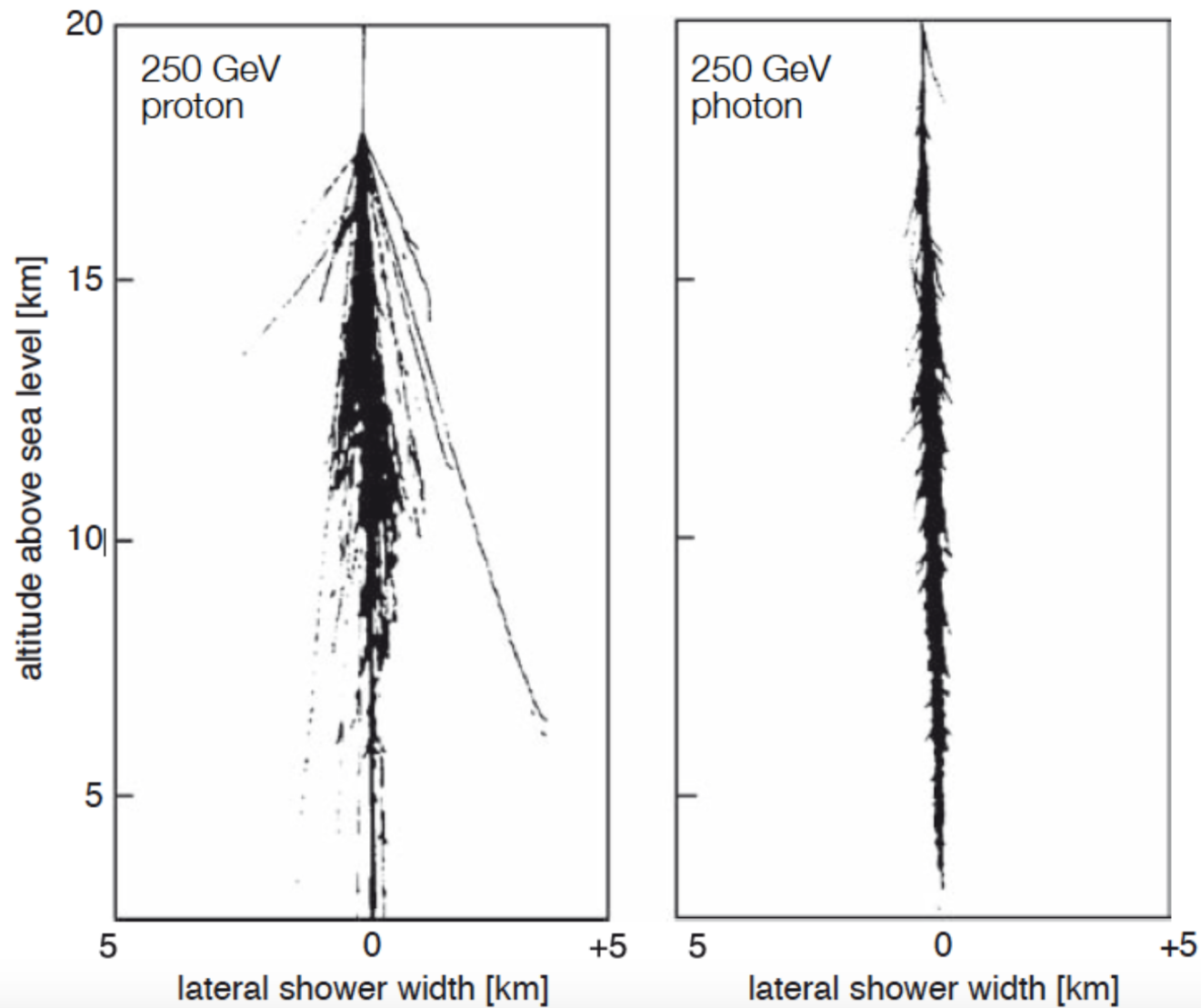


Inelastic:



Courtesy of H. C. Schoultz Coulon

Comparison hadronic vs EM showers

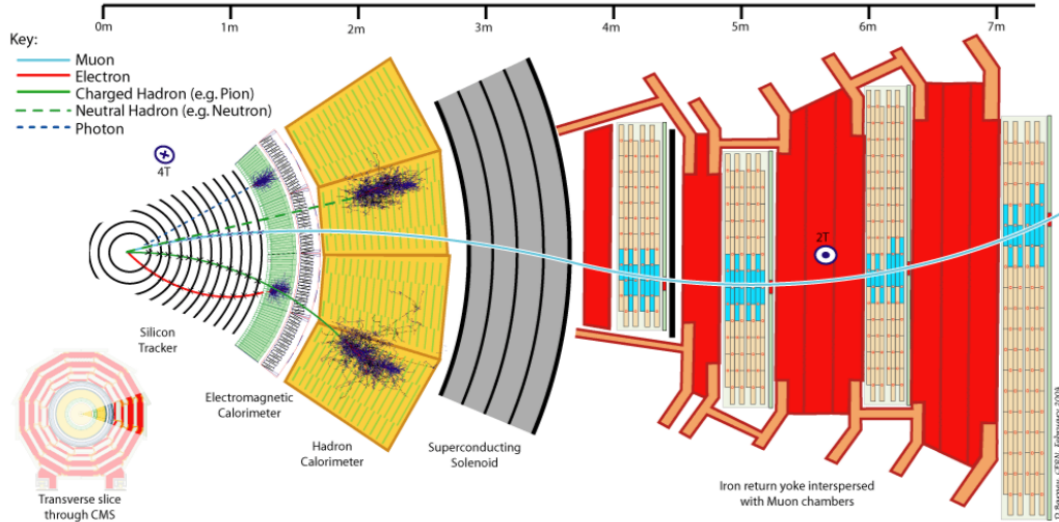
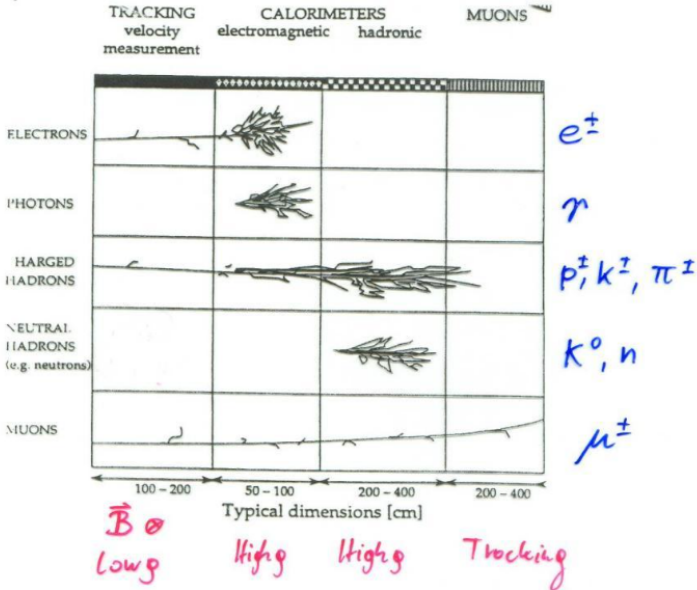


Simulated air showers

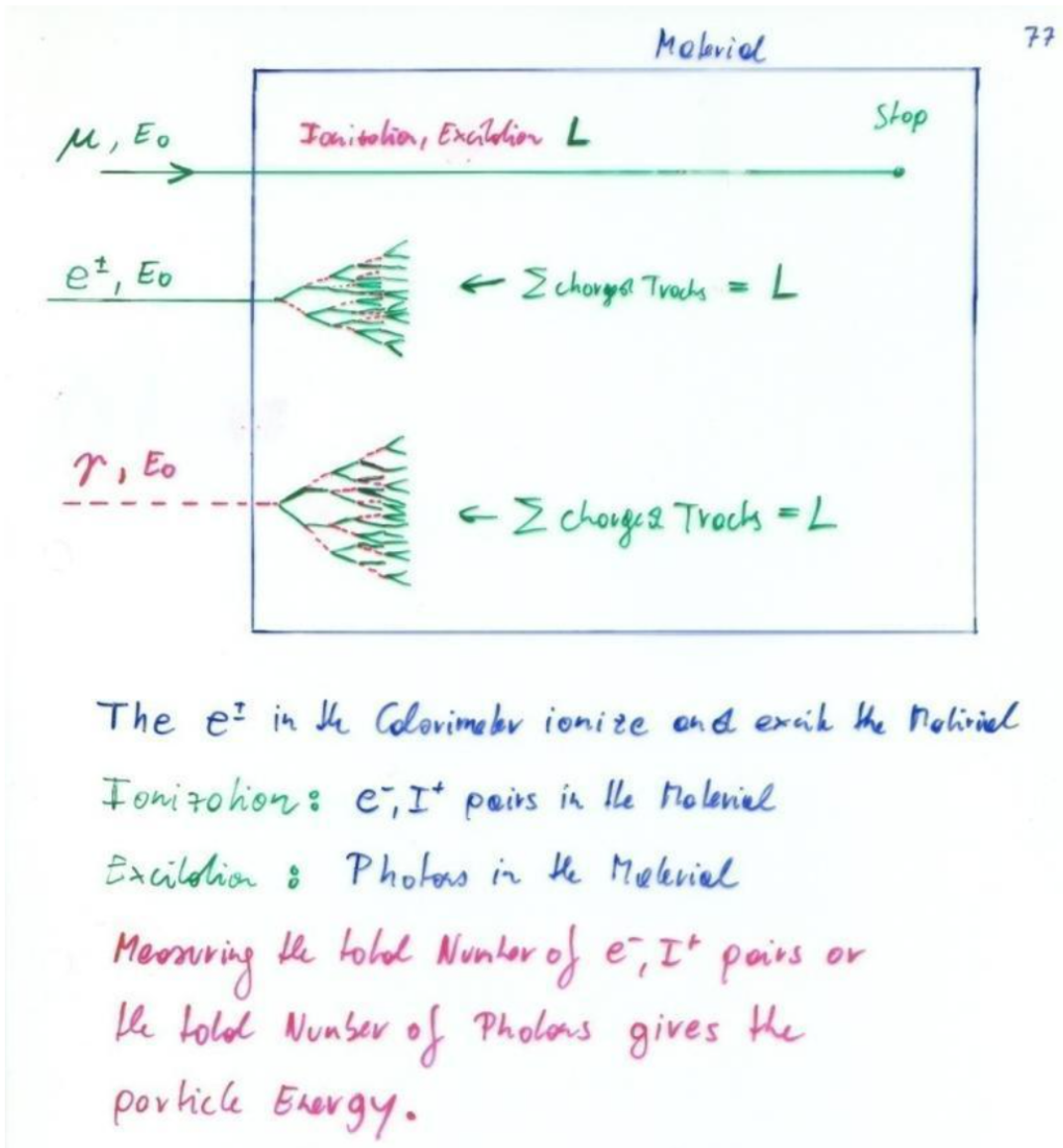
Astrofisica Nucleare e Subnucleare

Calorimeters

Calorimetry



Calorimetry: Energy Measurement by total Absorption of Particles



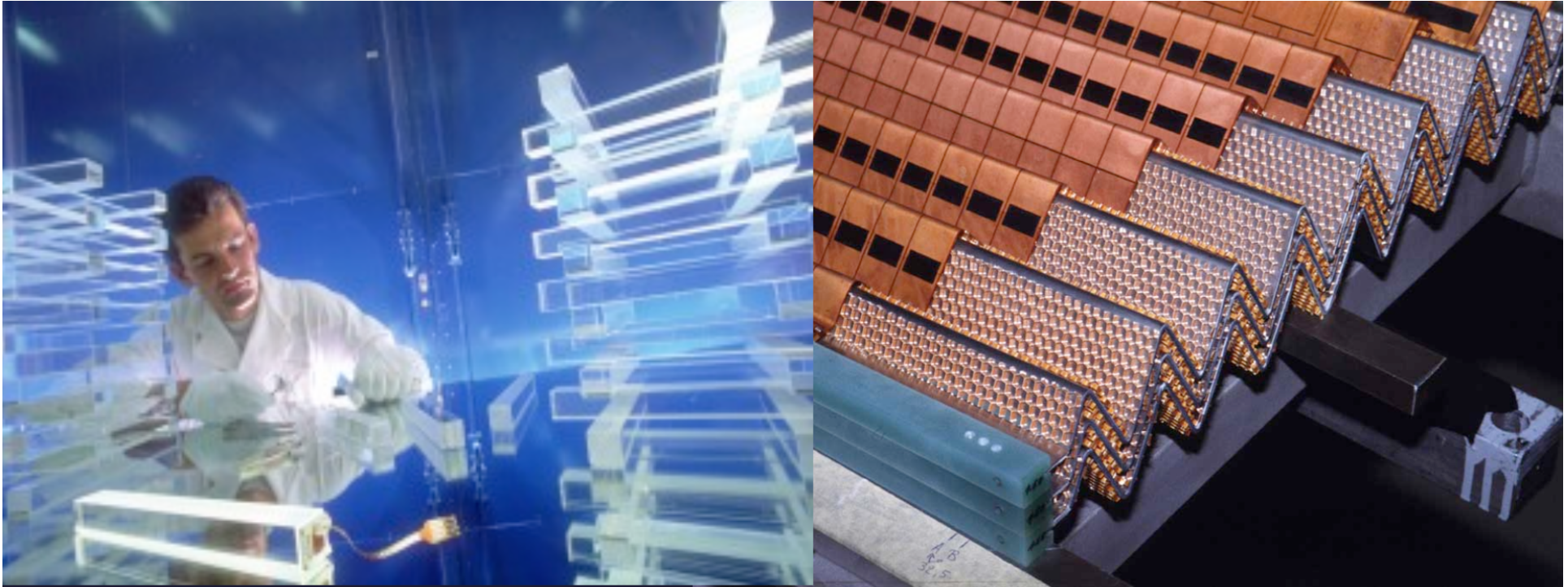
If N is the total Number of e^-, I^+ pairs or photons, or $N = c_1 E_0$:

$$\Delta N = \sqrt{N} \text{ (Poisson Statistics)}$$

$$\frac{\Delta E}{E} = \frac{\Delta N}{N} = \frac{1}{\sqrt{N}} = \frac{a}{\sqrt{E}} \rightarrow \text{Resolution}$$

Only Electrons and High Energy Photons show EM cascades at current GeV-TeV level Energies.

Strongly interacting particles like Pions, Kaons, produce hadronic showers in a similar fashion to the EM cascade
 → Hadronic calorimetry



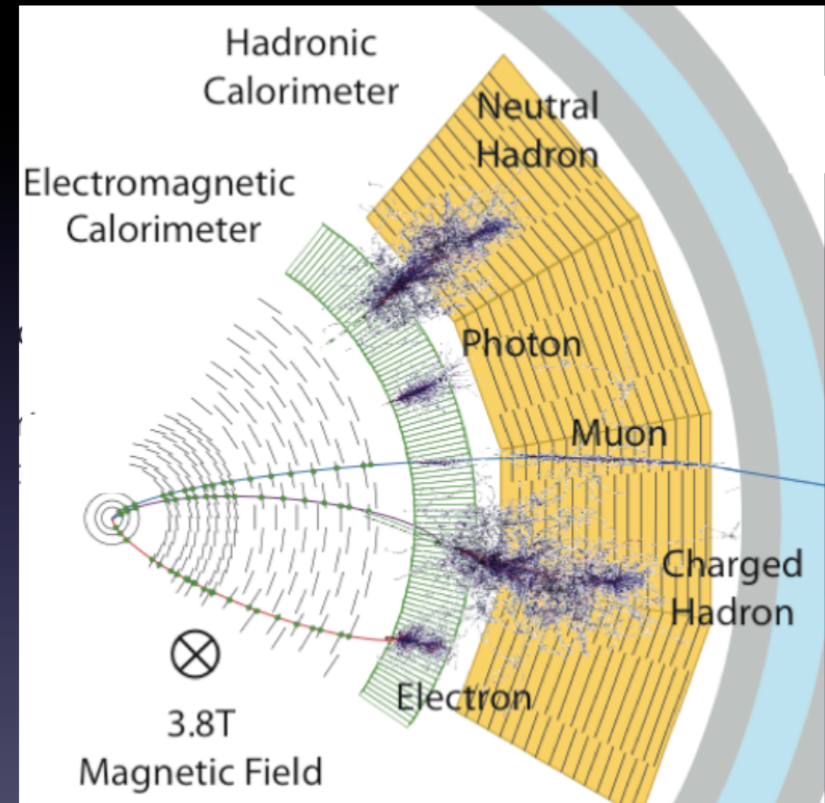
Detectors for Particle Physics

Calorimetry

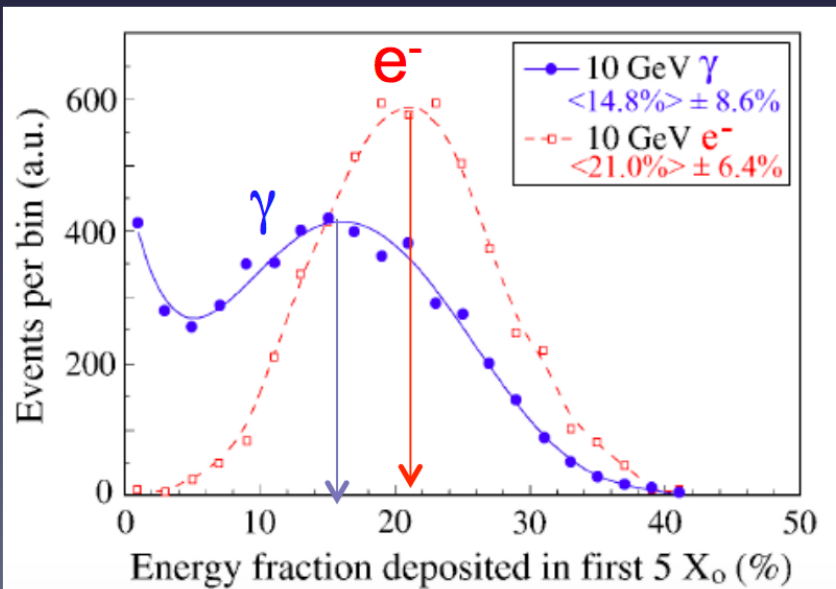
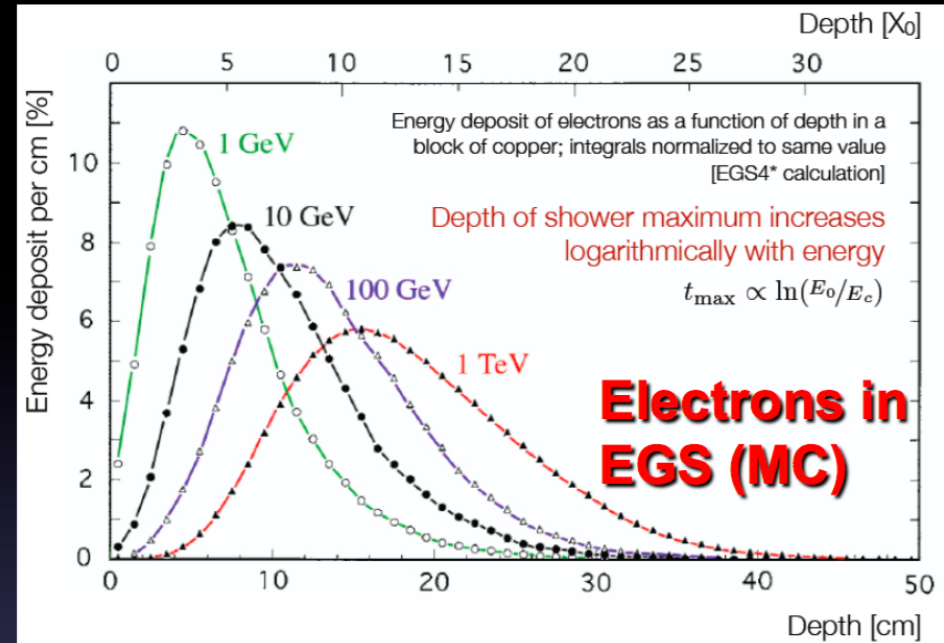
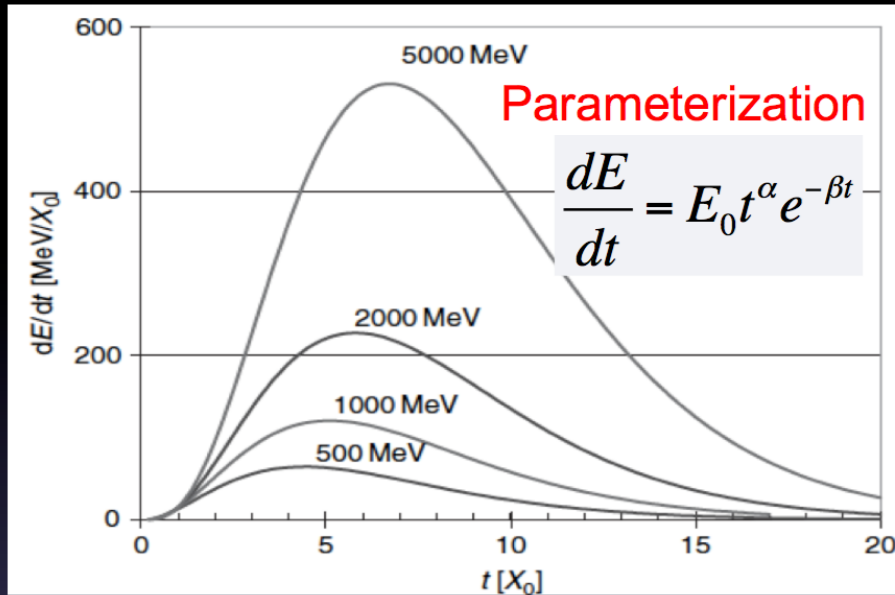
D. Bortoletto

What is a calorimeter ?

- In nuclear and particle physics calorimetry refers to the detection of particles through total absorption in a block of matter
 - The measurement process is destructive for almost all particle
 - The exception are muons (and neutrinos) → identify muons easily since they penetrate a substantial amount of matter
- In the absorption, almost all particle's energy is eventually converted to heat → calorimeter
- Calorimeters are essential to measure neutral particles



Longitudinal shower distribution



- Differences between electrons and photons generated showers
- Some photons penetrating (almost) the entire slab without interacting (peak at 0)

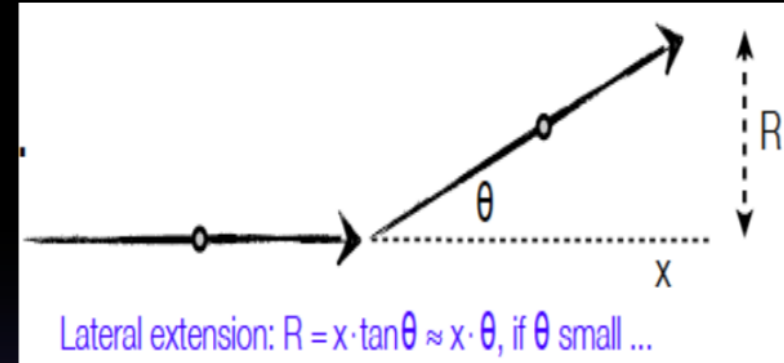
$$t_{\max} = \ln\left(\frac{E_0}{E_c}\right) + C_{ey}$$

$C_{ey} = -0.5$ for photons
 $C_{ey} = -1$ for electrons

Lateral development of EM shower

- Opening angle:
 - bremsstrahlung and pair production

$$\langle \theta^2 \rangle \approx \left(\frac{m_e c^2}{E_e} \right)^2 = \frac{1}{\gamma^2}$$



- multiple coulomb scattering [Molière theory]

$$\langle \theta \rangle = \frac{E_s}{E_e} \sqrt{\frac{x}{X_0}} \quad \text{where} \quad E_s = \sqrt{\frac{4\pi}{\alpha}} (m_e c^2) = 21.2 \text{ MeV}$$

- Main contribution from low energy e^- as $\langle \theta \rangle \sim 1/E_e$, i.e. for e^- with $E < E_c$

Molière Radius

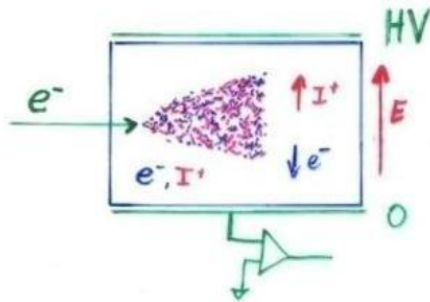
$$R_M = \frac{E_s}{E_c} X_0 \approx \frac{21.2 \text{ MeV}}{E_c} X_0$$

- Assuming the approximate range of electrons to be X_0 yields $\langle \theta \rangle \approx 21.2 \text{ MeV}/E_e \rightarrow$ lateral extension: $R = \langle \theta \rangle X_0$

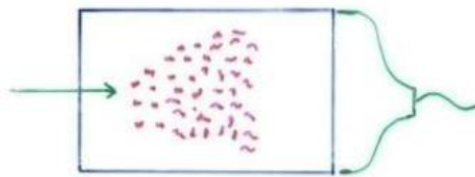
Calorimetry: Energy Measurement by total Absorption of Particles

The measurement is destructive. The particle can not be subject to further study.

Energy Measurement by



Collecting the produced Charge



Measuring the Photons produced by the collision of the e^\pm with Atom Electrons of the Material.

**Liquid Nobel Gases
(Nobel Liquids)**

**Scintillating Crystals,
Plastic Scintillators**

Total Amount of e^-, I^+ pairs or Photons is proportional to the total track length is proportional to the particle Energy.

EM Calorimeter configurations

■ Total absorption

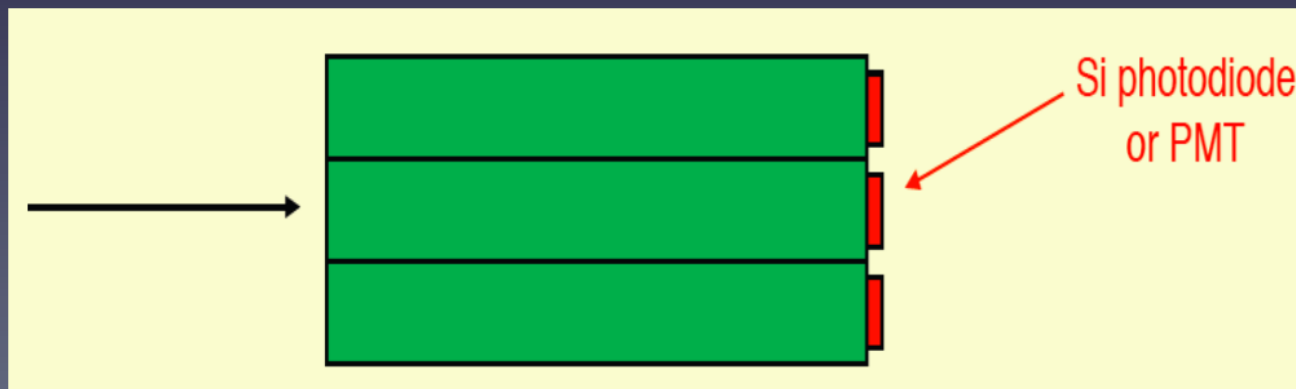
- Electrons and photons stop in calorimeter
- Scintillation proportional to energy of electron
- Usually non-organic scintillator (BGO, PbWO_4, \dots) or liquid Xe
- Advantage: Excellent energy resolution
 - see all charged particles in the shower (but for shower leakage) → best statistical precision
 - Uniform response → good linearity
- Disadvantages:
 - cost and limited segmentation

If W is the mean energy required to produce a signal (eg an e-ion pair in a noble liquid or a 'visible' photon in a crystal)

$$\frac{\sigma_E}{E} = \frac{1}{\sqrt{n}} = \frac{1}{\sqrt{E/W}}$$

■ Examples:

- B factories: small photon energies
- CMS ECAL which was optimized for $H \rightarrow \gamma\gamma$



EM Calorimeter configurations

■ Sampling Calorimeter

- One material to induce showering (high Z)
- Another to detect particles (typically by counting number of charged tracks)
- Many layers sandwiched together
- Resolution $\propto E^{-1/2}$

■ Advantages

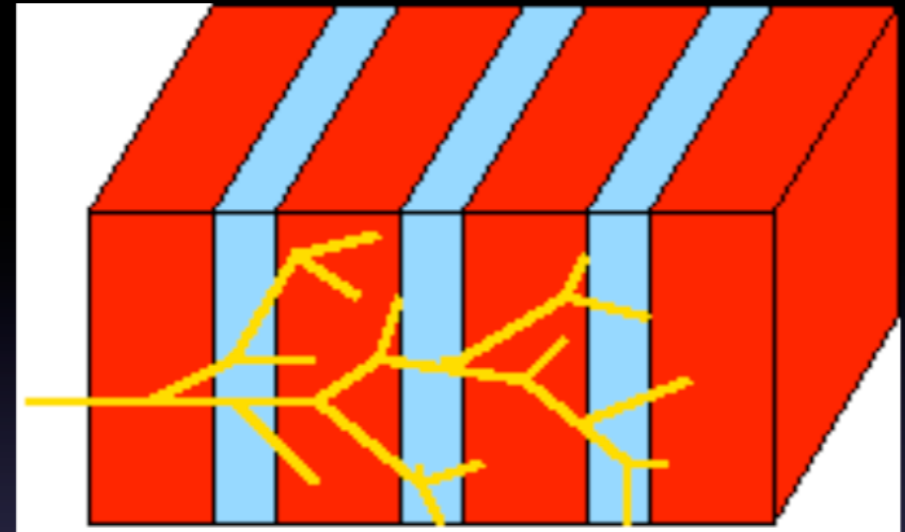
- Depth segmentation
- Spatial segmentation

■ Disadvantages:

- Only part of shower seen, less precise

■ Examples

- ATLAS ECAL
- Most HCALs



■ Sampling fraction

$$f_{\text{sampling}} = \frac{E_{\text{visible}}}{E_{\text{deposited}}}$$

Crystals for Homogeneous EM Calorimetry

	NaI(Tl)	CsI(Tl)	CsI	BGO	PbWO ₄
Density (g/cm ³)	3.67	4.53	4.53	7.13	8.28
X_0 (cm)	2.59	1.85	1.85	1.12	0.89
R_M (cm)	4.5	3.8	3.8	2.4	2.2
Decay time (ns)	250	1000	10	300	5
slow component			36		15
Emission peak (nm)	410	565	305	410	440
slow component			480		
Light yield γ /MeV	4×10^4	5×10^4	4×10^4	8×10^3	1.5×10^2
Photoelectron yield (relative to NaI)	1	0.4	0.1	0.15	0.01
Rad. hardness (Gy)	1	10	10^3	1	10^5

**Barbar@PEPII,
10ms
interaction
rate, good light
yield, good S/N**

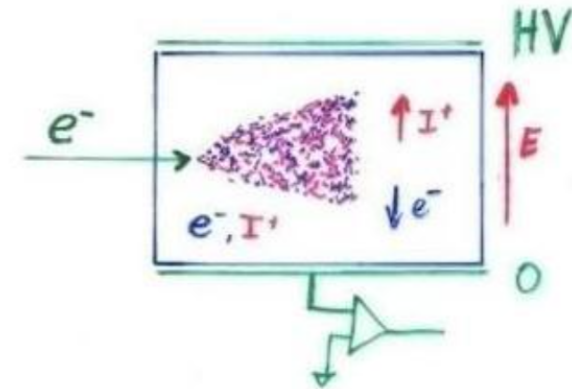
**KTeV@Tev
atron,
High rate,
Good
resolution**

**L3@LEP,
25us
bunch
crossing,
Low
radiation
dose**

**CMS@LHC,
25ns bunch
crossing,
high
radiation
dose**

Noble Liquids for Homogeneous EM Calorimetry

	Ar	Kr	Xe
Z	18	36	58
A	40	84	131
X_0 (cm)	14	4.7	2.8
R_M (cm)	7.2	4.7	4.2
Density (g/cm ³)	1.4	2.5	3.0
Ionization energy (eV/pair)	23.3	20.5	15.6
Critical energy ϵ (MeV)	41.7	21.5	14.5
Drift velocity at saturation (mm/ μ s)	10	5	3



When a charge particle traverses these materials, about half the lost energy is converted into ionization and half into scintillation.

The best energy resolution would obviously be obtained by collecting both the charge and light signal. This is however rarely done because of the technical difficulties to extract light and charge in the same instrument.

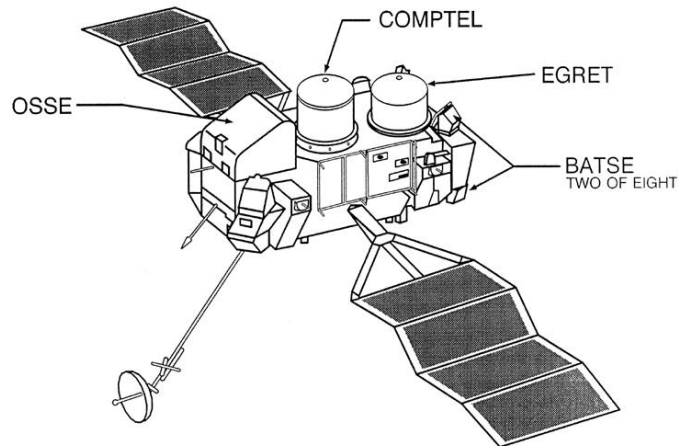
Krypton is preferred in homogeneous detectors due to small radiation length and therefore compact detectors. Liquid Argon is frequently used due to low cost and high purity in sampling calorimeters (see later).

GeV Gamma-ray Astrophysics

The EGRET legacy

EGRET

COMPTON OBSERVATORY INSTRUMENTS



The Instruments on CGRO Cover Six Orders of Magnitude in Photon Energy

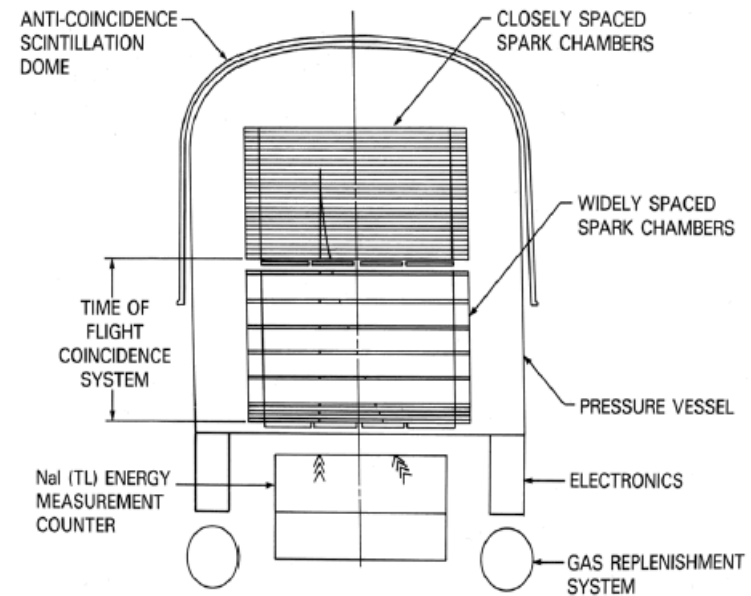
BATSE

OSSE

COMPTEL

EGRET

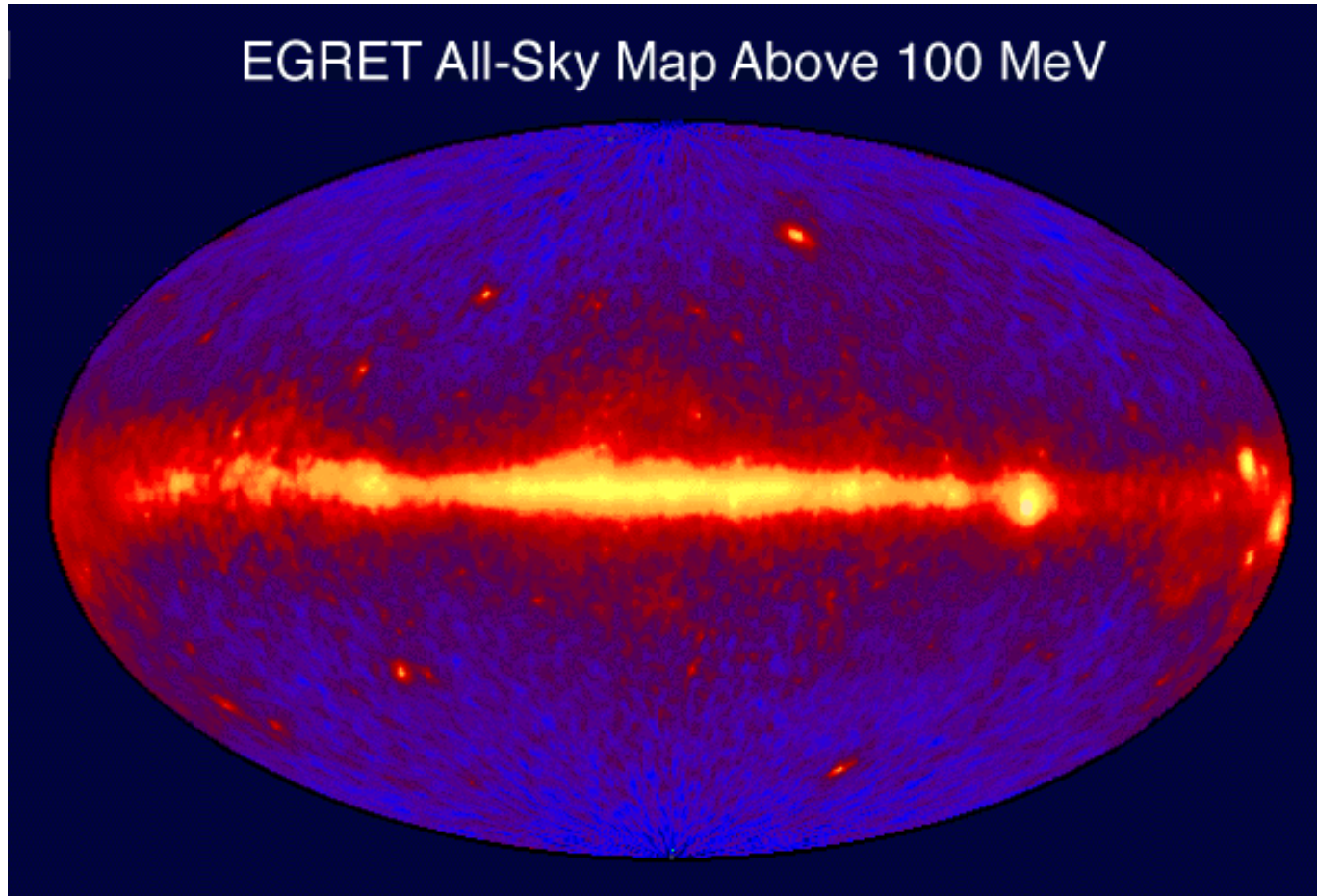
10 keV 100 keV 1 MeV 10 MeV 100 MeV 1 GeV 10 GeV 100 GeV



EGRET

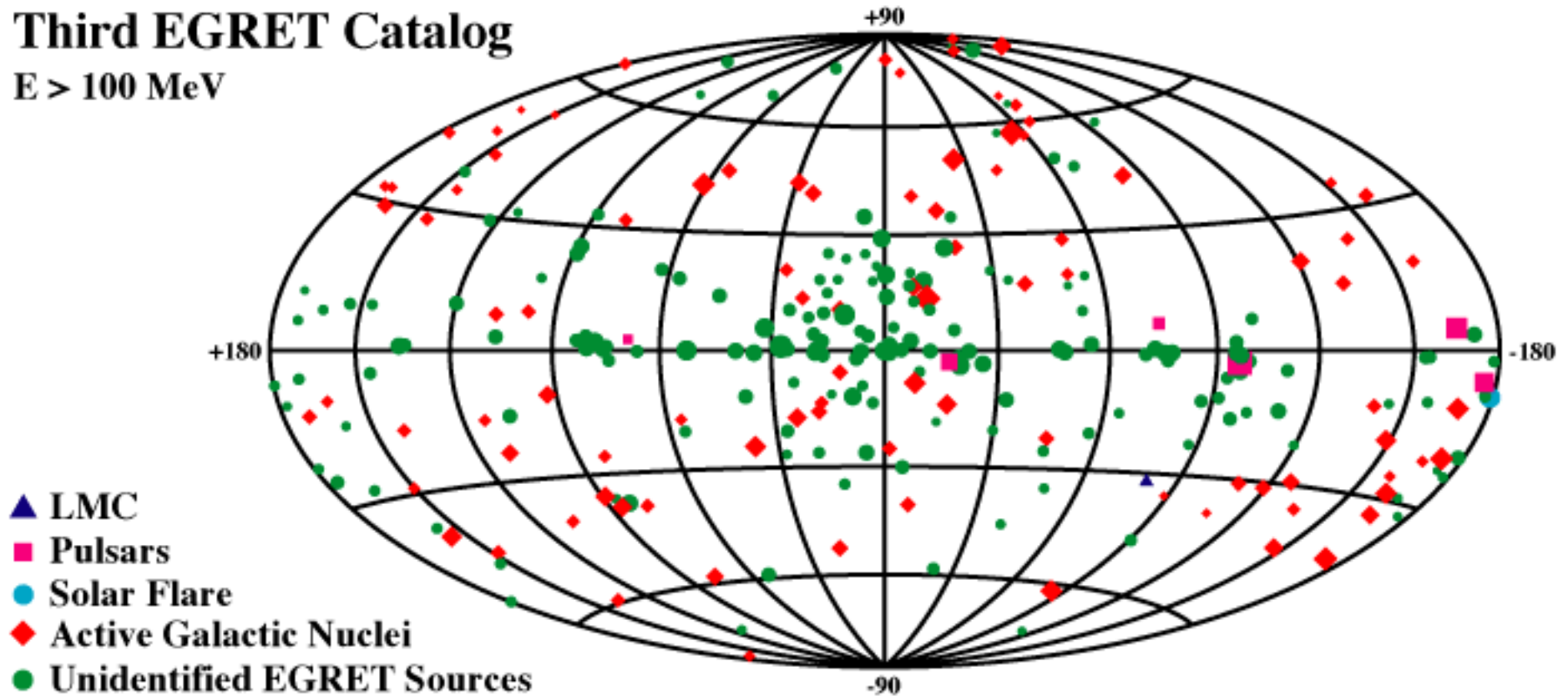
- 1991-2000
- 30 MeV - 30 GeV
- AGN, GRB, Unidentified Sources, Diffuse Bkg

The HE sky from EGRET



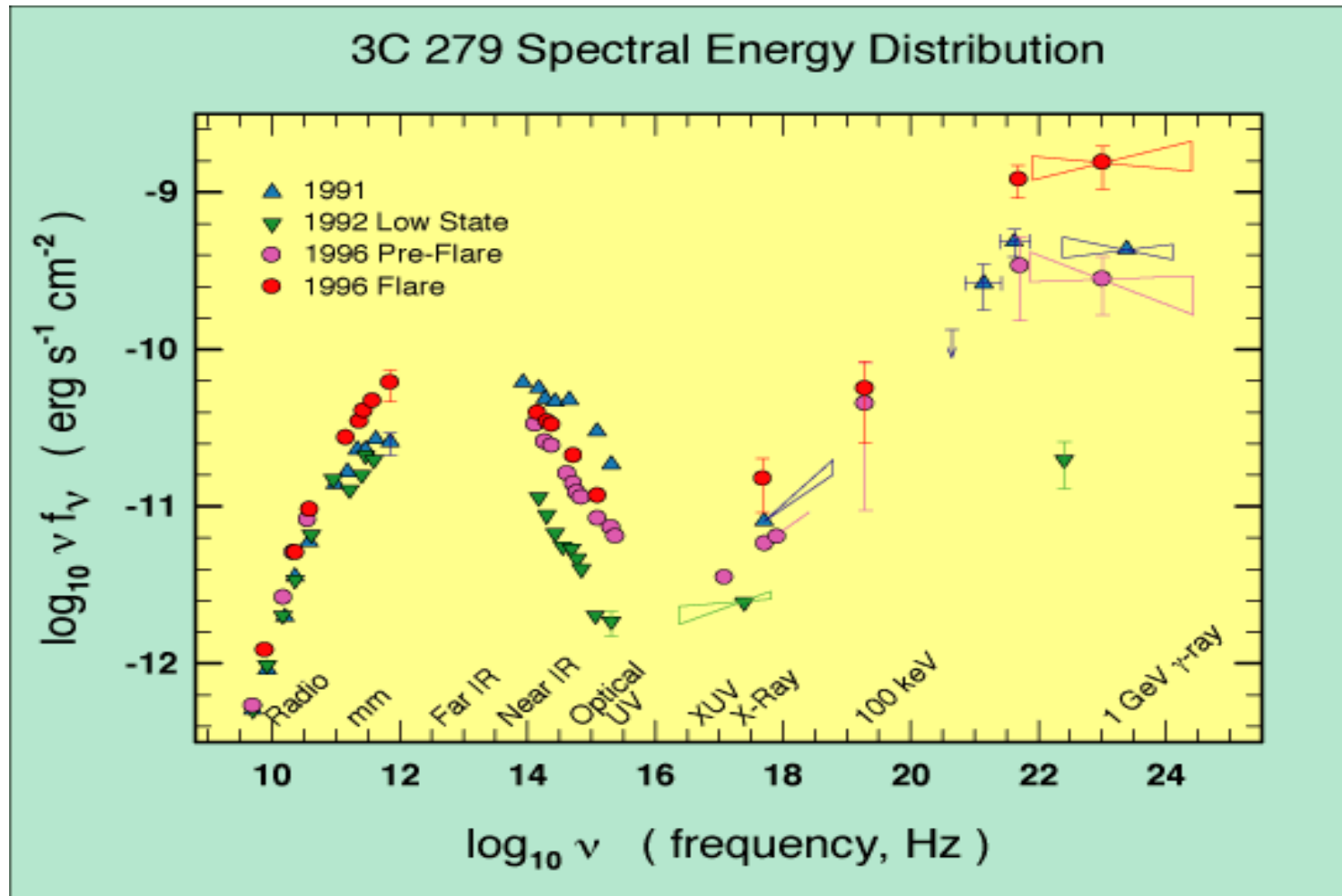
EGRET Gamma-ray Sources

Third EGRET Catalog
 $E > 100 \text{ MeV}$



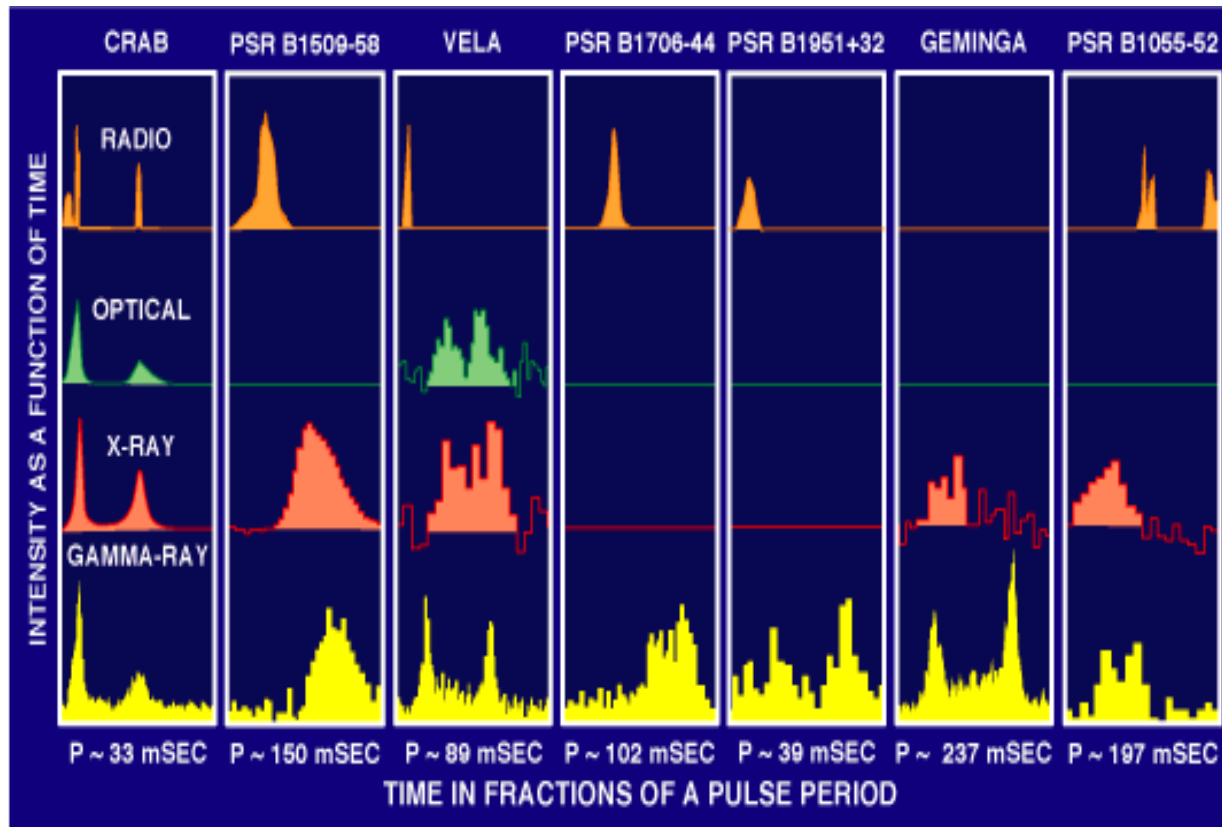
Challenge # 1

- Need simultaneous multiwavelength data to study variability and emission processes



Challenge # 2

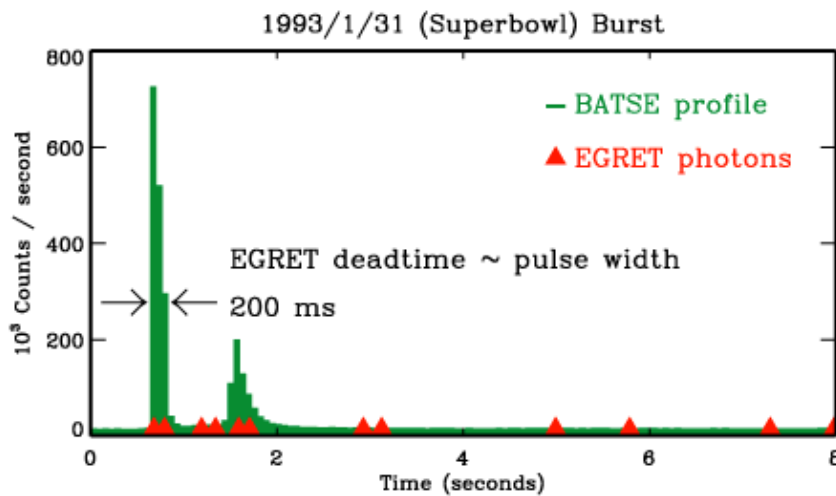
- Need more exposure and optimal timing (and radio monitoring) to discover more gamma-ray PSRs.



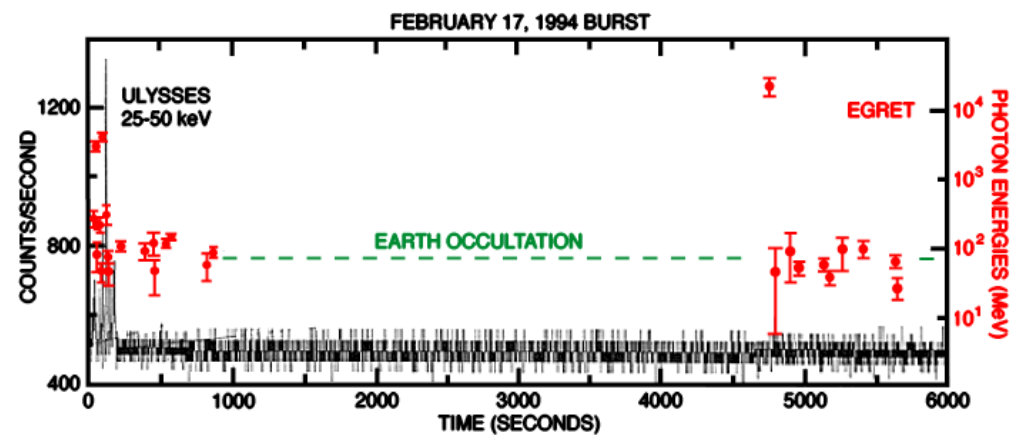
Challenge # 3

- Need fast timing for gamma-ray detection (improving EGRET deadtime, 100 msec → 100 microsec or less).

Prompt Emission (GRB 930131)

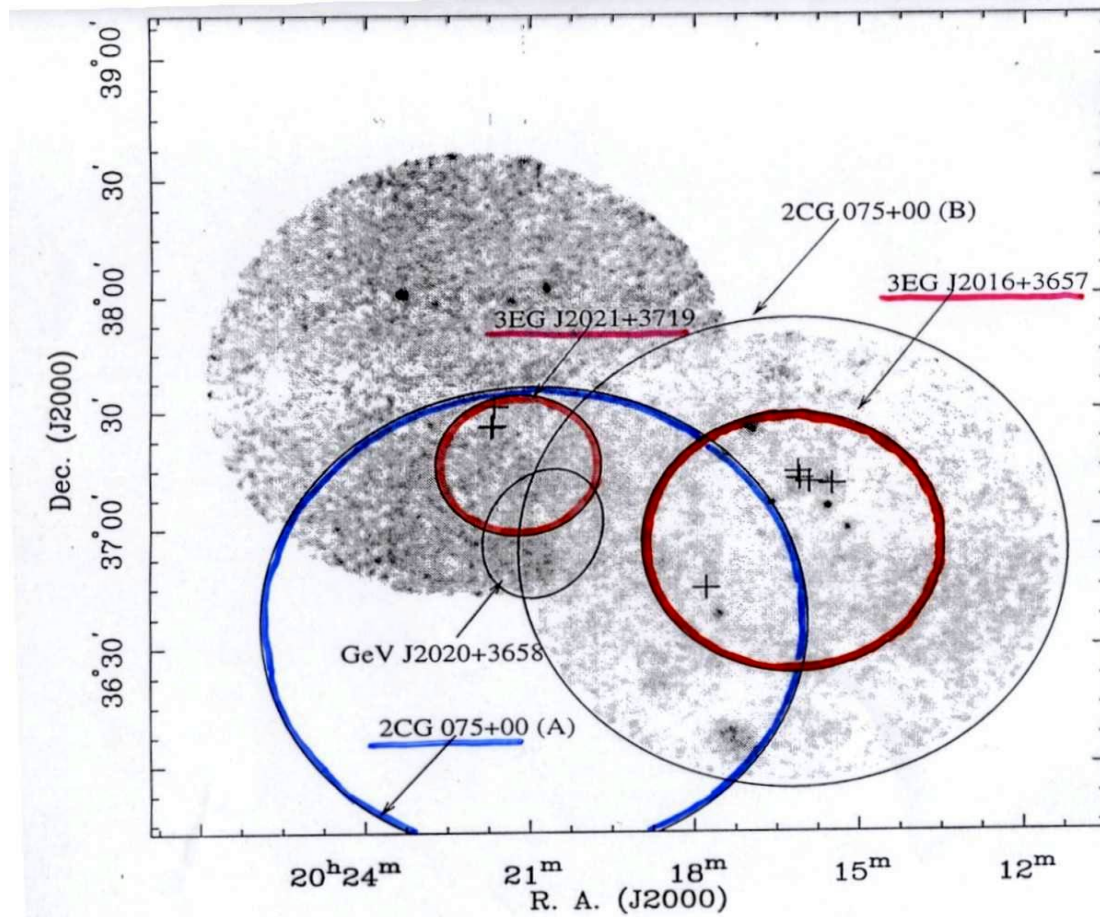


Delayed Emission (GRB 940217)



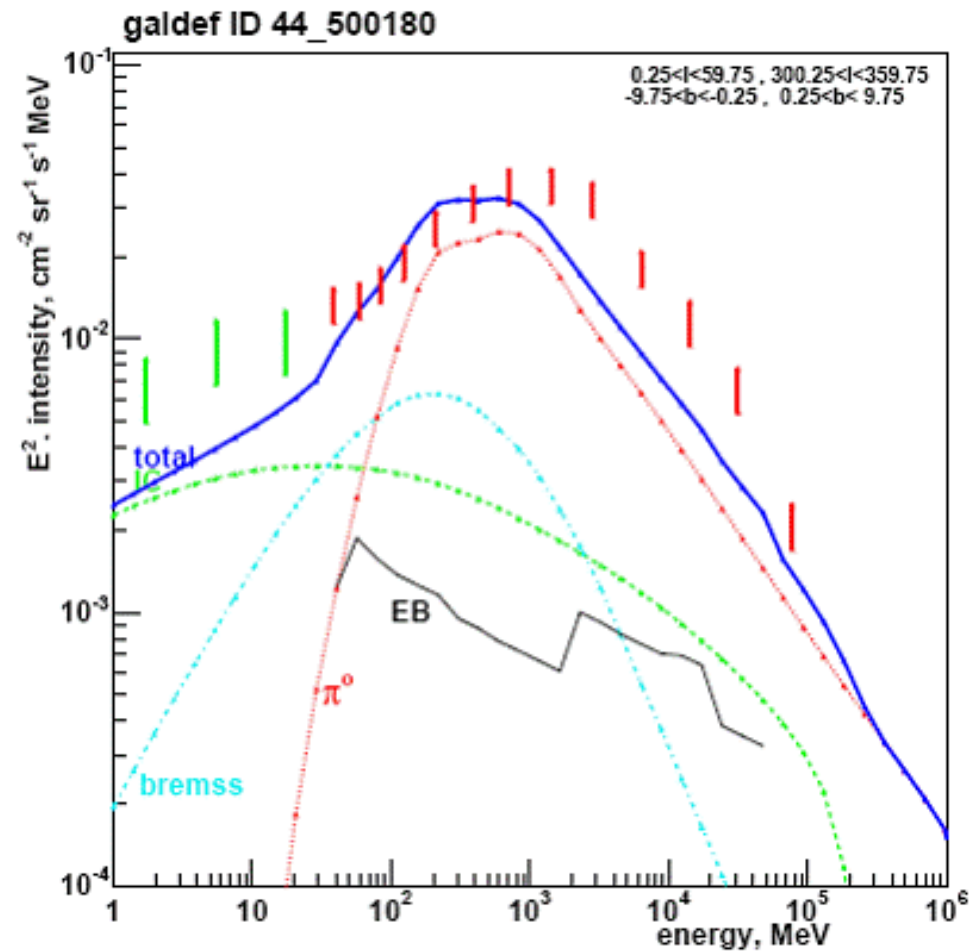
Challenge # 4

- Need arcminute positioning of gamma-ray sources (improving EGRET error box radii by a factor of 2-10).

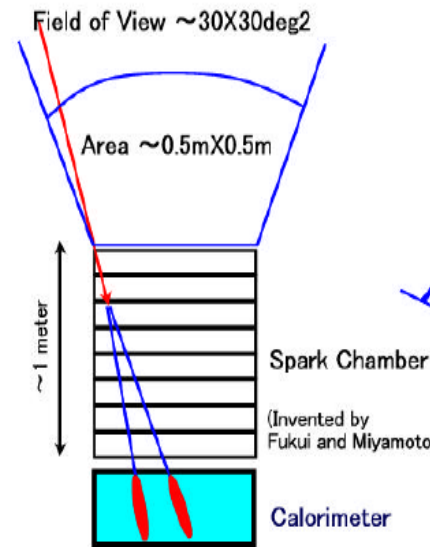
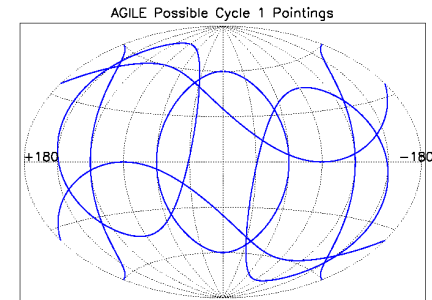
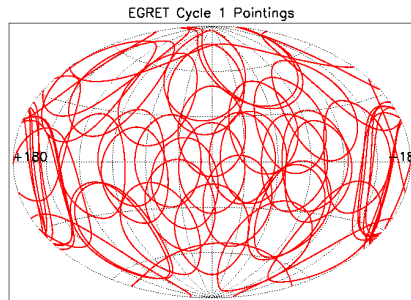
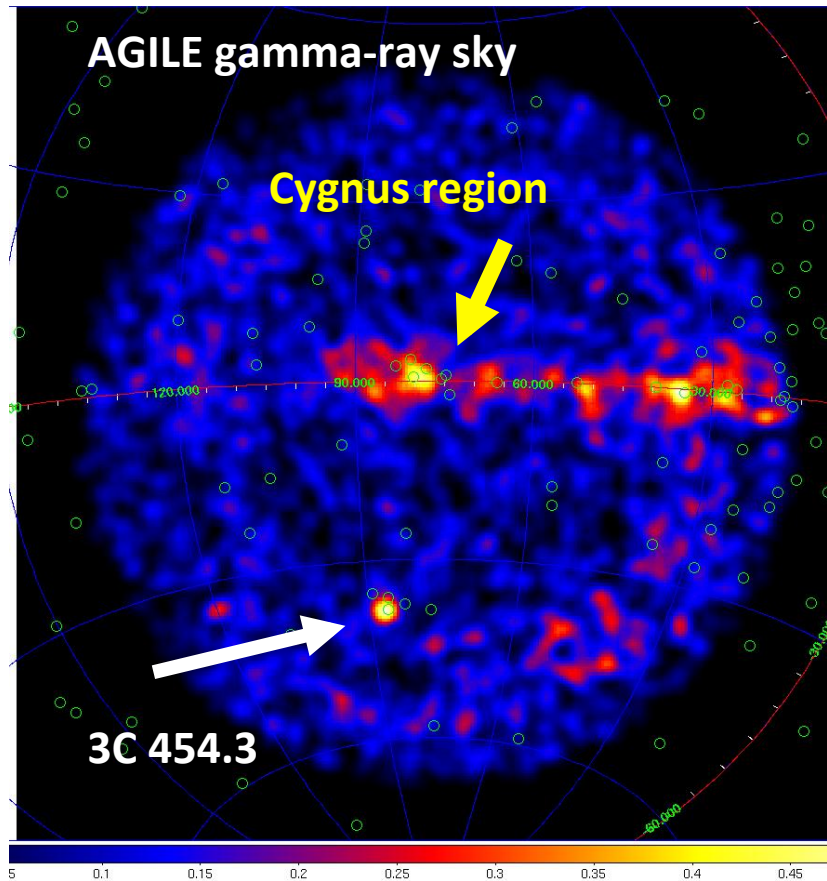


Challenge # 5

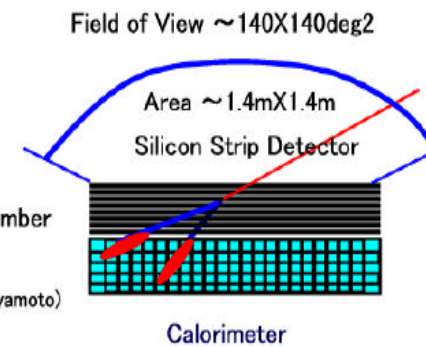
- Need improvements in Spectral Resolution fo check for DM signals



Technology impact - FoV

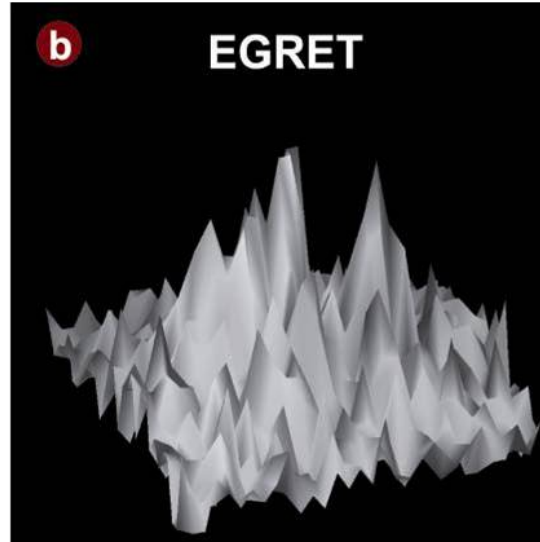
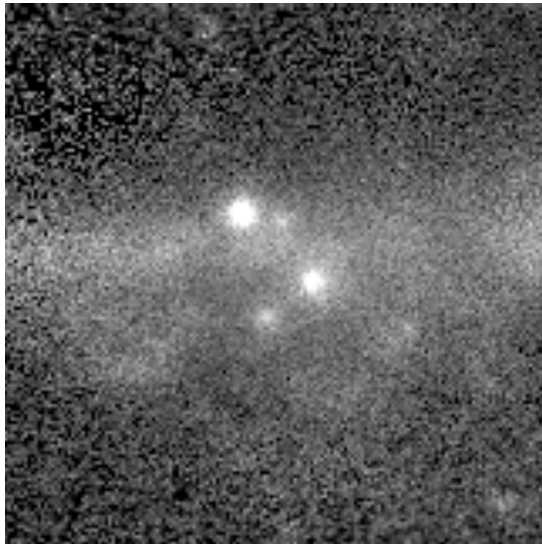


EGRET on Compton GRO



GLAST Large Area Telescope

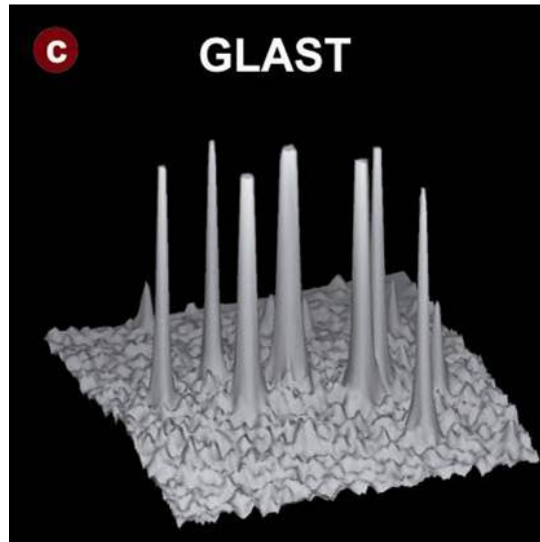
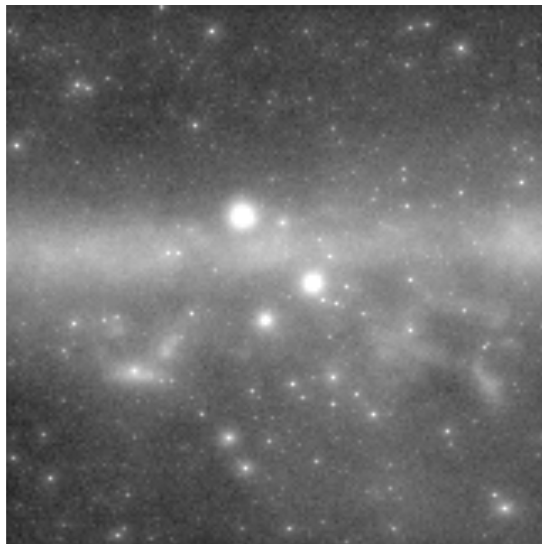
Technology impact -- PSF



EGRET
(1991-2000)
Phases 1-5

Spark chamber

- sense electrode spacing \sim mm
- sensitive layer depth \sim cm
 - *up to 28 hit over $>1m$*



LAT
(2008- >2013)
1-yr simulation



Si-strip detectors

- sense electrode spacing $\sim 0.2mm$
 - *better single hit resolution*
- sensitive layer depth $\sim 0.4mm$
 - *up to 36 hit over $0.8m$*
 - *converter proximity to minimize MCS*

Cygnus region ($15^\circ \times 15^\circ$), $E_\gamma > 1 GeV$

Multiple Scattering

Multiple Scattering

Statistical (quite complex) analysis of multiple collisions gives:

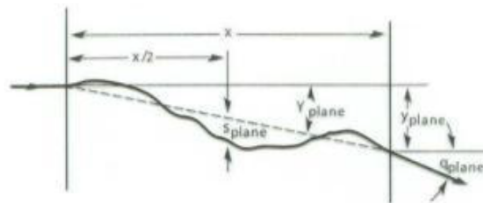
Probability that a particle is deflected by an angle θ after travelling a distance x in the material is given by a Gaussian distribution with sigma of:

$$\Theta_0 = \frac{0.0136}{\beta c p [\text{GeV}/c]} Z_1 \sqrt{\frac{x}{X_0}}$$

X_0 ... Radiation length of the material

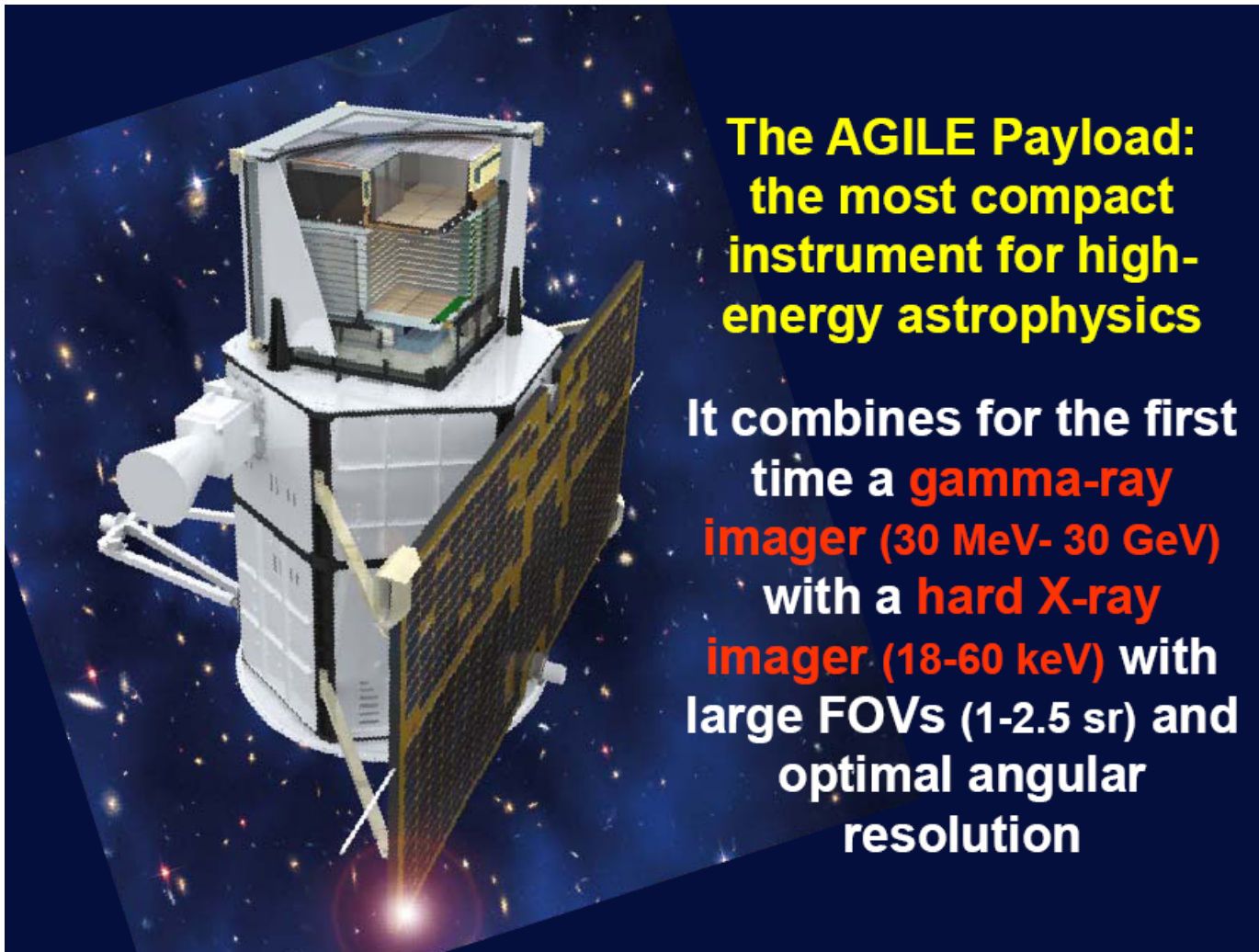
Z_1 ... Charge of the particle

p ... Momentum of the particle



AGILE

AGILE instrument



**The AGILE Payload:
the most compact
instrument for high-
energy astrophysics**

It combines for the first
time a **gamma-ray
imager (30 MeV- 30 GeV)**
with a **hard X-ray
imager (18-60 keV)** with
large FOVs (1-2.5 sr) and
optimal angular
resolution

AGILE



INAF



Carlo Gavazzi Space SpA



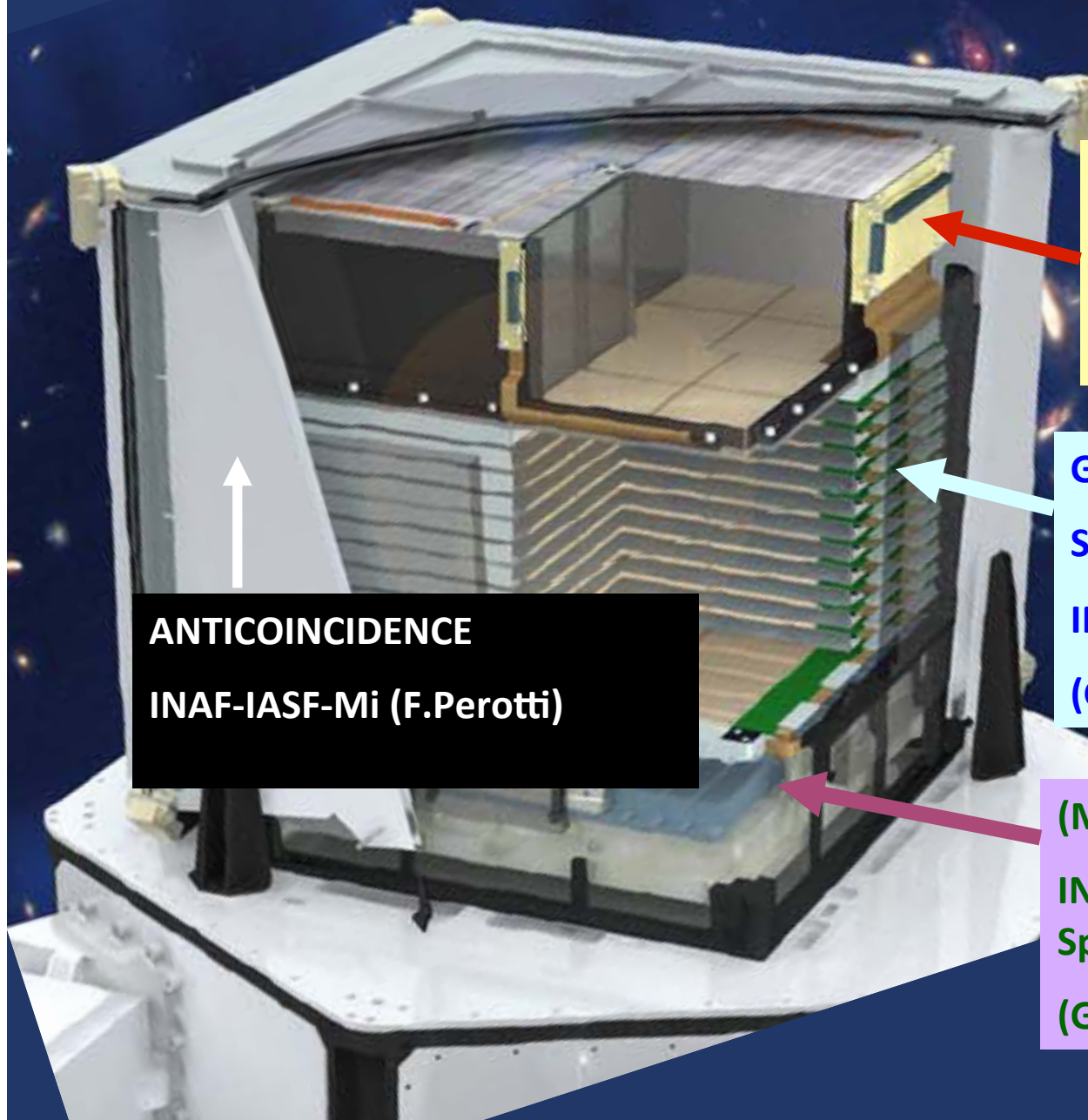
OERLIKON
CONTRAVES



ENEA



AGILE: inside the cube...



**HARD X-RAY IMAGER
(SUPER-AGILE)**
**INAF-IASF-Rm (E.Costa, M.
Feroci)**

**GAMMA-RAY IMAGER
SILICON TRACKER**
**INFN-Trieste
(G.Barbiellini, M. Prest)**

↑
**ANTICOINCIDENCE
INAF-IASF-Mi (F.Perotti)**

(MINI) CALORIMETER
**INAF-IASF-Bo, Thales-Alenia
Space (LABEN)**
(G. Di Cocco, C. Labanti)

The Silicon Tracker

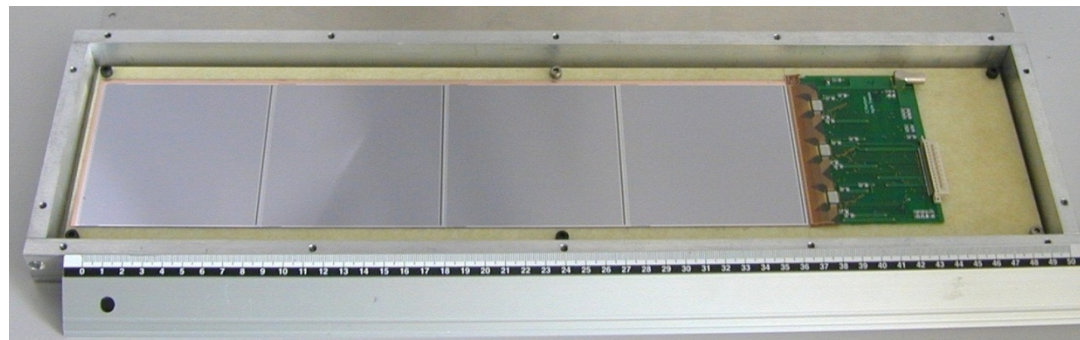
The AGILE silicon detectors

Detector specifications:

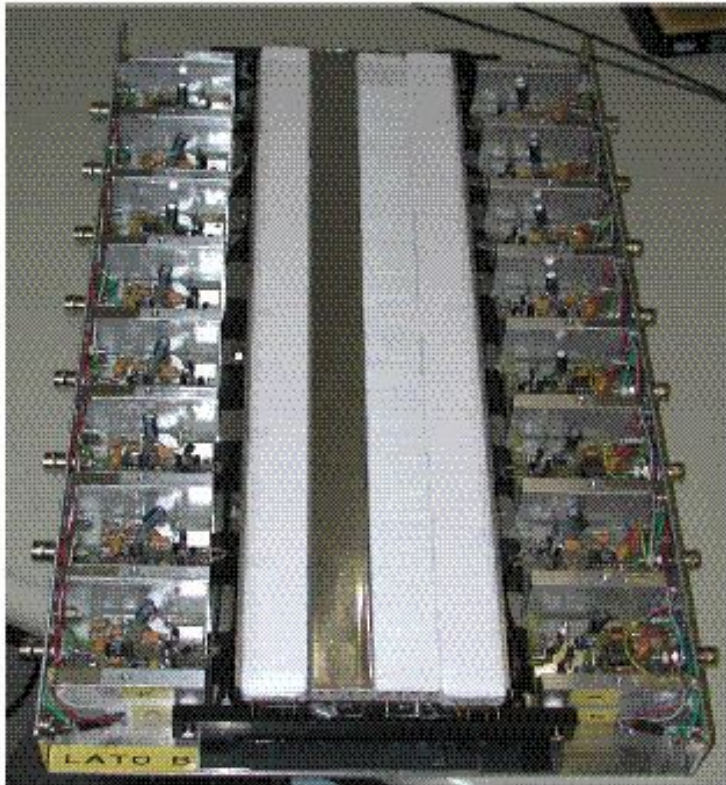
- dimension: $9.5 \times 9.5 \text{ cm}^2$
- thickness: $410 \text{ }\mu\text{m}$ (6 inch technology)
- readout pitch: $242 \text{ }\mu\text{m}$;
physical pitch: $121 \text{ }\mu\text{m}$ (one floating strip)
- number of strips/ladder: 384
- Single side and AC-coupled
- leakage current: 2 nA/cm^2 at $V_{\text{bias}} = 2.5 \cdot V_{\text{FD}} = 200 \text{ V}$
- polarization resistor: $40 \text{ M}\Omega$
- coupling capacitor: 55 pF/cm
- Al strip resistance: $4.3 \text{ }\Omega/\text{cm}$
- max number of bad strips: $<1\%$
- average number of bad strips: $<0.5\%$

The AGILE frontend chip: TA1 \rightarrow TAA1

- low noise, low power, **SELF-TRIGGERING**
- technology: $1.2 \text{ }\mu\text{m}$ CMOS, double poly, double metal (final: $0.8 \text{ }\mu\text{m}$ BiCMOS on epitaxial layer)
- features:
 - 128 channels
 - gain: 25 mV/fC ; range: 18 fC
 - noise (e^- rms): $165 + 6.1/\text{pF}$ for $T_{\text{peak}} = 2 \text{ }\mu\text{s}$
 - power: $<0.4 \text{ mW/channel}$**
 - power rails: $\pm 2 \text{ V}$
 - readout frequency: 5 Mhz
 - gain spread: $<1.5\%$
 - threshold offset spread (TA1): 20% (in TAA1 will be implemented a 3 bit DAC per channel)



The CsI Mini-Calorimeter



MINI-CALORIMETER

DETECTOR

- 30 CsI bars wrapped with tight diffusion material organized in 2 orthogonal trays
- bar dimension: $40 \times 2.3 \times 1.5 \text{ cm}^3$
 - total radiation length: $1.5X_0$ (in axis)

FRONTEND ELECTRONICS

- 1 photodiode on each side of the bar
- optically coupled

GOAL

- measure energy deposit of the photon conversion pair (GRID mode)
- detect GRBs and transients in the range 0.25-250MeV (BURST mode)

SCIENTIFIC FEATURES

- energy resolution: 22-24%(FWHM) @ 1MeV
0.7% @ 100MeV
- spatial resolution: 15mm @ 1MeV
2mm @ 100MeV
- timing resolution: $2\mu\text{s}$ (BURST mode)

SuperAGILE X-ray detector



SUPER-AGILE

DETECTOR

- plane with 16 silicon tiles organized in 4 1D detectors
- each detector: 1536 readout strips (0.121mm pitch)
- a coded mask system

FRONTEND ELECTRONICS

- 12 self-triggering readout ASICs (128 channels each) per each detector, positioned on a kapton-FR4 hybrid

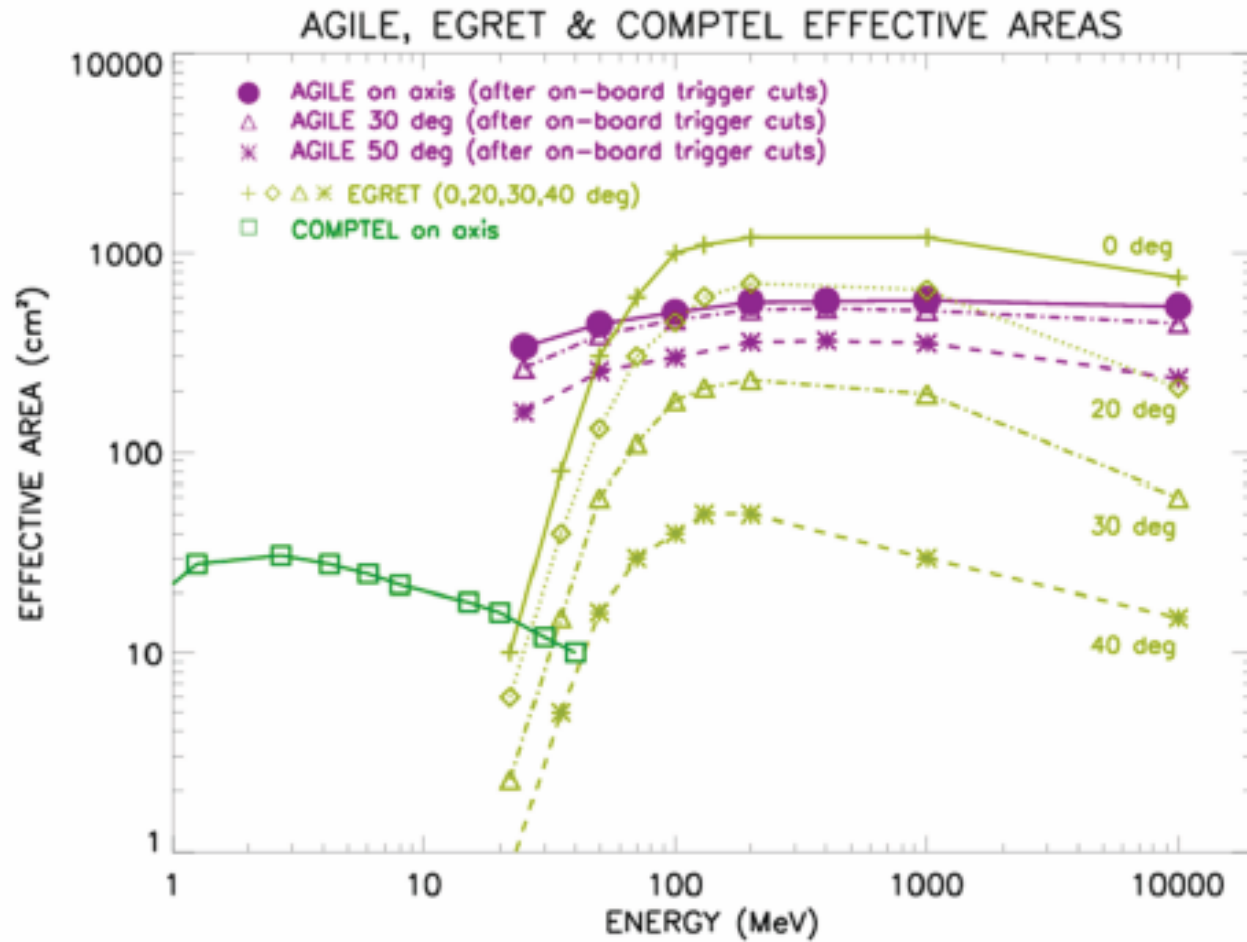
GOAL

measure X-rays in the energy range 10-40keV to detect GRBs, transients, galactic and extra-galactic sources

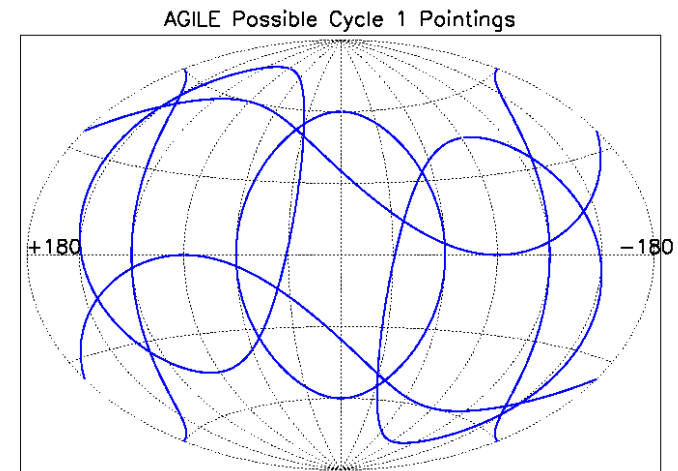
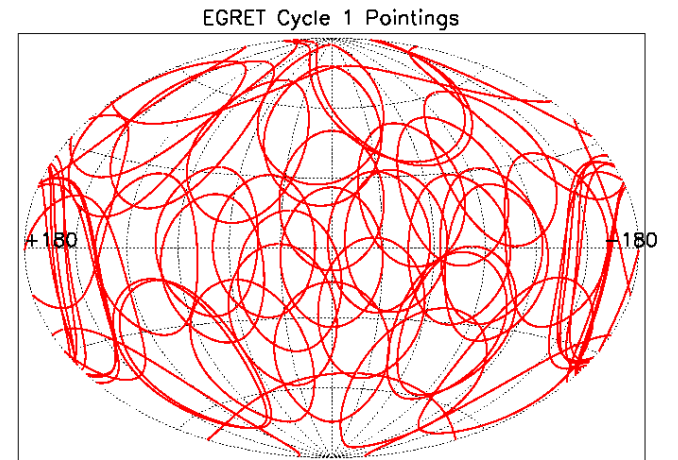
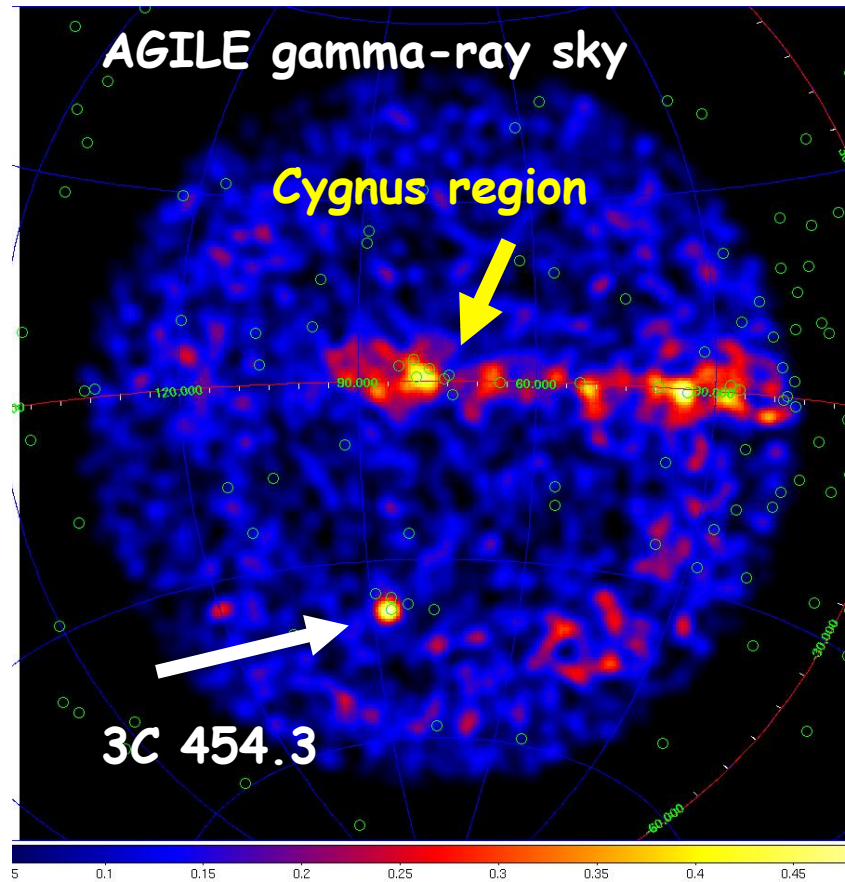
SCIENTIFIC FEATURES

- imaging: 1'-3' at ~20mCrab
- timing resolution: 5 μ s
- energy resolution: 4keV (FWHM)
- flux sensitivity: ~5mCrab (15keV)

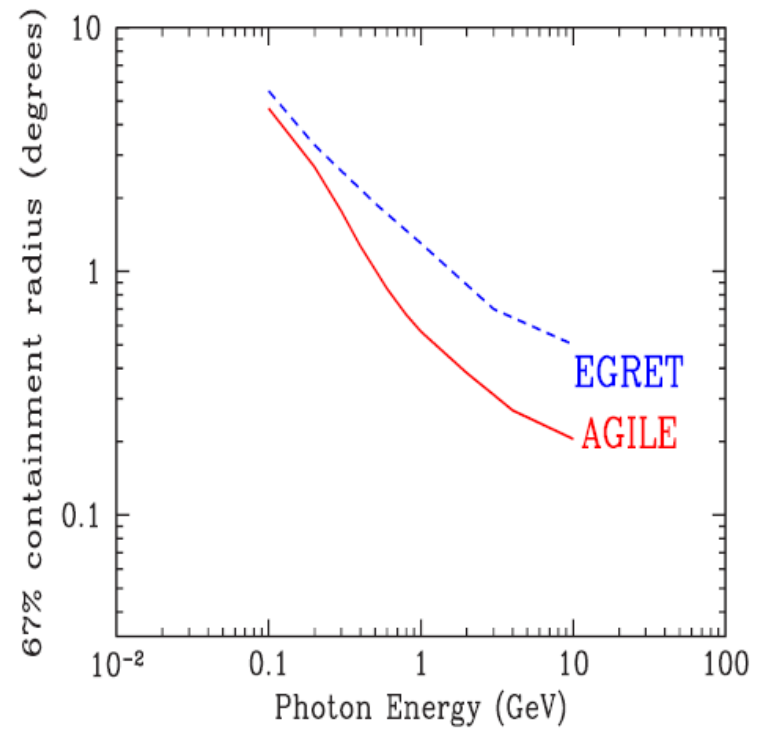
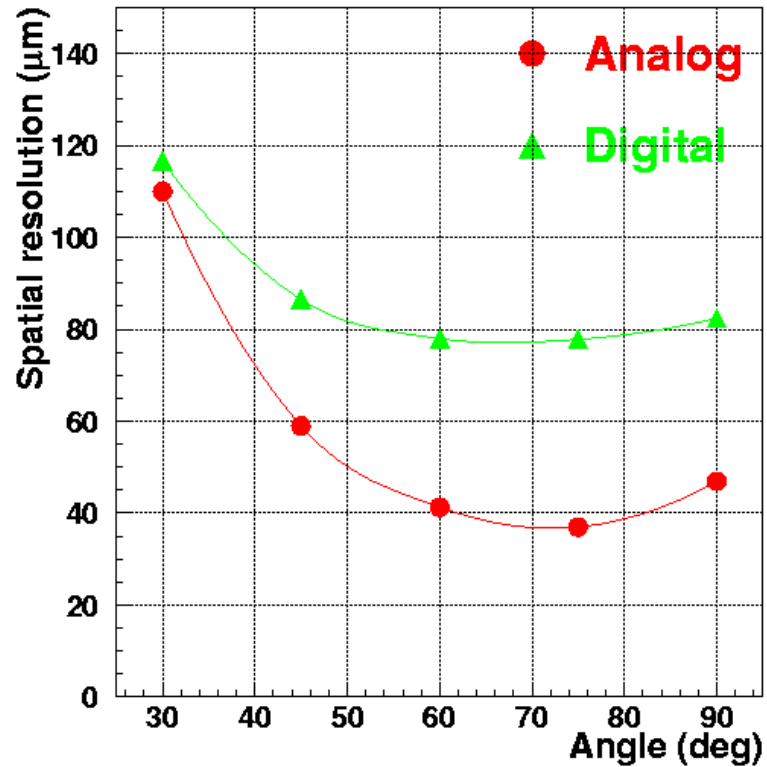
Performance



Si Self Trigger and FoV



Analog readout and PSF

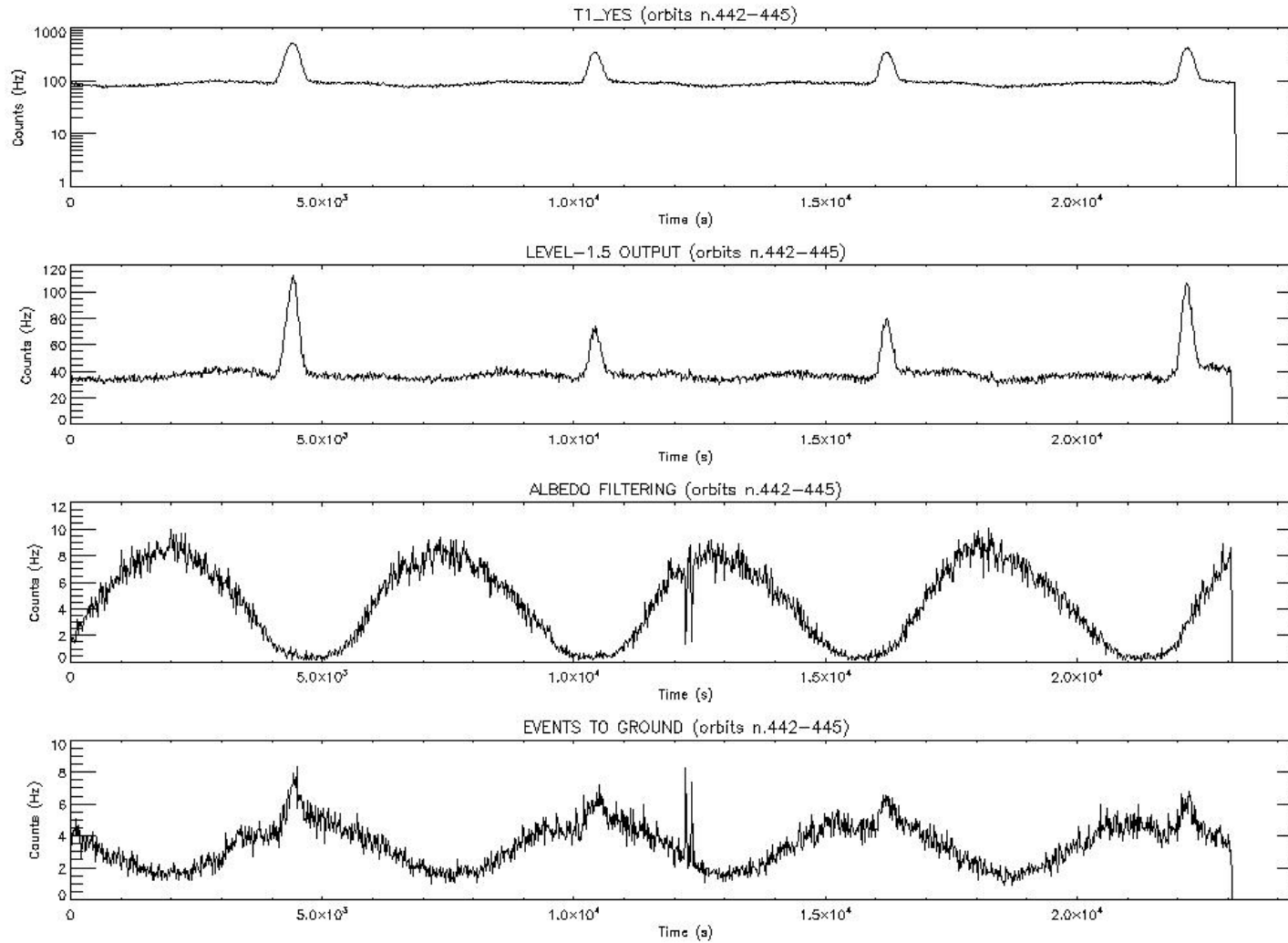


The AGILE launch



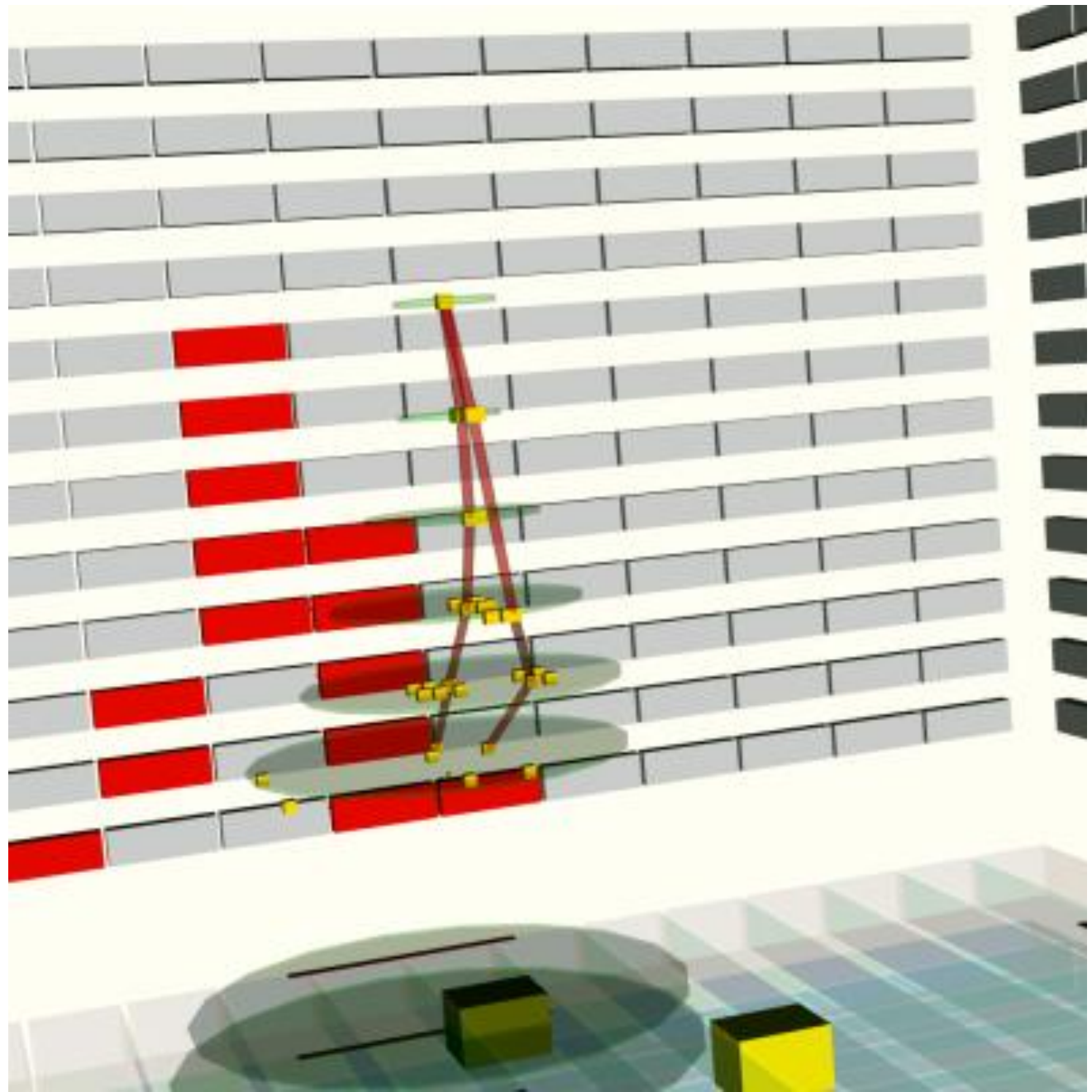
AGILE in orbit

AGILE in orbit

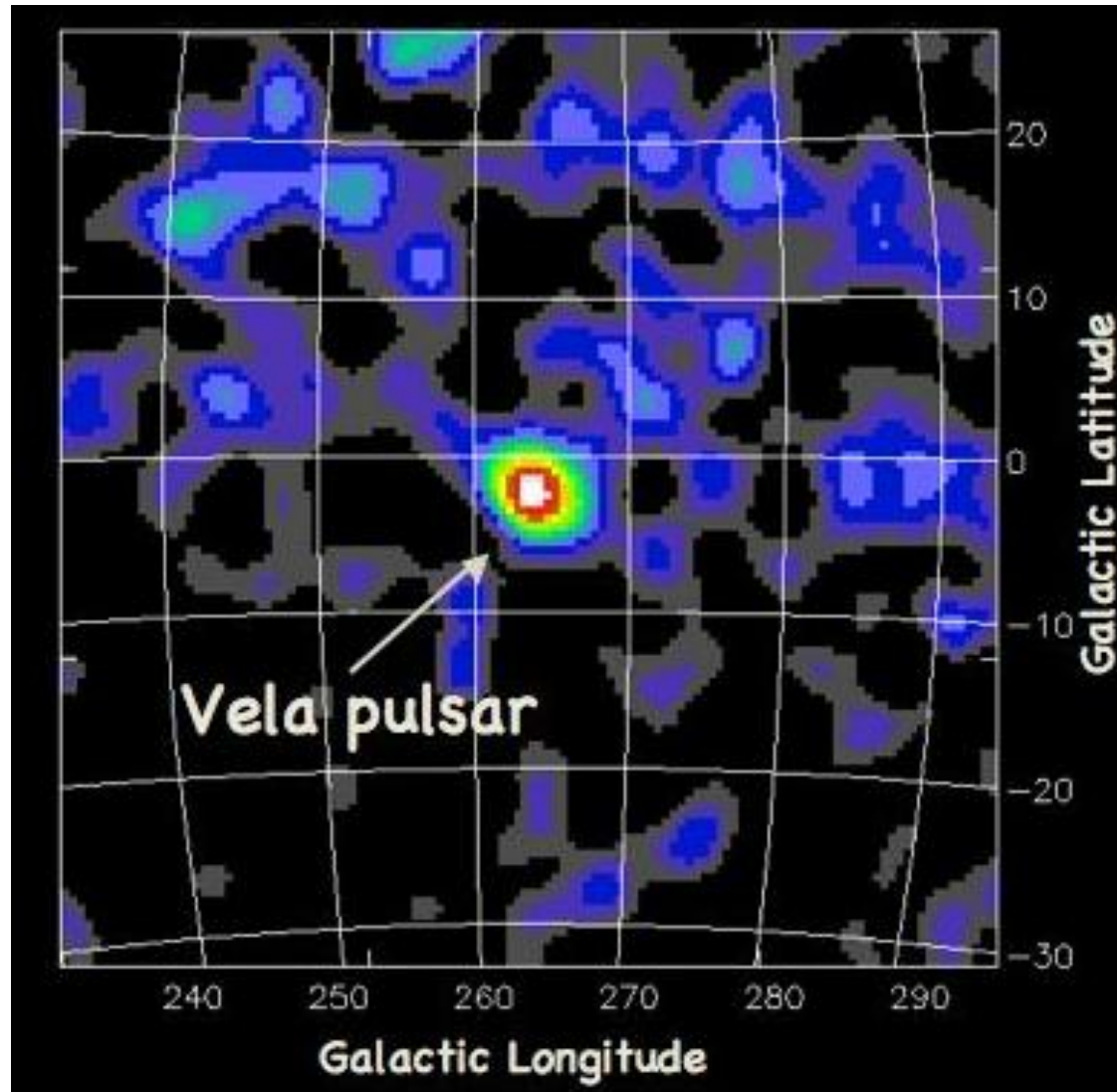


On Orbit Trigger Rates

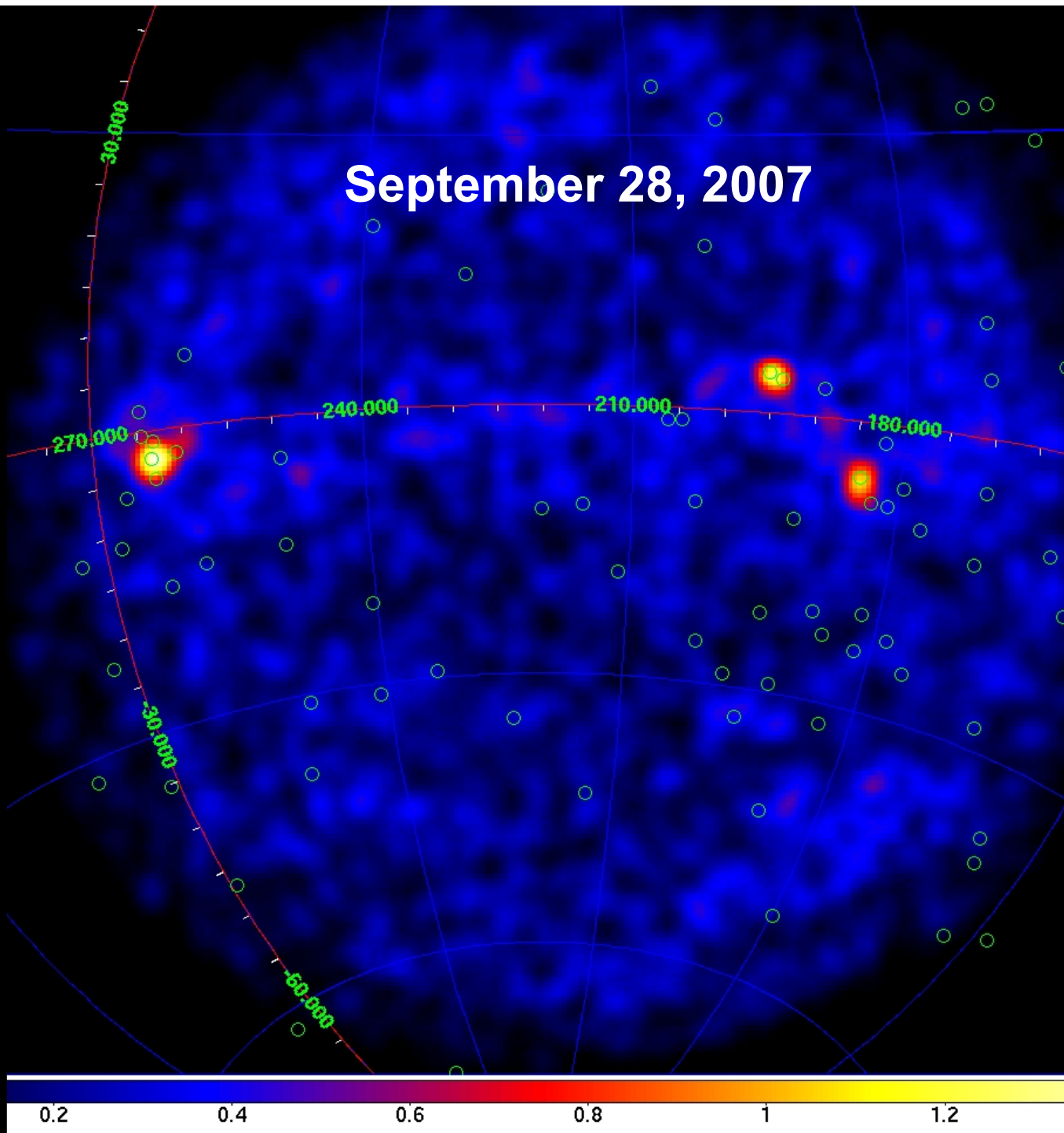
**First gamma-ray
detected in orbit
with the nominal
GRID trigger
configuration
(May 10, 2007)**



First Light



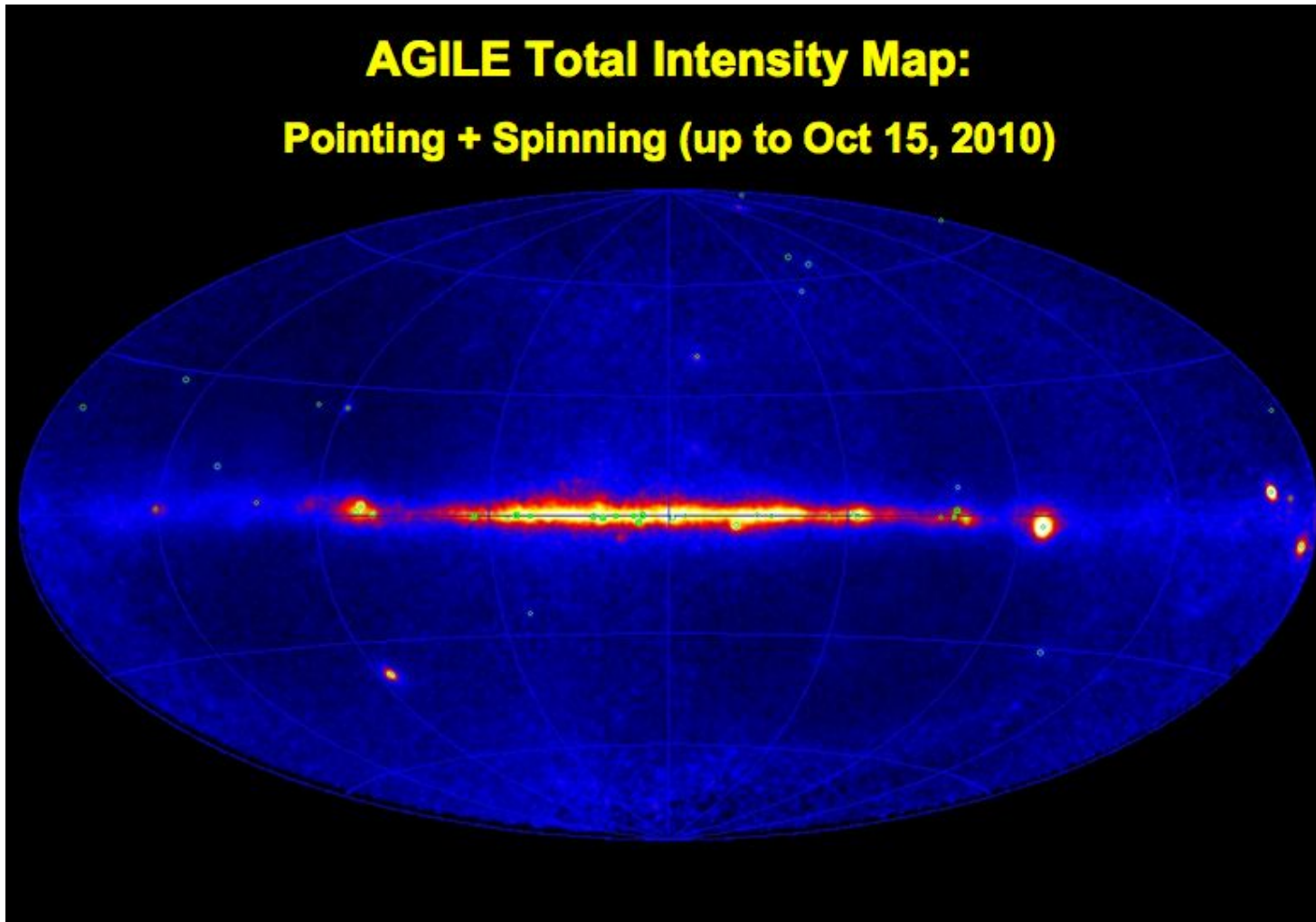
September 28, 2007



AGILE two lives

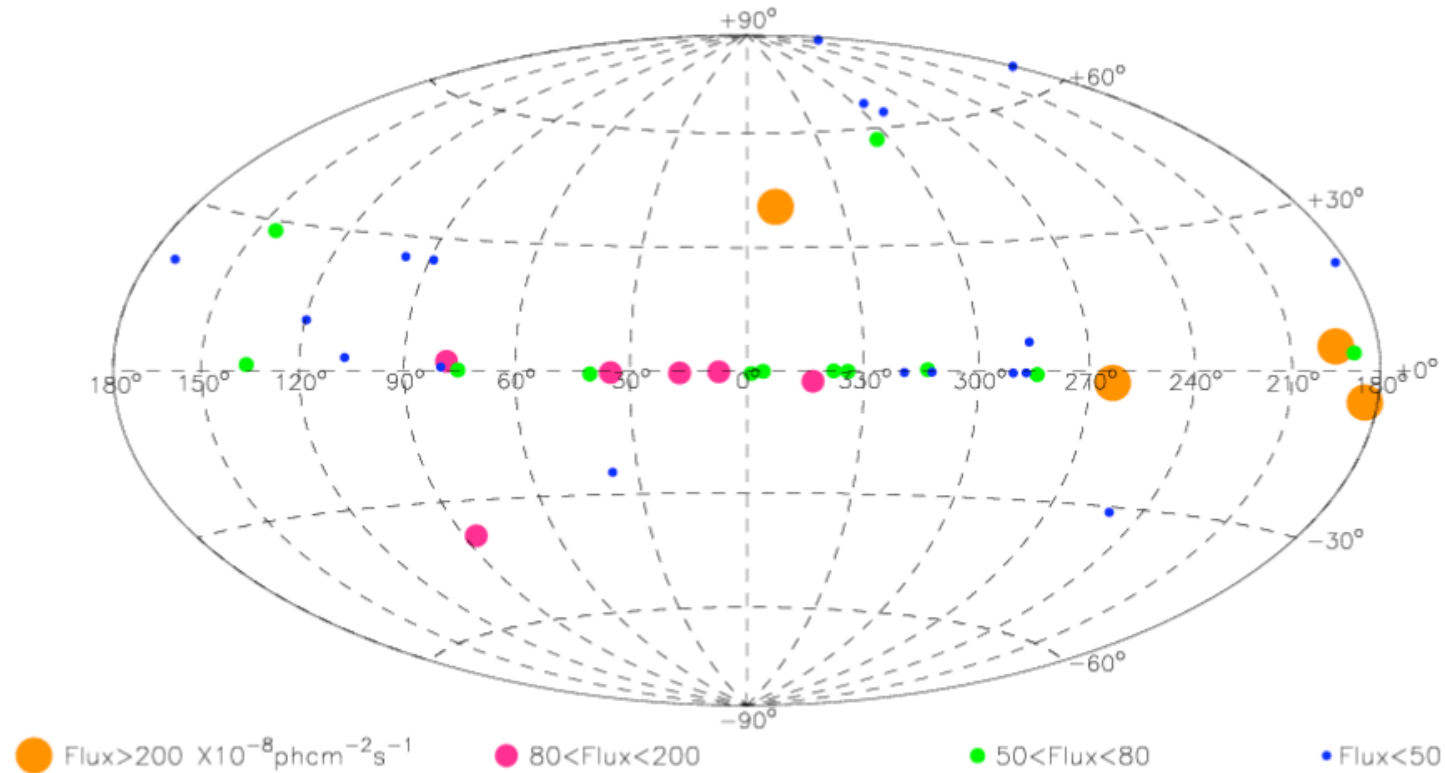
	pointing- AGILE	spinning- AGILE
time period	Jul.07 – Oct.09	Nov. 2010 -
attitude	fixed	variable (spinning, 1°/sec)
sky coverage	1/5	~ 70%
source livetime fraction	~ 0.5	~ 0.2
1-day exposure (30 degree off-axis, 100 MeV)	~ 2 10⁷ (cm² sec)	(0.5-1) 10⁷ (cm² sec)

The AGILE sky



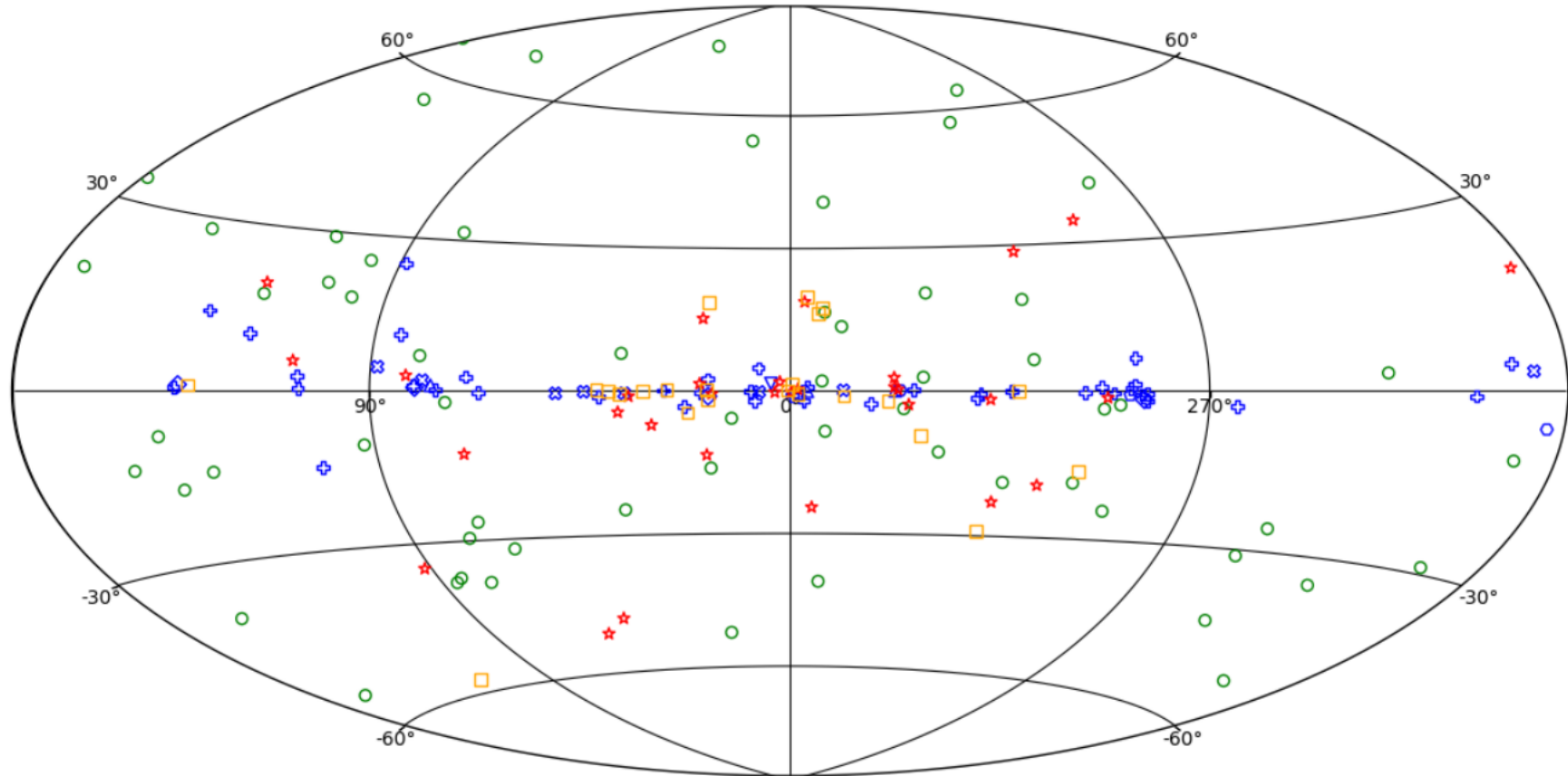
AGILE sources

AGILE GRID First Source Catalogue
Period July 2007 -- June 2008



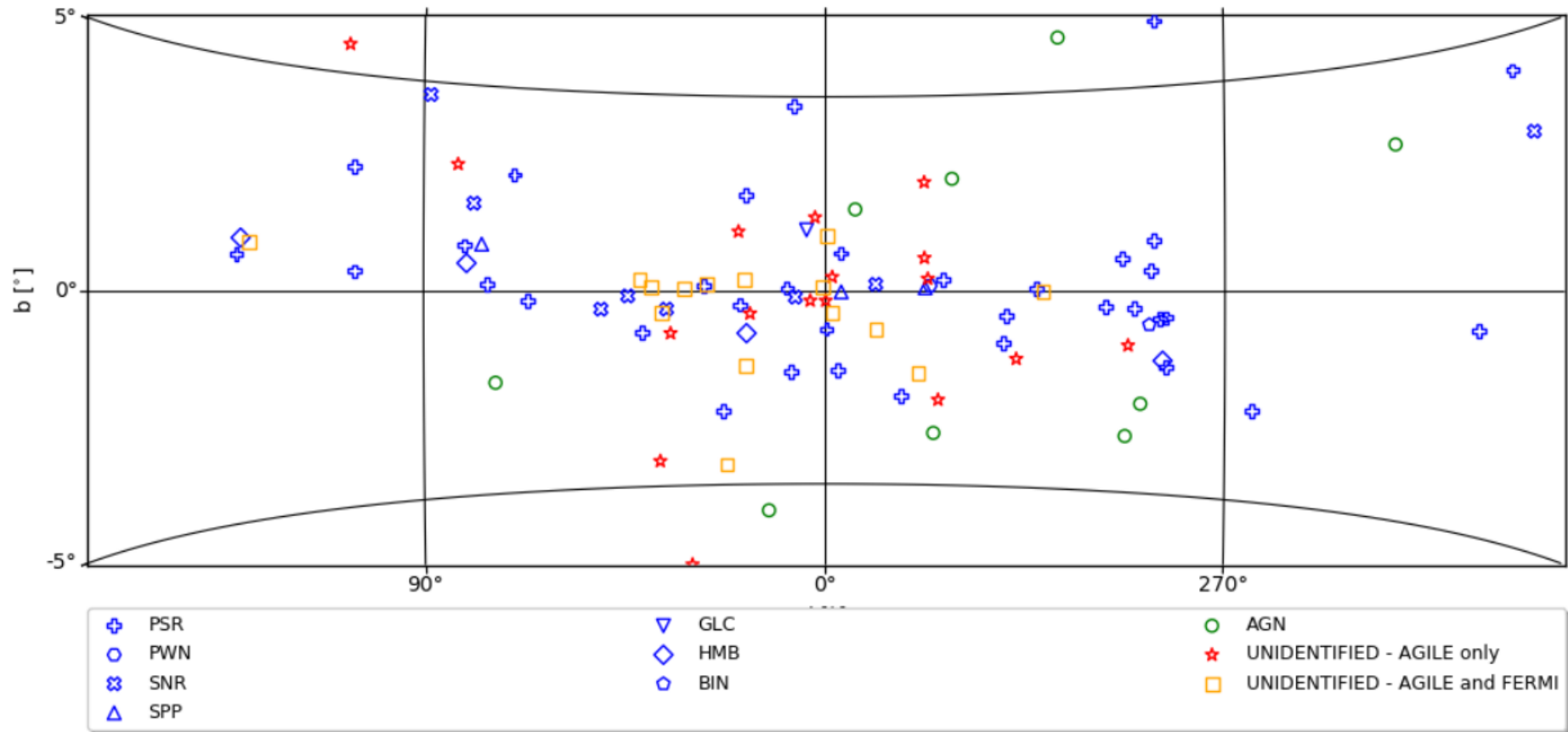
Pittori et al. 2009

AGILE sources



Bulgarelli et al. 2019

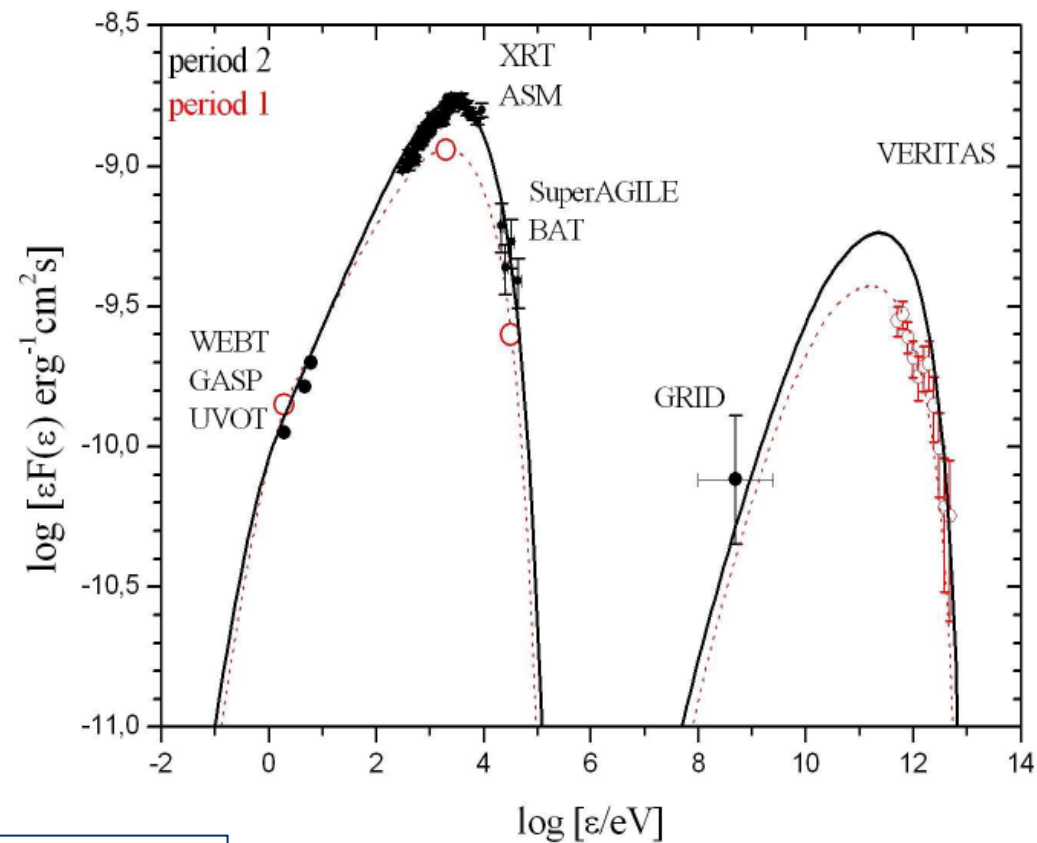
AGILE sources



Bulgarelli et al. 2019

Challenge # 1 – AGN

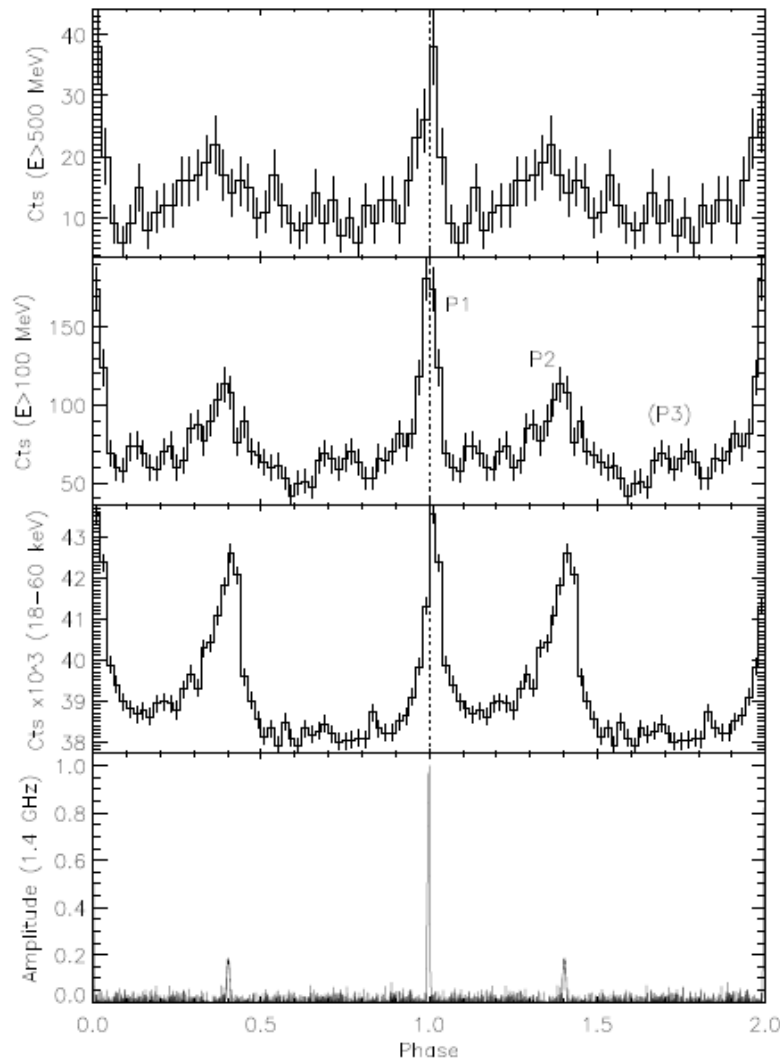
Joint campaign with MAGIC and VERITAS on Mkn 421



Donnarumma et al. 2009

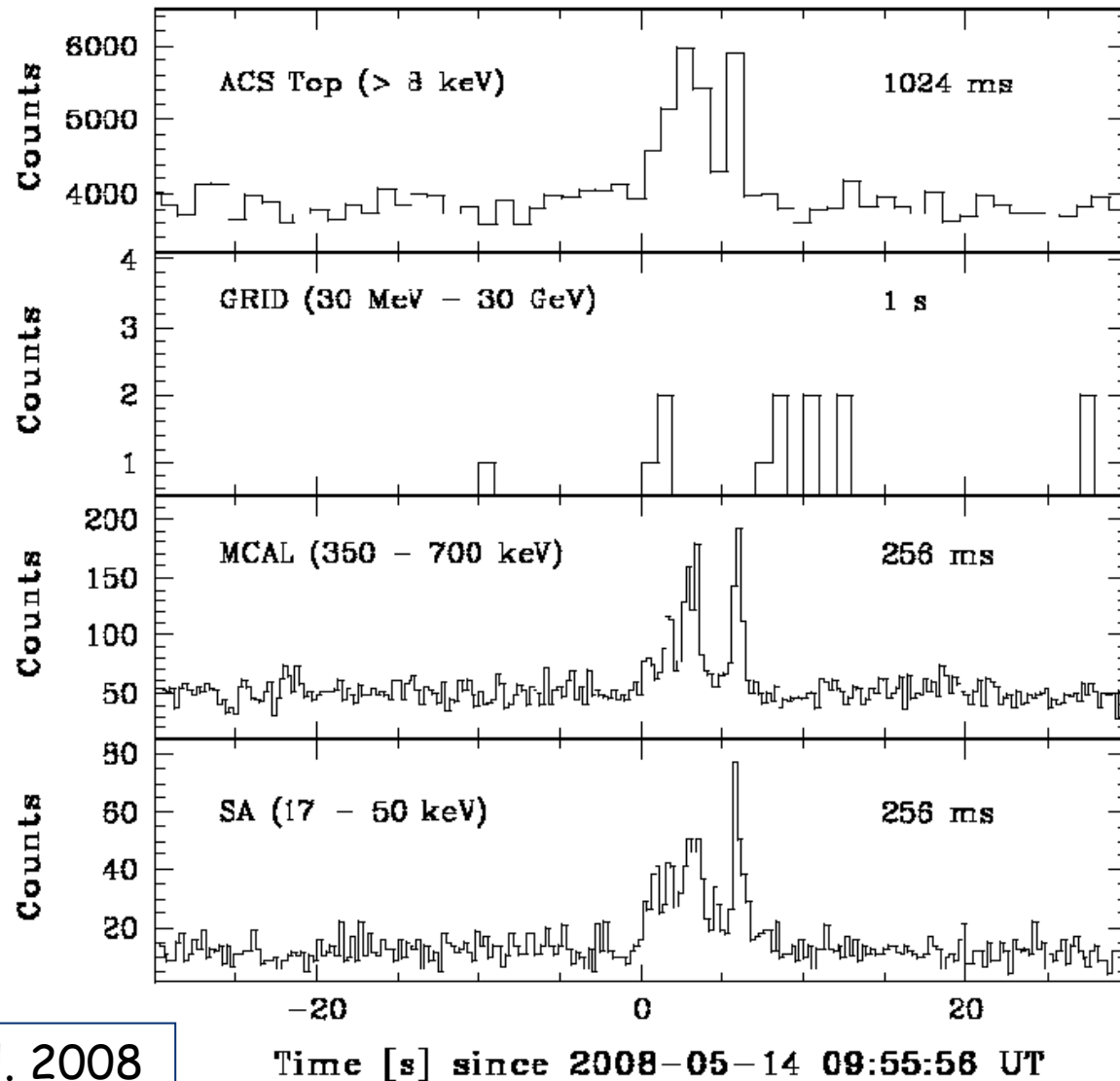
Challenge # 2 – Pulsar

High Precision
Timing (eg.
Crab PSR)



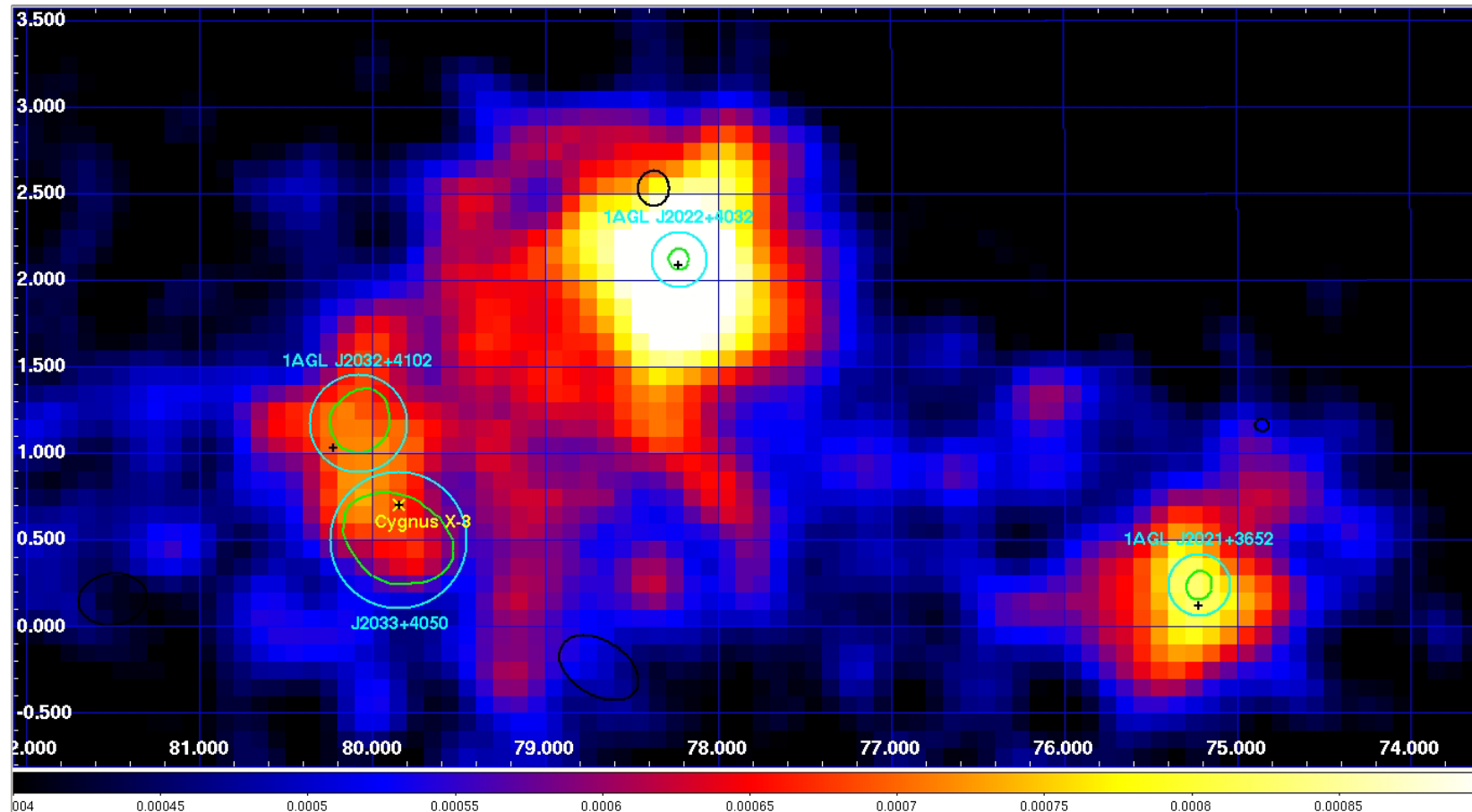
Pellizzoni et al. 2009

Challenge # 3 – GRB



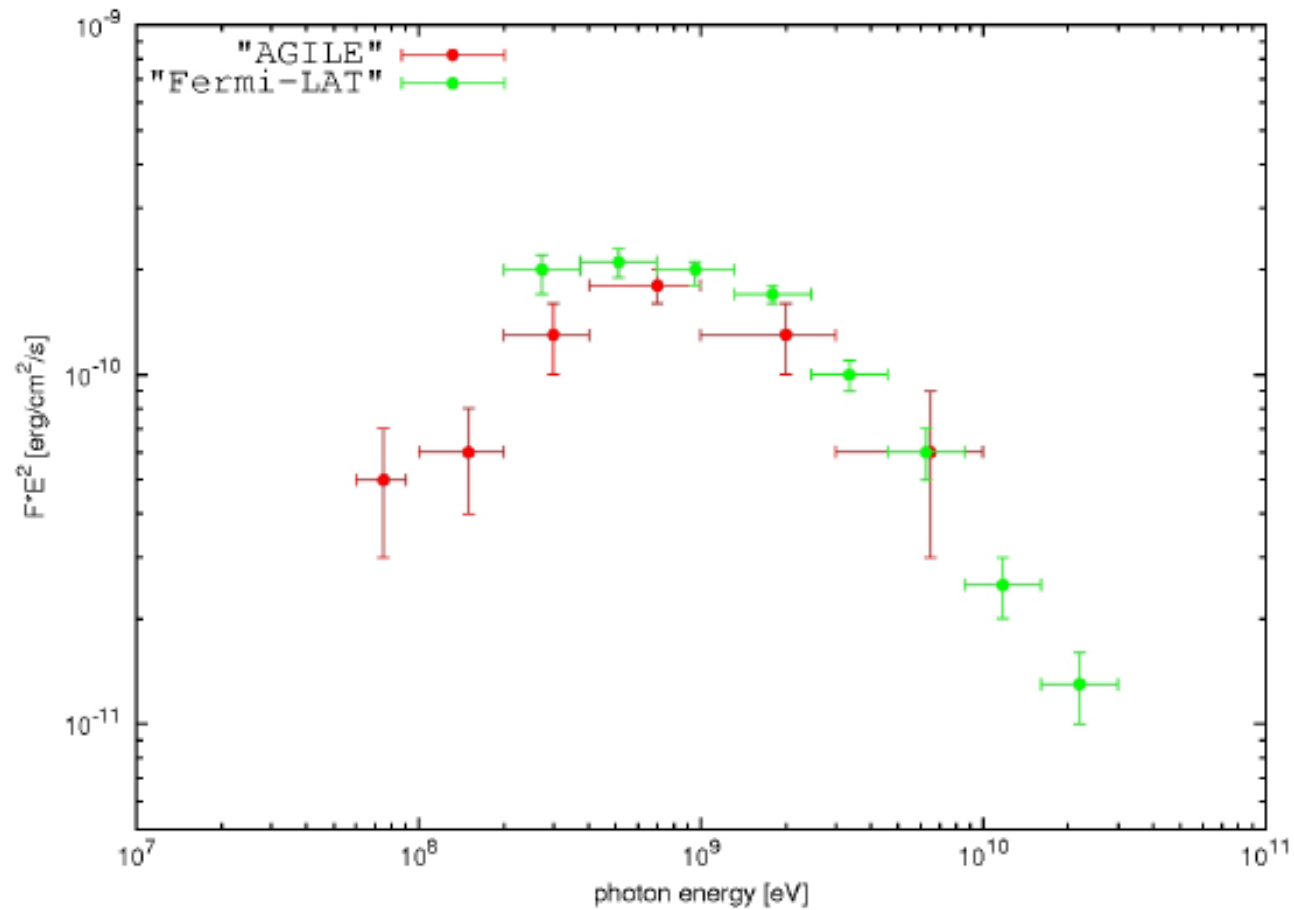
Giuliani et al. 2008

Challenge # 4 – Unidentified



Chen et al. 2011

Challenge # 5 – Spectral resolution

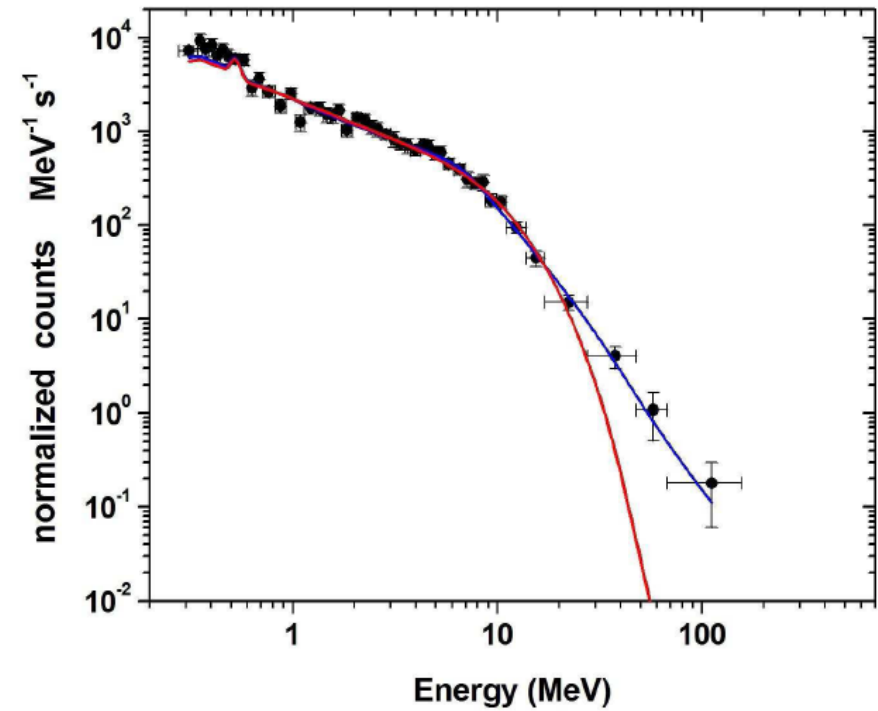
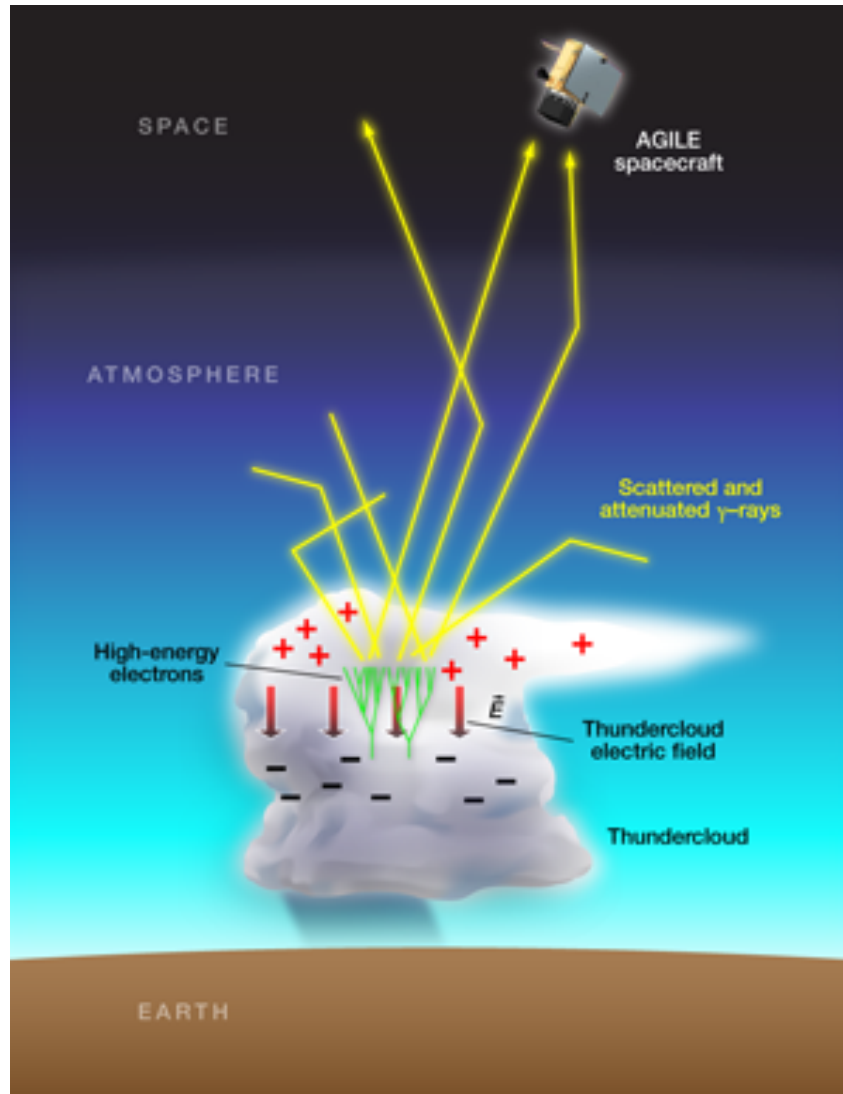


Giuliani et al. 2011

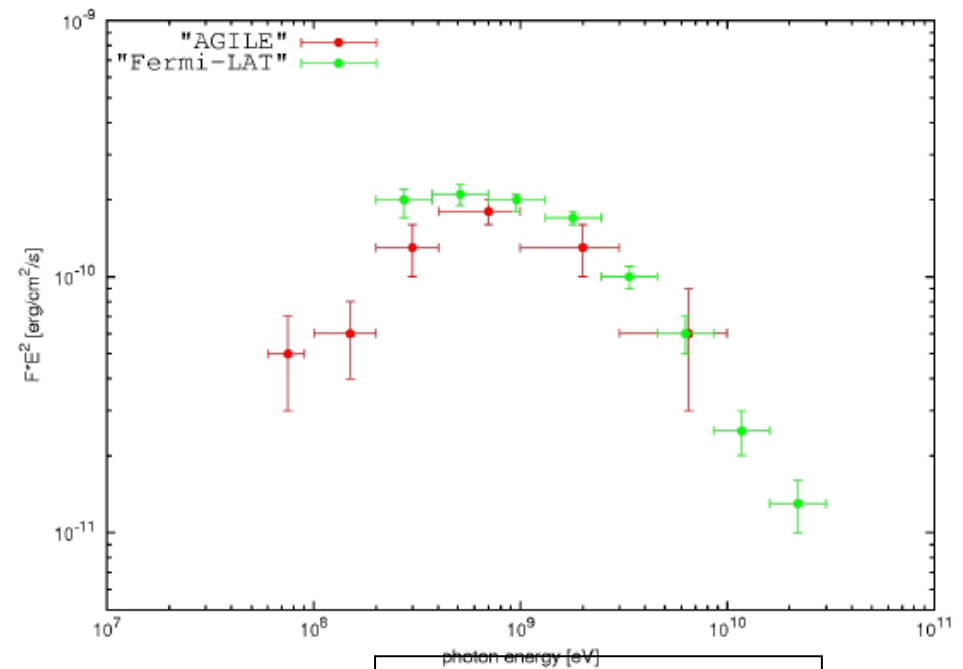
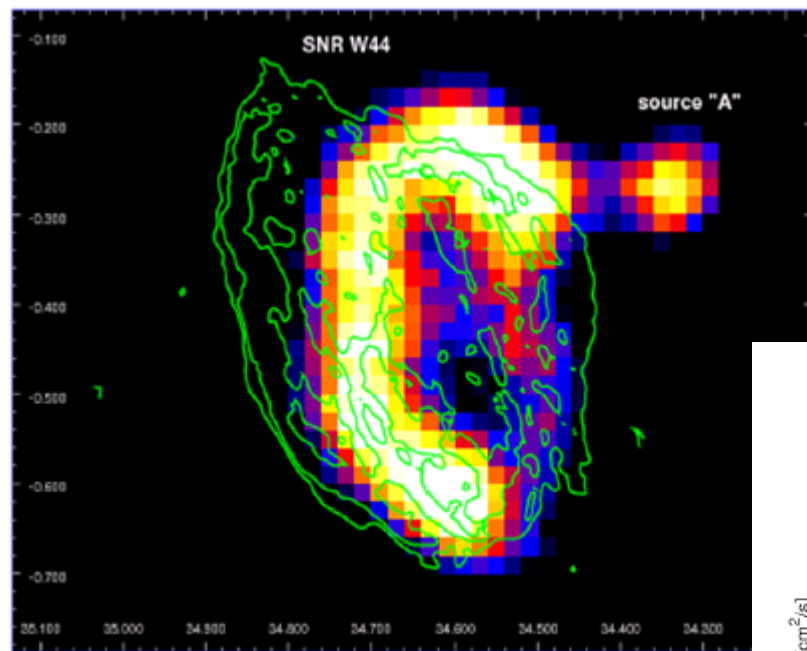
Key AGILE results

Terrestrial Gamma Ray Flashes

Marisaldi et al. 2010

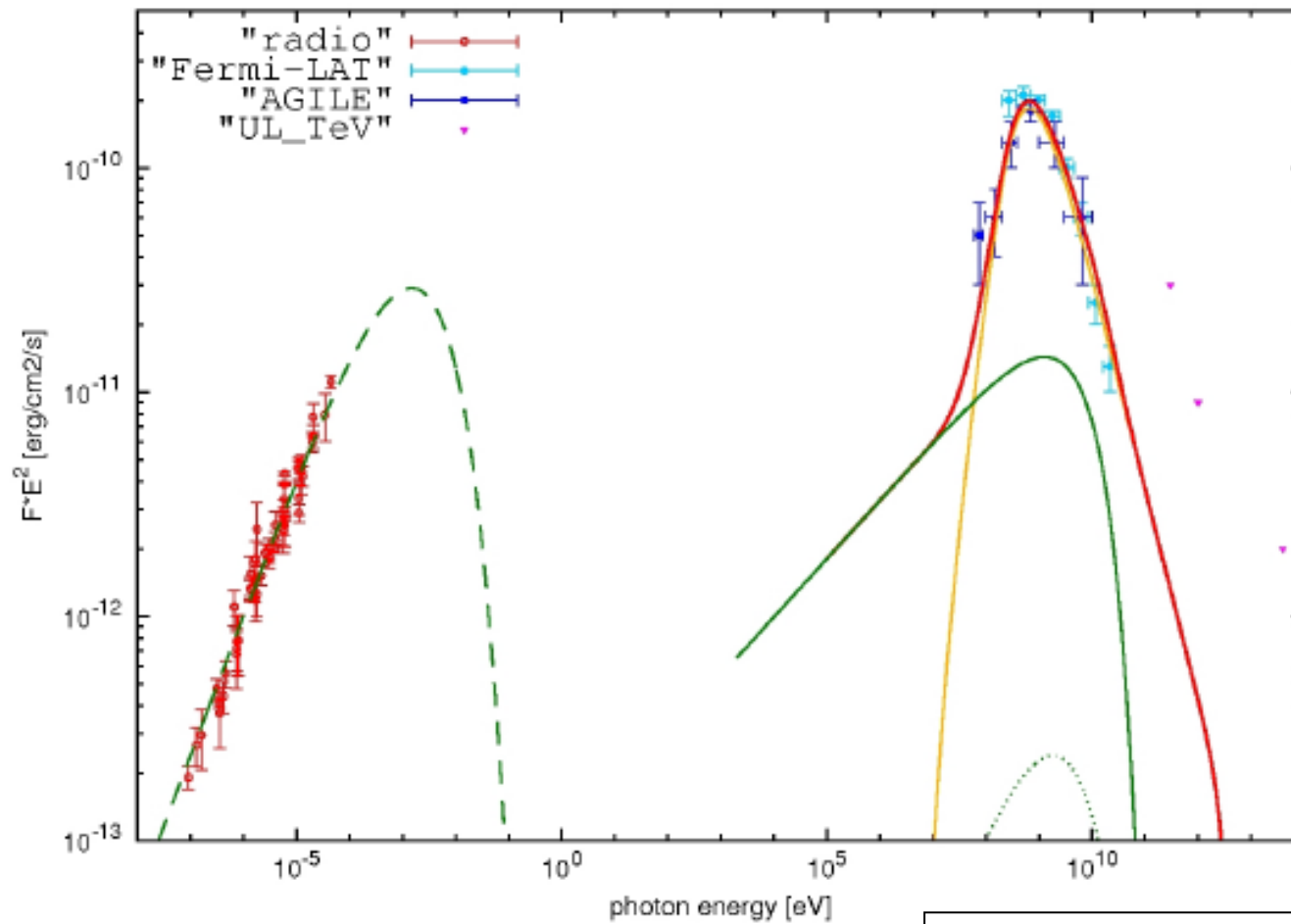


SNR W44



Giuliani et al. 2011

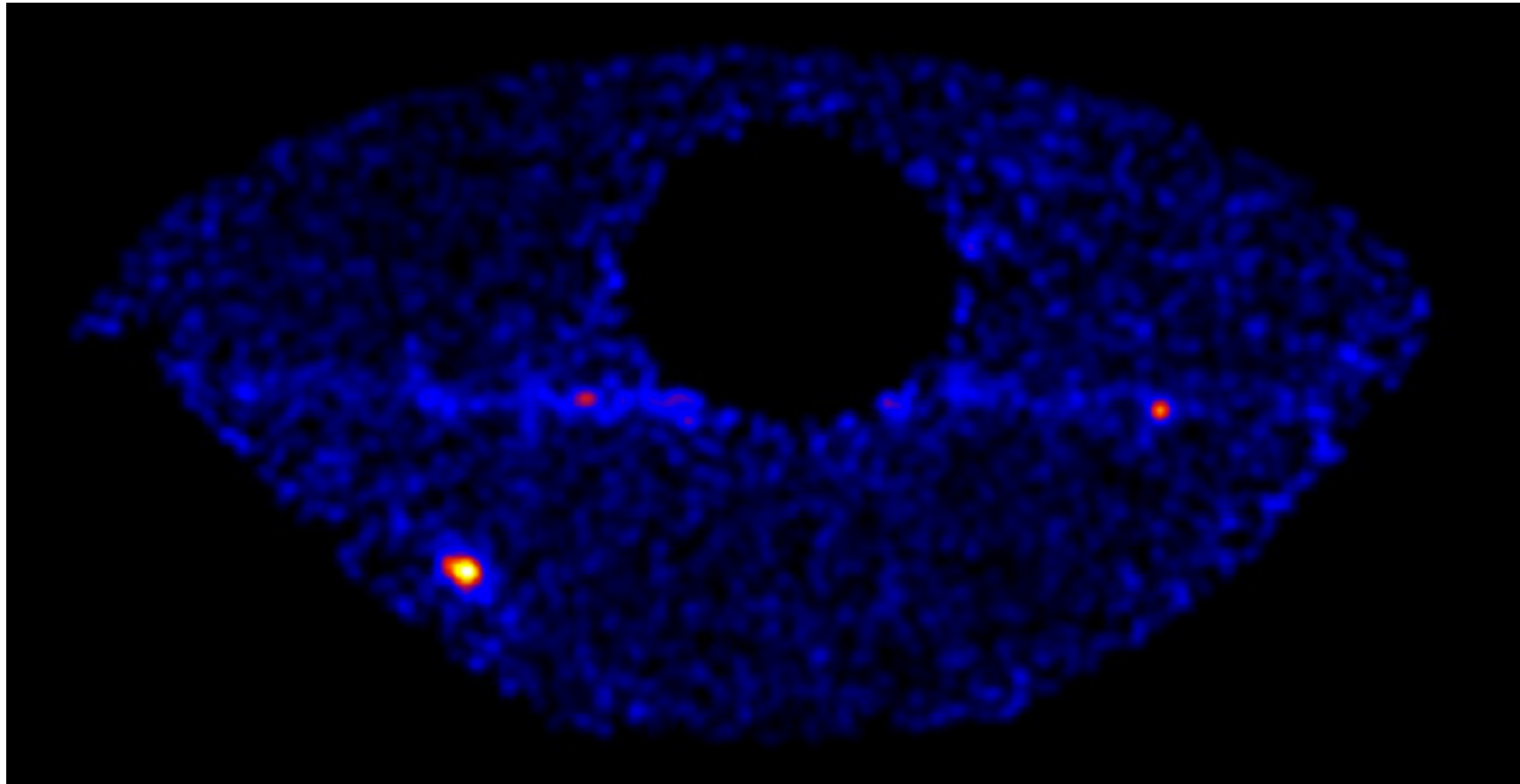
SNR W44



Giuliani et al. 2011

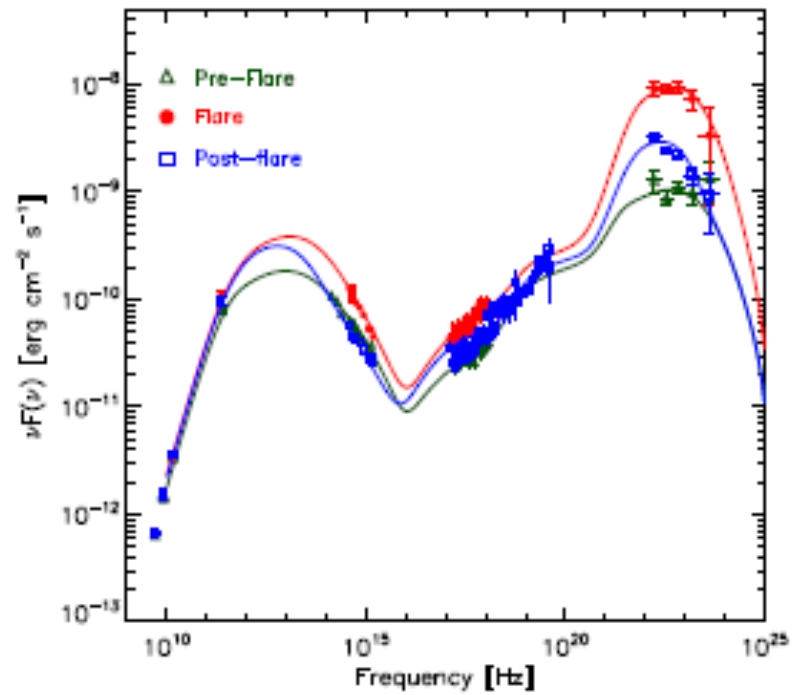
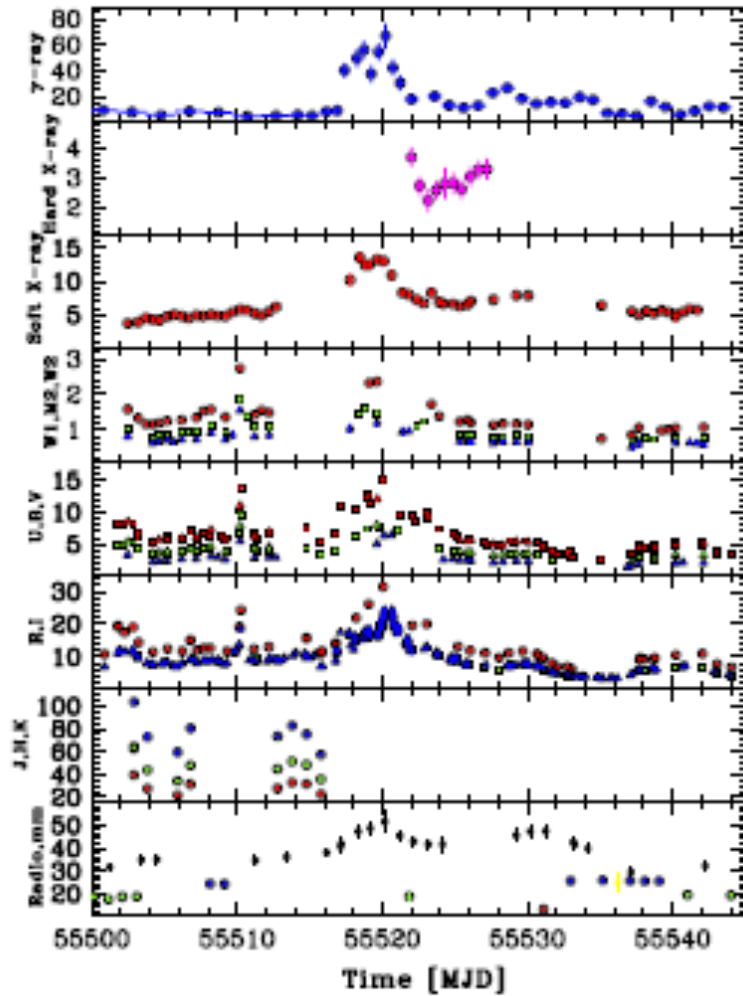
The Flaring 3C454.3

Vercellone et al. 2010

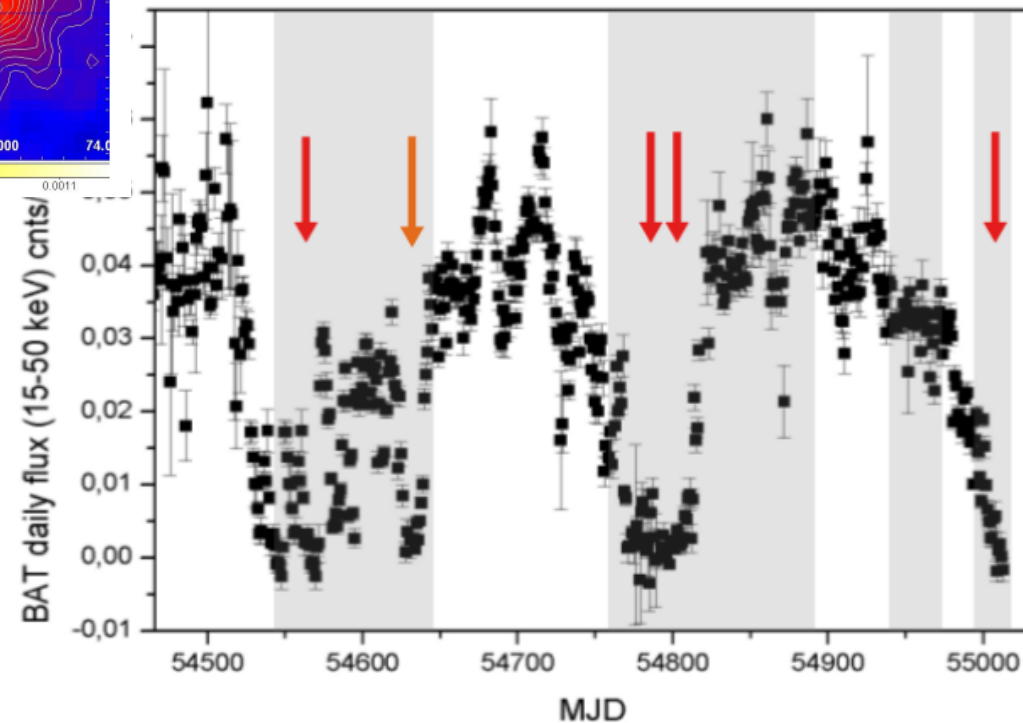
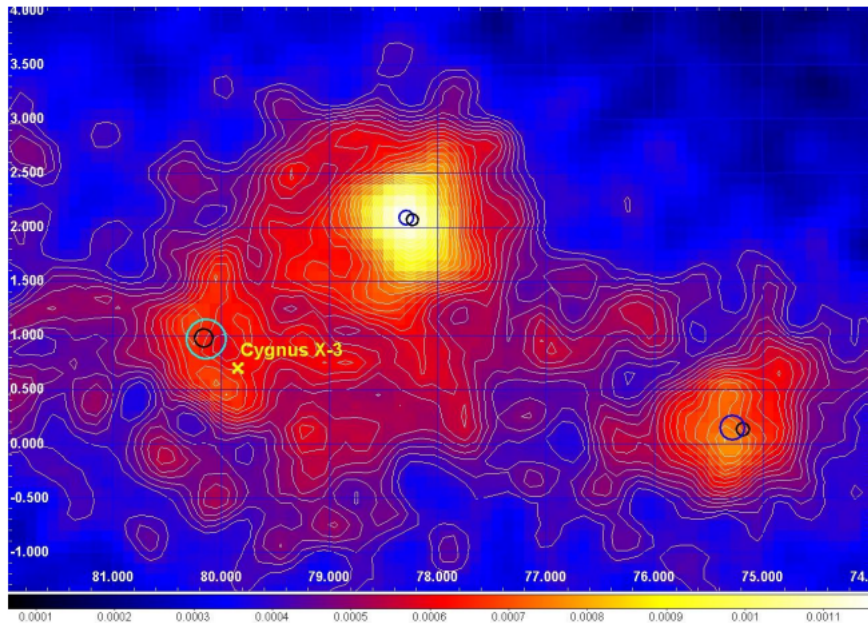


Blazar 3C454.3

Vercellone et al. 2011

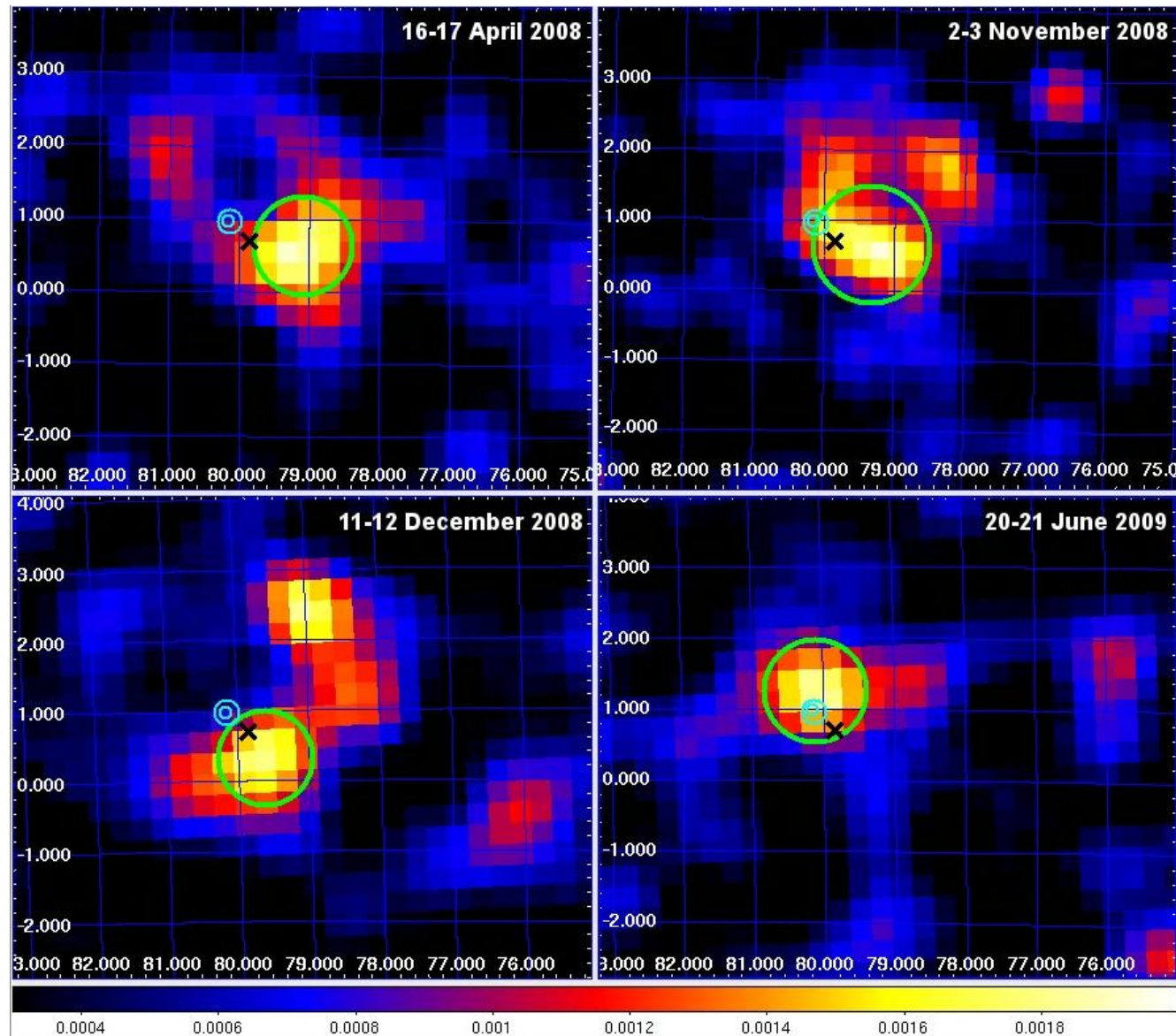


Galactic Transients: Cygnus X3



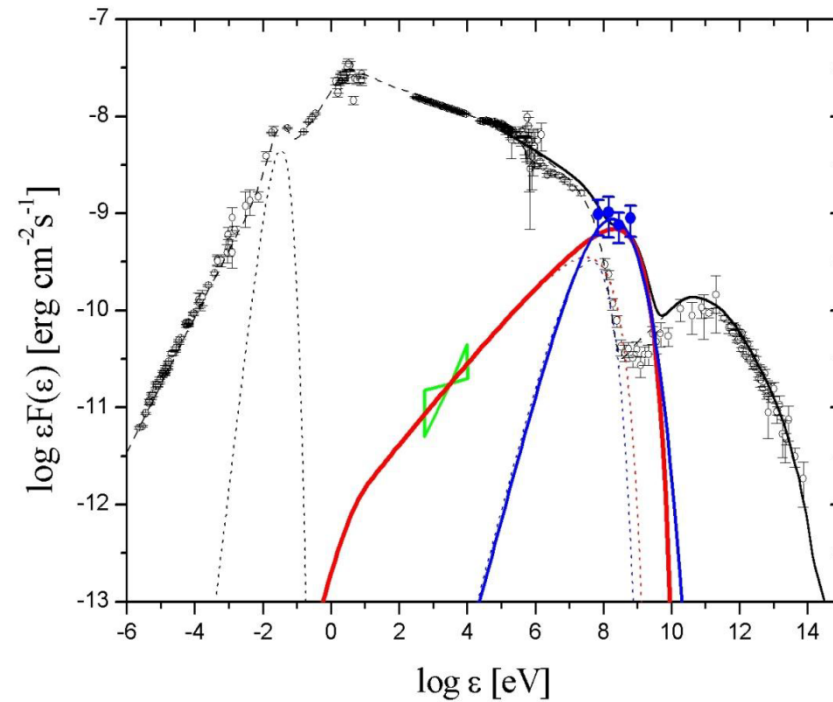
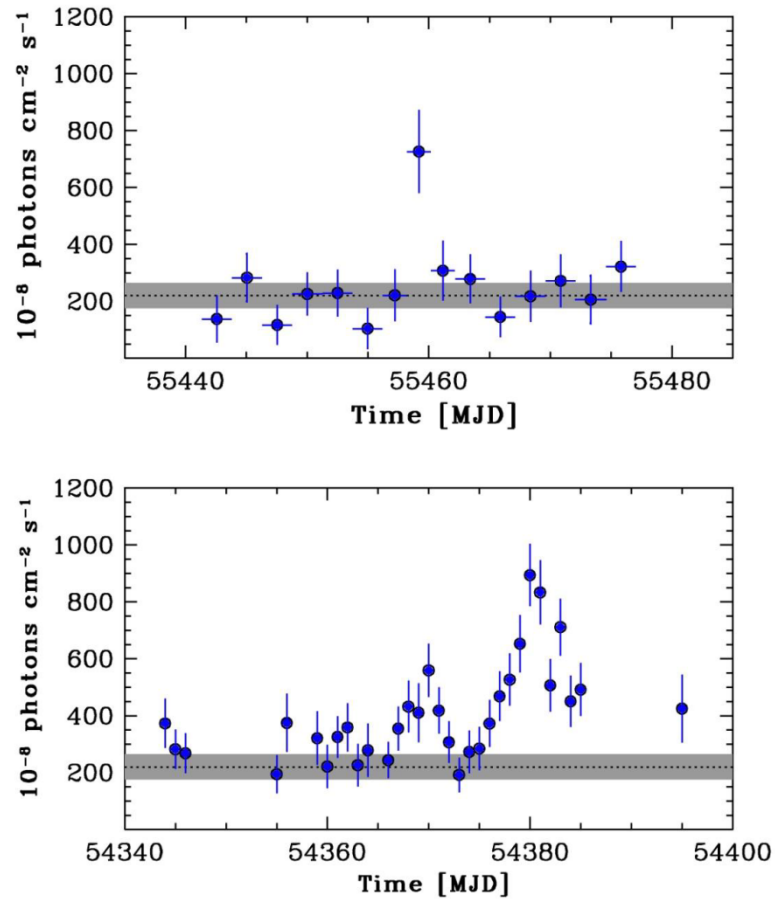
Tavani et al. 2009

AGILE discovery of transient gamma-ray emission from Cygnus X-3



Galactic Transients: The Flaring Crab

Tavani et al. 2011



The Flaring Crab

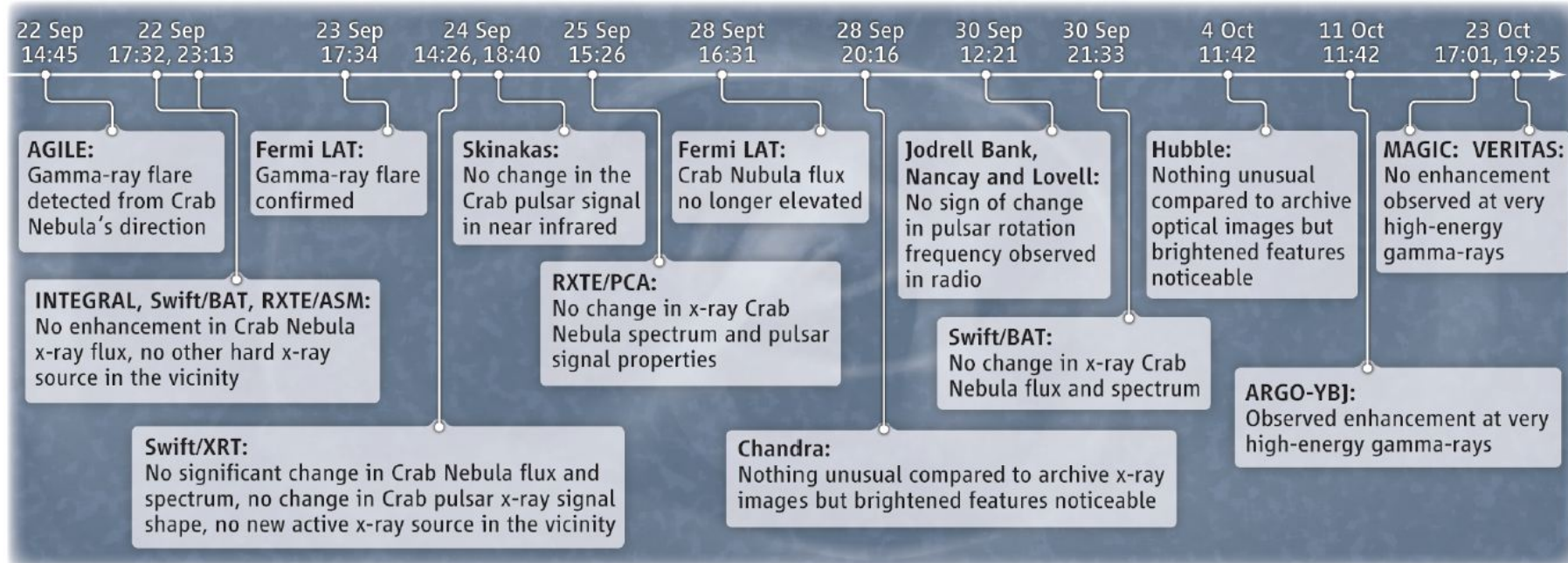
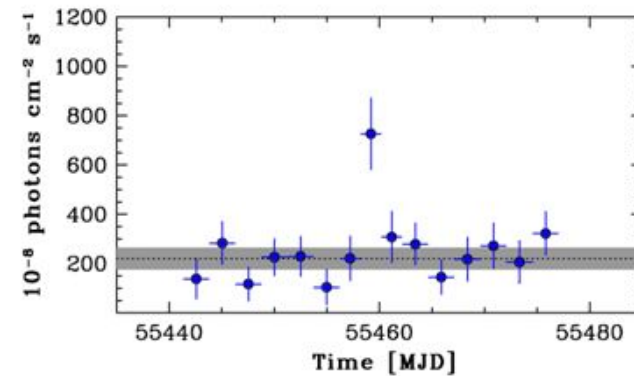
AGILE detection of enhanced gamma-ray emission from the Crab Nebula region

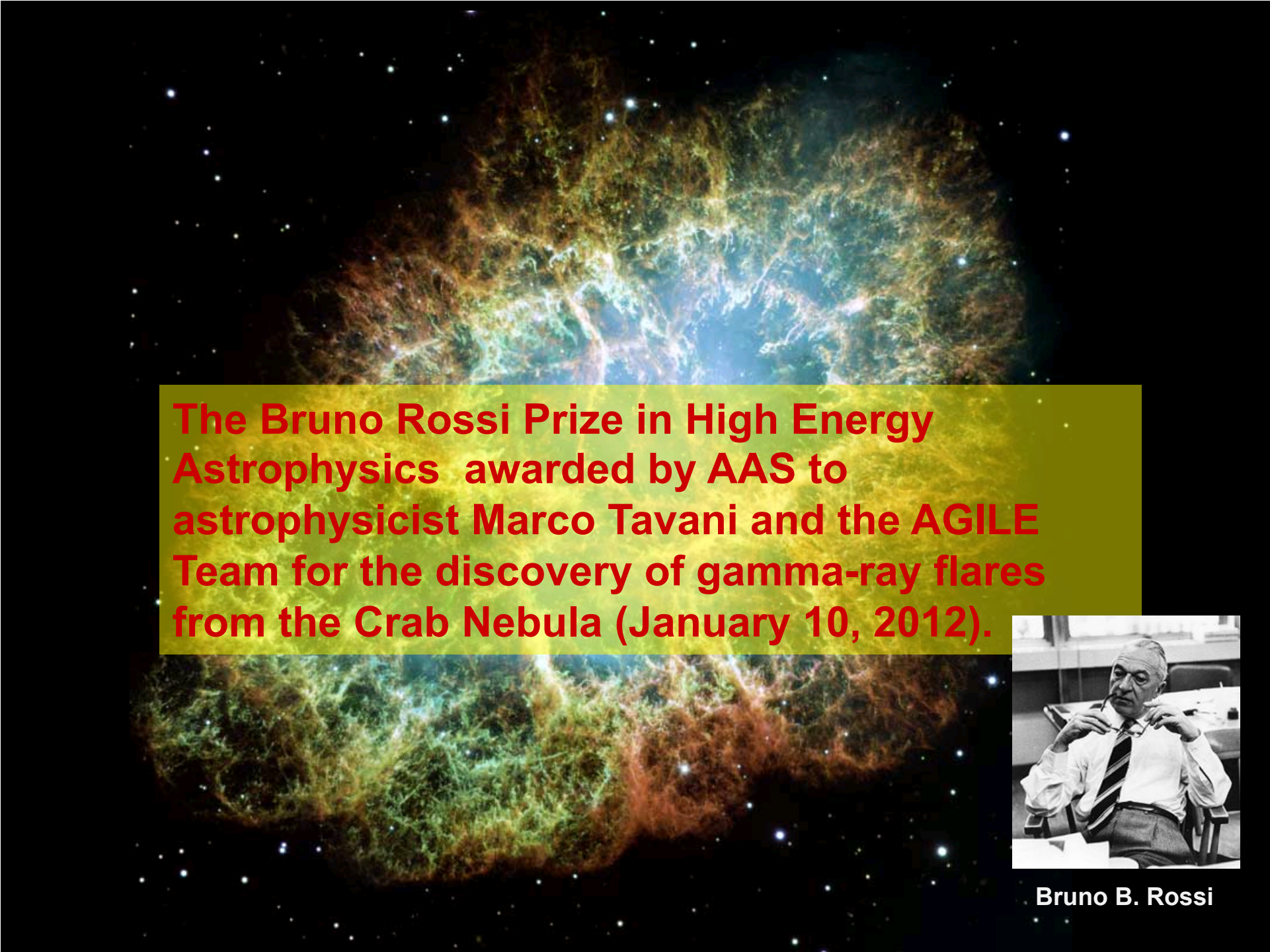
ATel #2855: *M. Tavani (INAF/IASF Roma), E. Striani (Univ. Tor Vergata), A. Bulgarelli (INAF/IASF Bologna), F. Gianotti, M. Trifoglio (INAF/IASF Bologna), C. Pittori, F. Verrecchia (ASDC), A. Argan, A. Trois, G. De Paris, V. Vittorini, F. D'Ammando, S. Sabatini, G. Piano, E. Costa, I. Donnarumma, M. Feroci, L. Pacciani, E. Del Monte, F. Lazzarotto, P. Soffitta, Y. Evangelista, I. Lapshov (INAF-IASF-Rm), A. Chen, A. Giuliani (INAF-IASF-Milano), M. Marisaldi, G. Di Cocco, C. Labanti, F. Fuschino, M. Galli (INAF/IASF Bologna), P. Caraveo, S. Mereghetti, F. Perotti (INAF/IASF Milano), G. Pucella, M. Rapisarda (ENEA-Roma), S. Vercellone (IASF-Pa), A. Pellizzoni, M. Pilia (INAF/OA-Cagliari), G. Barbiellini, F. Longo (INFN Trieste), P. Picozza, A. Morselli (INFN and Univ. Tor Vergata), M. Prest (Universita' dell'Insubria), P. Lipari, D. Zanella (INFN Roma-1), P.W. Cattaneo, A. Rappoldi (INFN Pavia), P. Giommi, P. Santolamazza, F. Lucarelli, S. Colafrancesco (ASDC), L. Salotti (ASI)*

on 22 Sep 2010; 14:45 UT

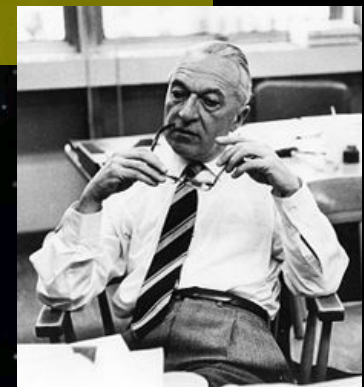
Distributed as an Instant Email Notice (Transients)

Password Certification: Marco Tavani (tavani@iasf-roma.inaf.it)



The background of the slide is a large, detailed image of the Crab Nebula, showing its intricate filamentary structure in shades of green, blue, and orange against a dark starry sky. A semi-transparent yellow-green rectangular box is overlaid on the center of the image, containing red text.

The Bruno Rossi Prize in High Energy Astrophysics awarded by AAS to astrophysicist Marco Tavani and the AGILE Team for the discovery of gamma-ray flares from the Crab Nebula (January 10, 2012).



Bruno B. Rossi

Where to find data?



Welcome to the AGILE Data Center Home Page at SSCD

These pages provide updated information and services in support to the general scientific community for the mission AGILE, which is a small Scientific Mission of the Italian Space Agency (ASI) with participation of INFN, IASF/INAF and CIFS .

AGILE is devoted to gamma-ray astrophysics and it is a first and unique combination of a gamma-ray (AGILE-GRID) and a hard X-ray (SuperAGILE) instrument, for the simultaneous detection and imaging of photons in the 30 MeV - 50 GeV and in the 18 - 60 keV energy ranges. AGILE has been operating nominally for more than 16 years, providing valuable data and important scientific results.

AGILE operations:

Launch date: 23 April, 2007 - Re-entry date: 14 February, 2024
Science observations ended on 18 January, 2024
Planned Nominal Phase: 2 + 2 extended years
Elapsed: 16 years and 10 months in orbit (6.141 days)

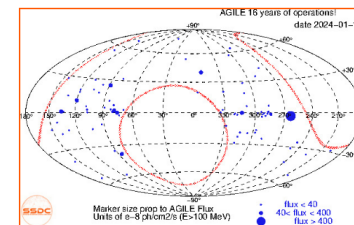
The AGILE Mission Board (AMB) has executive power overseeing all the scientific matters of the AGILE Mission and is composed of:

- AGILE Principal Investigator: Marco Tavani, INAF Rome (Chair)
- ASI Project Scientist: Paolo Giommi, ASI
- ASI Mission Director: Giovanni Valentini, ASI
(Former ASI Mission Directors: Luca Salotti: Apr 2007 - Sep 2010, Giovanni Valentini: Sep 2010 - Jan 2015, Fabio D'Amico: Jan 2015 - Jun 2023)
- AGILE Co-Principal Investigator: Guido Barbiellini, INFN Trieste
- 1 ASI representative: Elisabetta Tommasi di Vignano
(Former ASI representative: Sergio Colafrancesco up to June, 2010)
- INAF Project Scientist: Carlotta Pittori (from November 10, 2020)



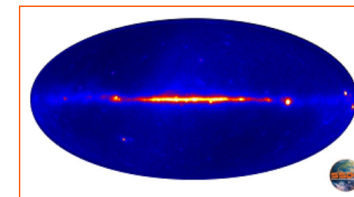
AGILE spinning sky view

[\(Click here for previous pointing details\)](#)



[Click here to access the AGILE Spinning FOV plotter](#)

[Click here to access the AGILE Real Data FOV Plotter](#)



AGILE total intensity map up to Sep. 30, 2017.

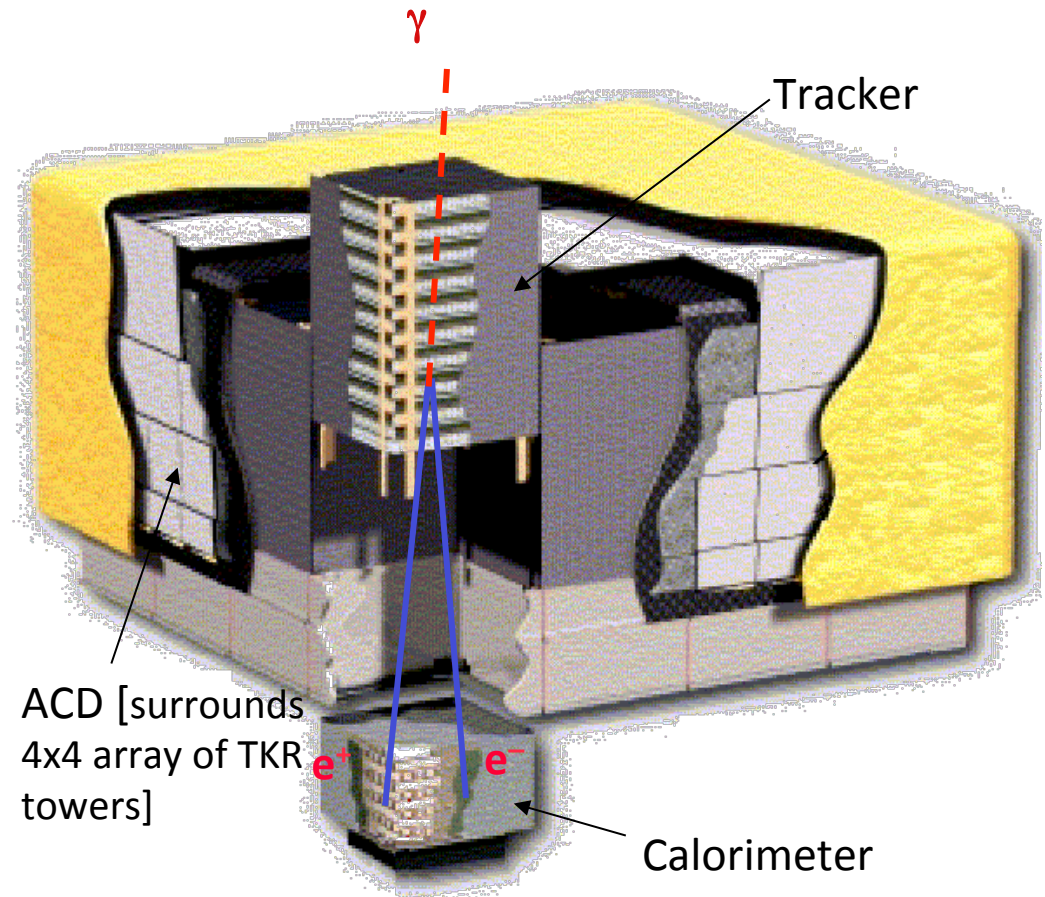
Conclusions

- AGILE crucial contributions to testing particle acceleration theories, plasma instabilities in the Universe and on the Earth !
 - Big surprise: discovery of gamma-ray flares from the Crab Nebula: 2012 Bruno Rossi Prize
 - Origin of cosmic rays, SNR W44, first direct evidence of neutral pion emission
 - Relativistic jets in microquasars and blazars
 - Gamma-ray emission up to 100 MeV from Terrestrial Gamma-Ray Flashes

Fermi LAT

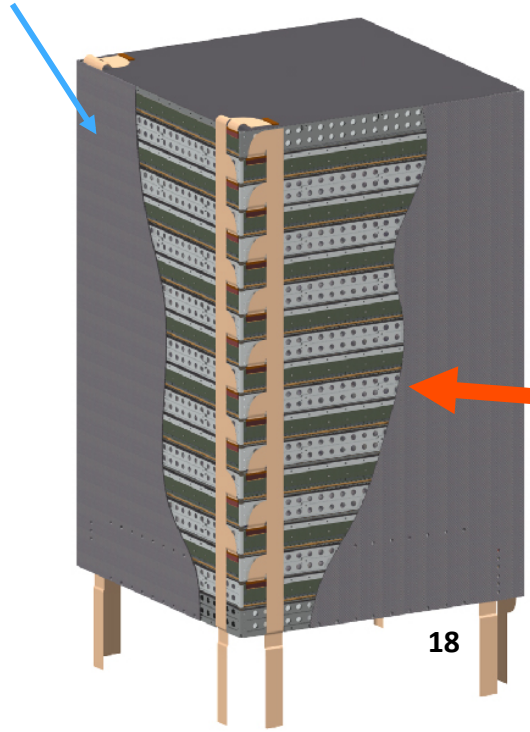
Overview of LAT

- Precision Si-strip Tracker (TKR) 18 XY tracking planes. Single-sided silicon strip detectors (228 μm pitch) Measure the photon direction; gamma ID.
- Hodoscopic Csl Calorimeter(CAL) Array of 1536 Csl(Tl) crystals in 8 layers. Measure the photon energy; image the shower.
- Segmented Anticoincidence Detector (ACD) 89 plastic scintillator tiles. Reject background of charged cosmic rays; segmentation removes self-veto effects at high energy.
- Electronics System Includes flexible, robust hardware trigger and software filters.



Systems work together to identify and measure the flux of cosmic gamma rays with energy 20 MeV - >300 GeV.

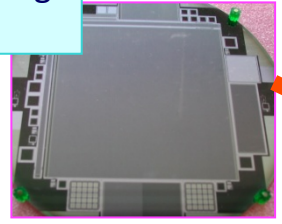
Tower Structure



Cable Plant UCSC

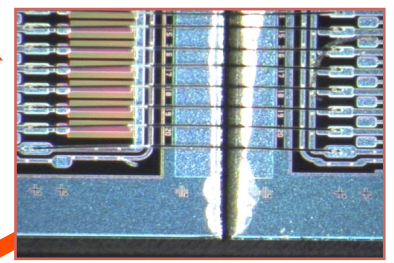
18

SSD Procurement, Testing
Japan, Italy, SLAC



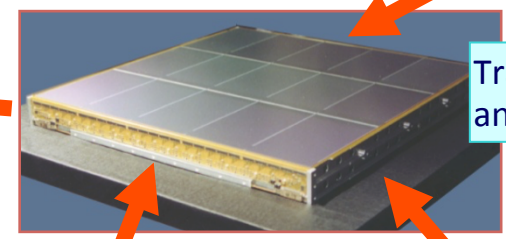
10,368

SSD Ladder Assembly



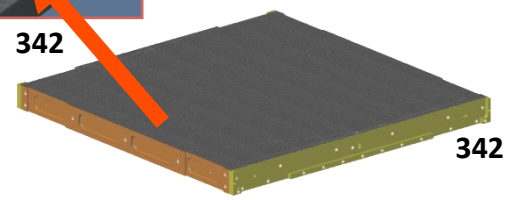
2592

Tower Assembly and Test



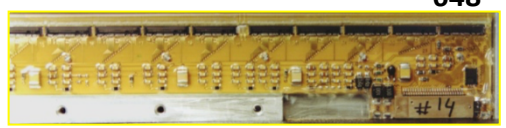
Tray Assembly and Test

342



342

Electronics



648

Composite Panel & Converters

Launch!

- Launch from Cape Canaveral Air Station
11 June 2008 at
12:05PM EDT
- Circular orbit, 565 km altitude (96 min period), 25.6 deg inclination.

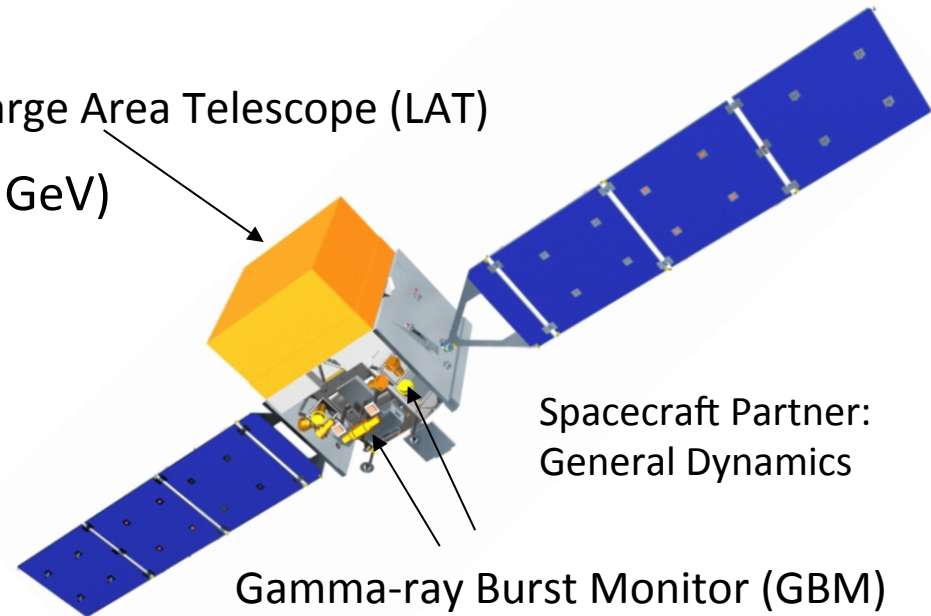


Key Features

- Two instruments:

- LAT:
 - high energy (20 MeV – >300 GeV)
- GBM:
 - low energy (8 keV – 40 MeV)

Large Area Telescope (LAT)



Spacecraft Partner:
General Dynamics

Gamma-ray Burst Monitor (GBM)

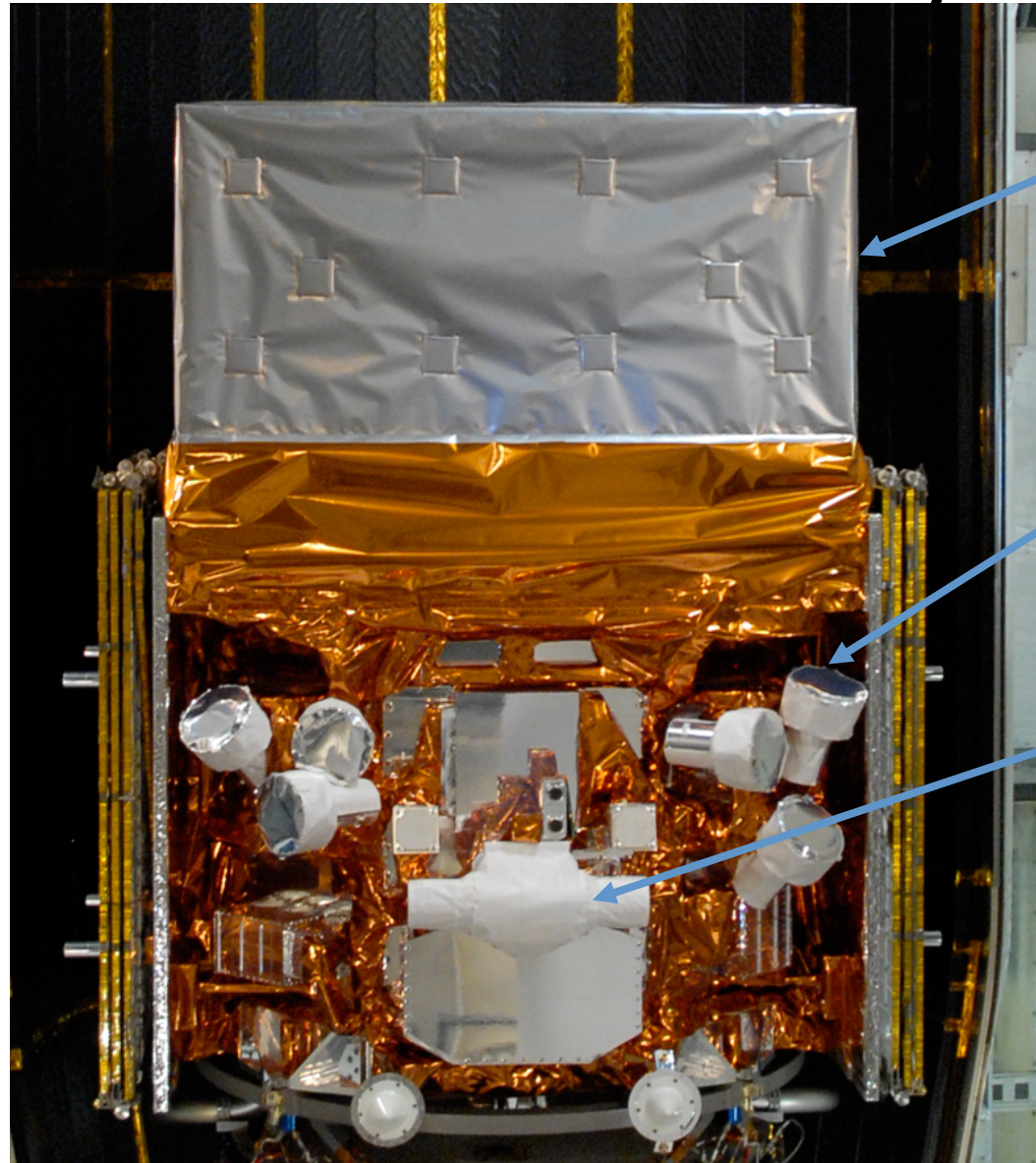
- Huge field of view

- LAT: 20% of the sky at any instant; in sky survey mode, expose all parts of sky for ~30 minutes every 3 hours. GBM: whole unocculted sky at any time.

- Huge energy range, including largely unexplored band 10 GeV - 100 GeV

- Large leap in all key capabilities. Great discovery potential.

The Observatory

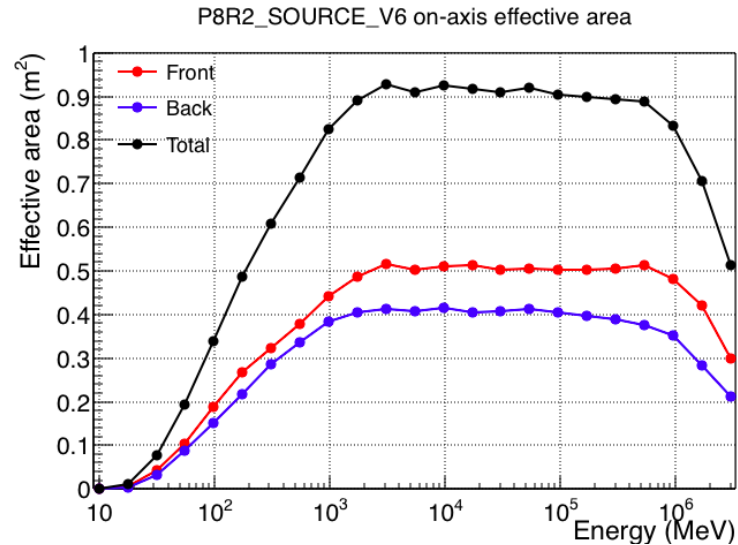


LAT

GBM
NaI
Detector

GBM
BGO
Detector

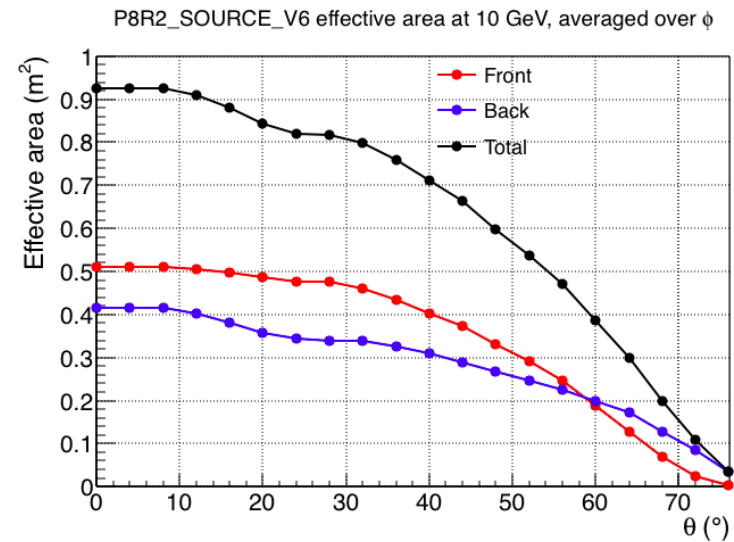
Effective Area (A_{eff})



< 100 MeV limited by 3-in a row requirement

< 1 GeV limited discriminating information

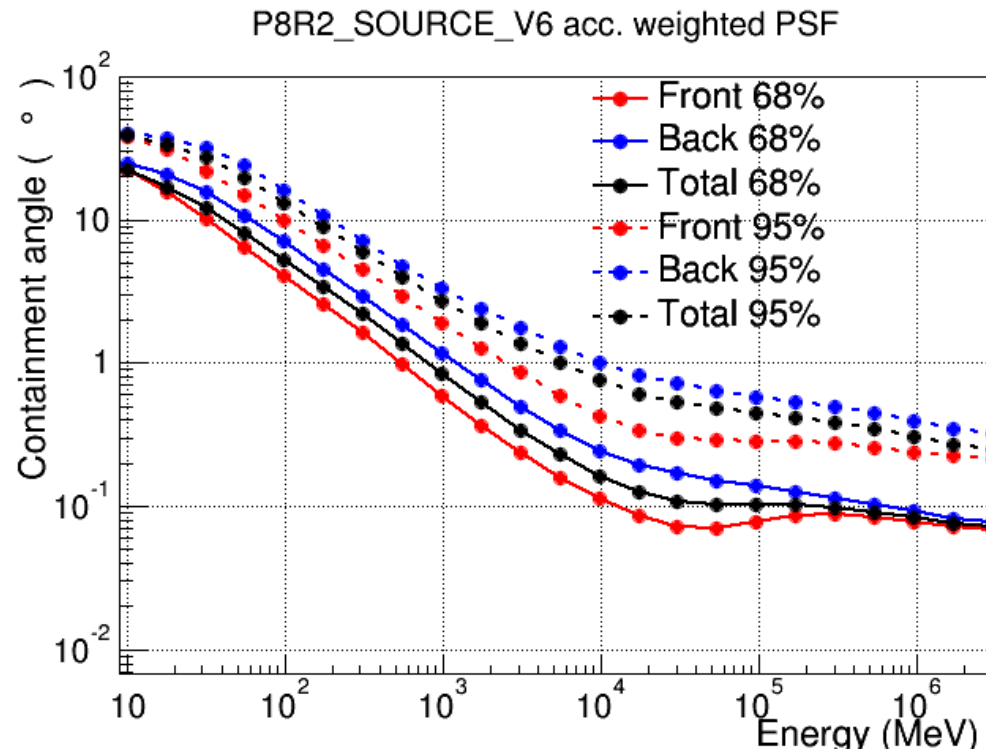
> 100 GeV self-veto from backslash



Off-axis: more material, less cross section

Shift from front/back events as we go off-axis

Point Spread Function (P)

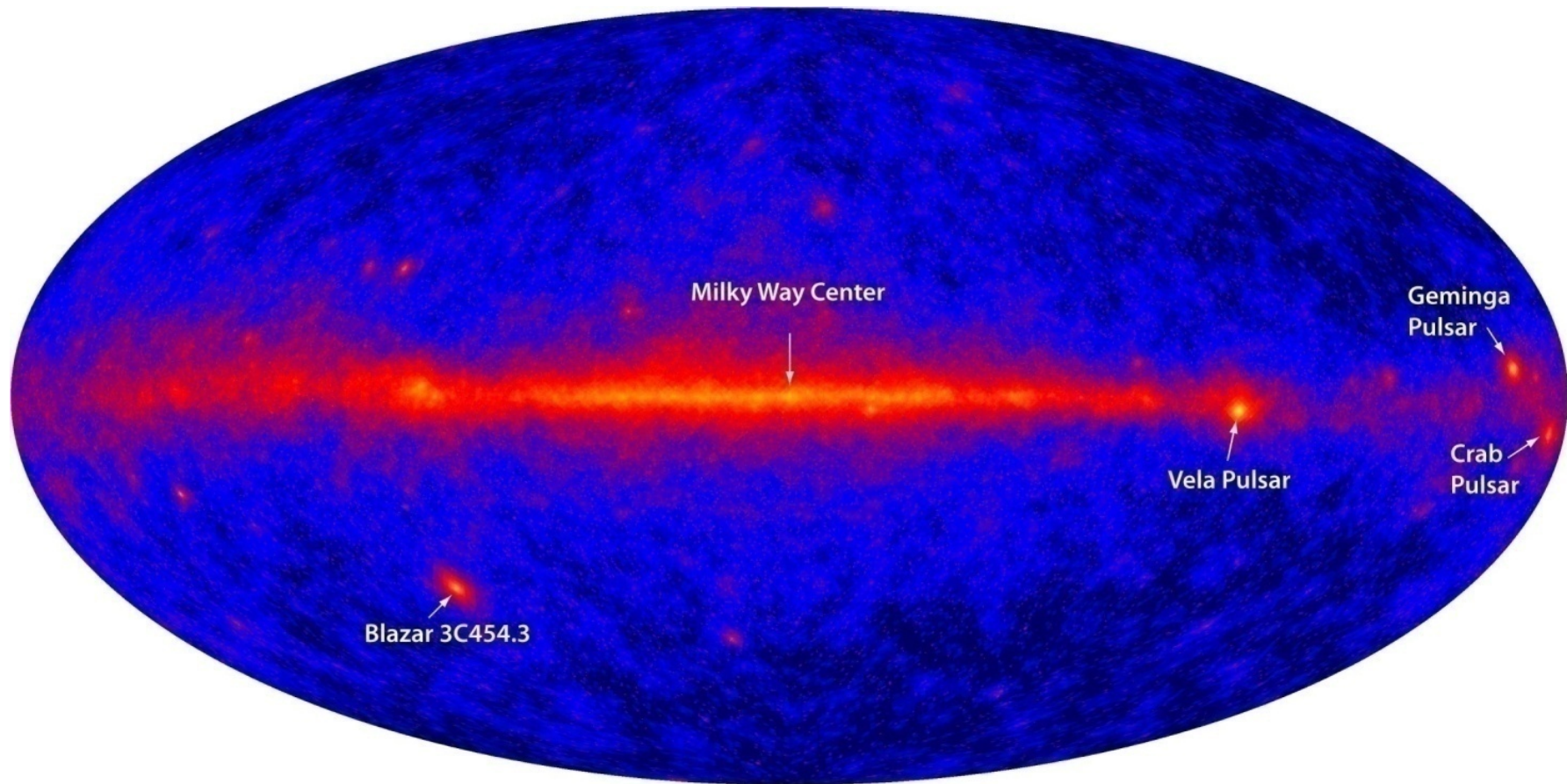


Low energy: dominated by MS

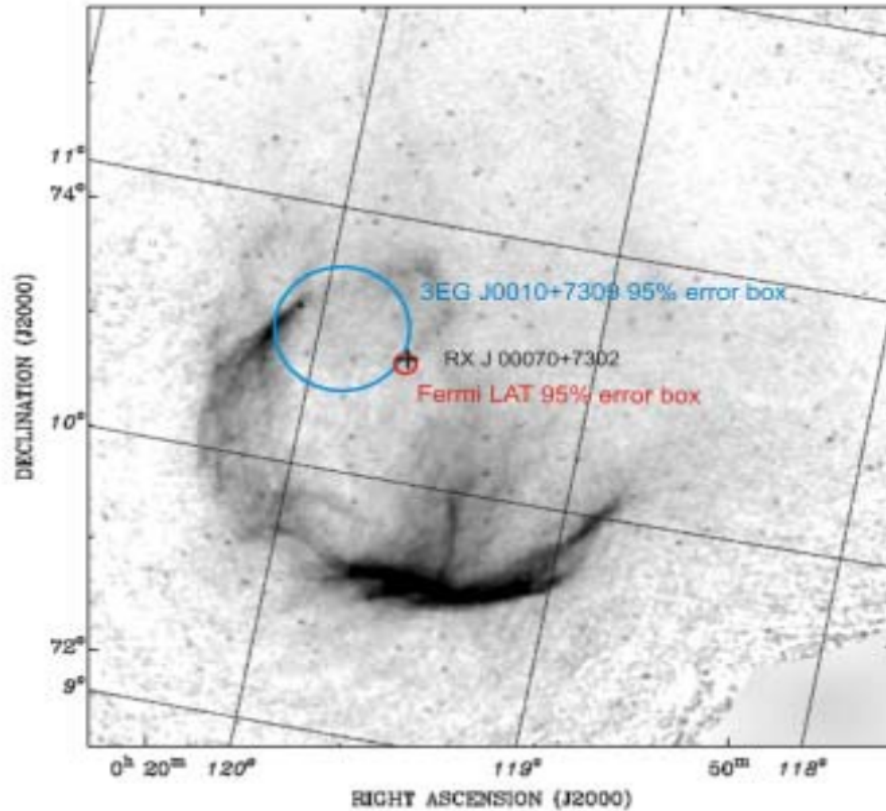
High energy: dominated by strip pitch

http://www.slac.stanford.edu/exp/glast/groups/canda/lat_Performance.htm

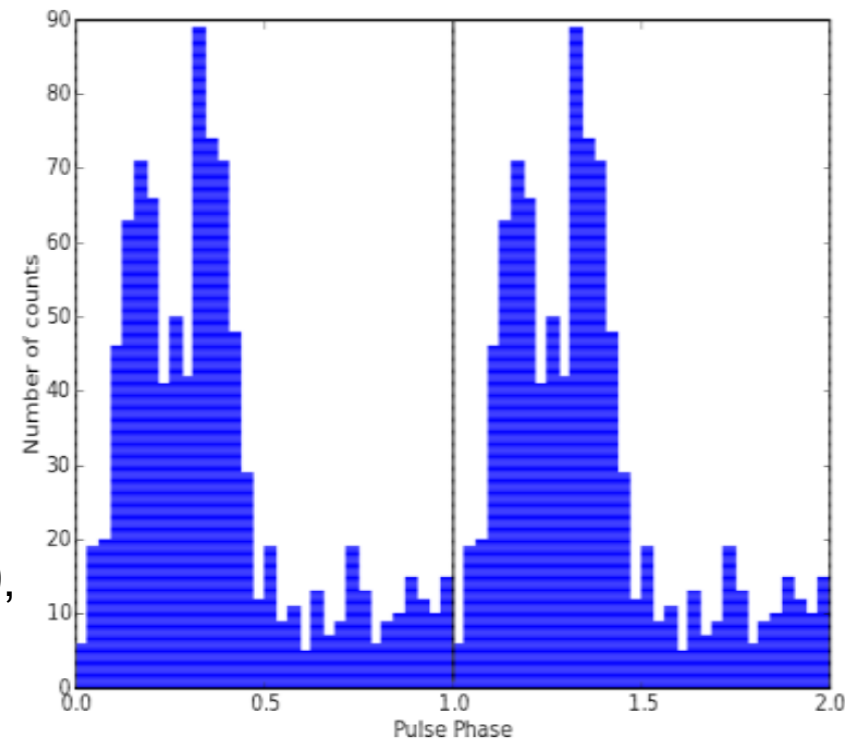
LAT first light



LAT discovers a radio-quiet pulsar!



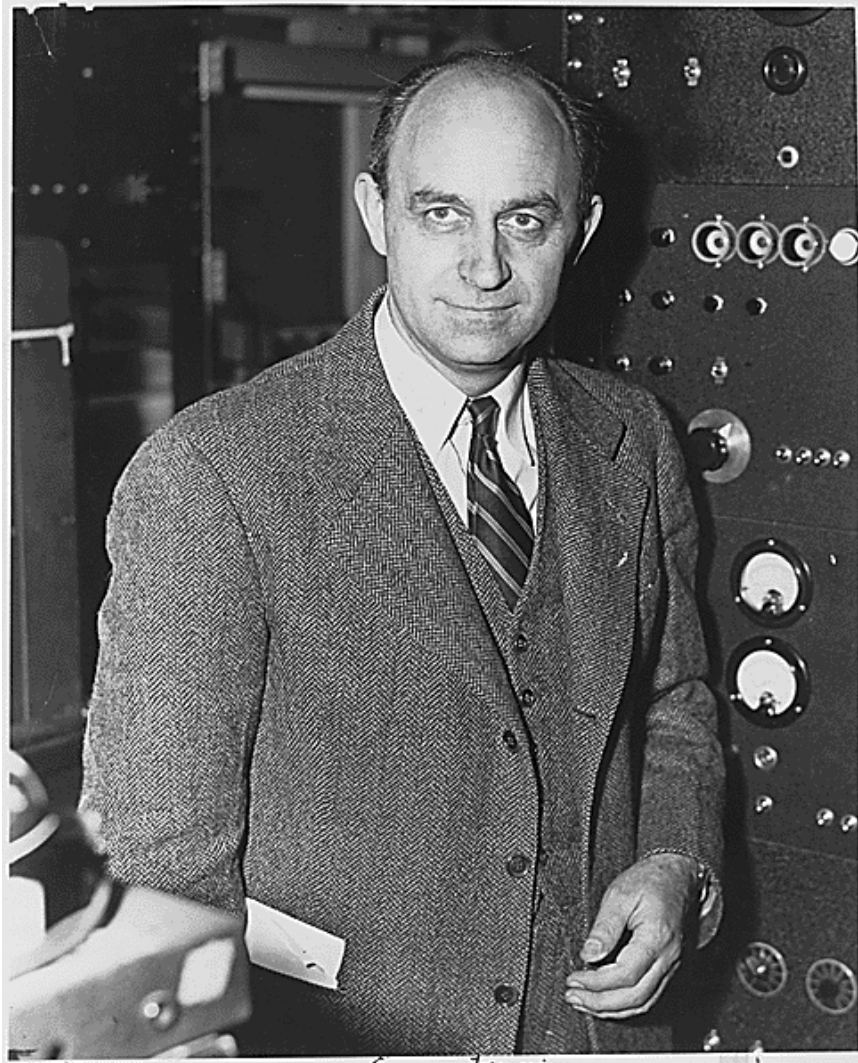
$P \sim 317$ ms
 $\dot{P} \sim 3.6E-13$
Characteristic age $\sim 10,000$ yrs



Location of EGRET source 3EG J0010+7309,
the Fermi-LAT source, and the central X-ray
source RX J0007.0+7303

Published in Science Express October 16, 2008

Fermi Gamma-ray Space Telescope

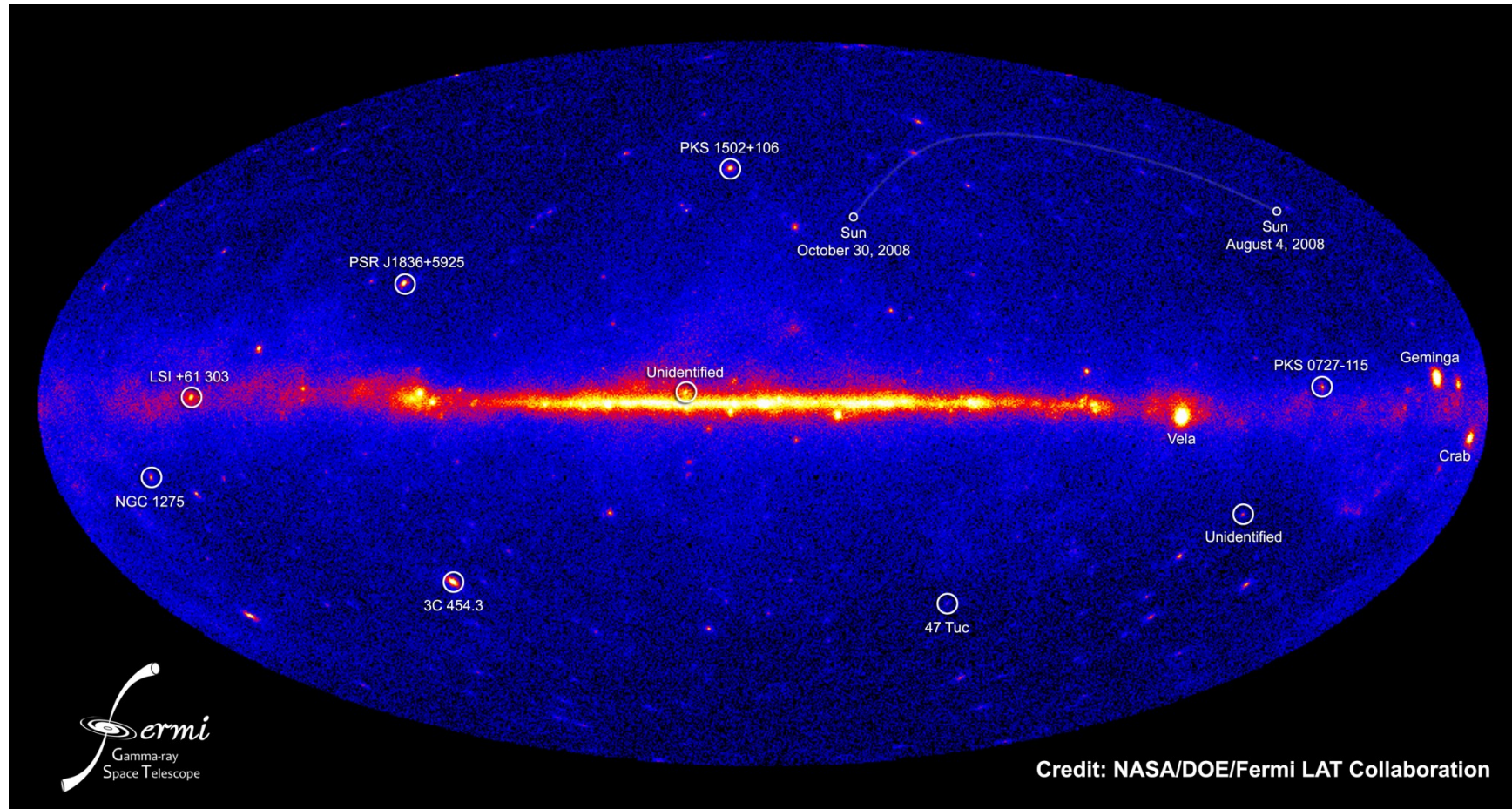


GLAST renamed *Fermi* by NASA on August 26, 2008

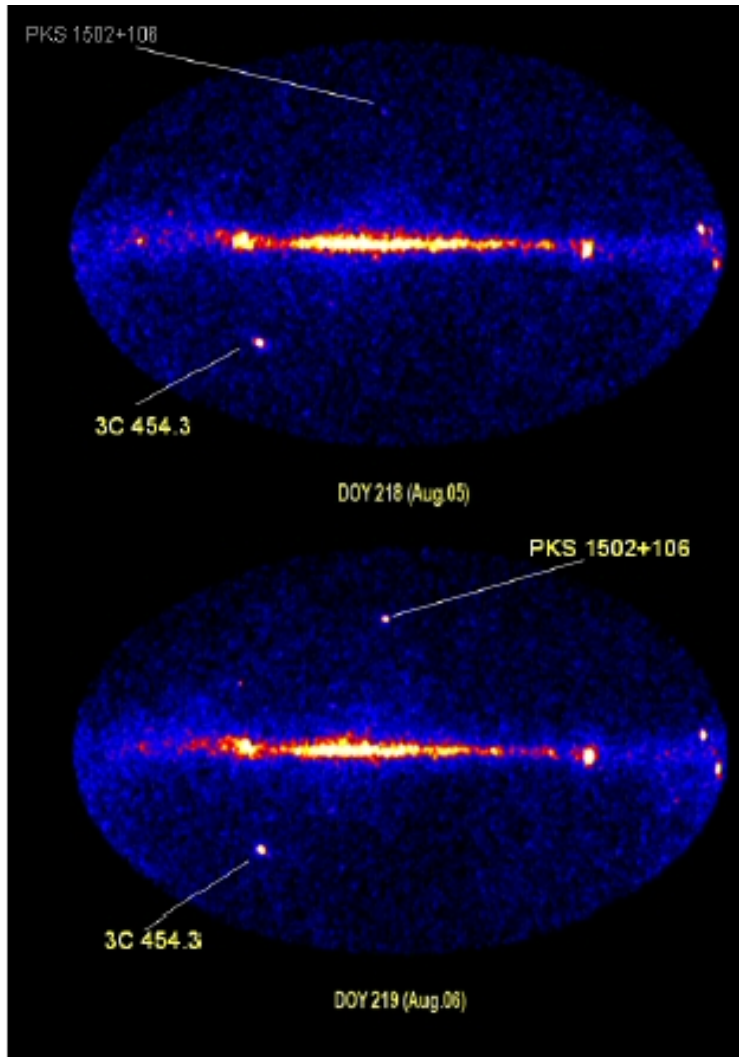
<http://fermi.gsfc.nasa.gov/>

“ Enrico Fermi (1901-1954) was an Italian physicist who immigrated to the United States. He was the first to suggest a viable mechanism for astrophysical particle acceleration. This work is the foundation for our understanding of many types of sources to be studied by NASA’s Fermi Gamma-ray Space Telescope, formerly known as GLAST. ”

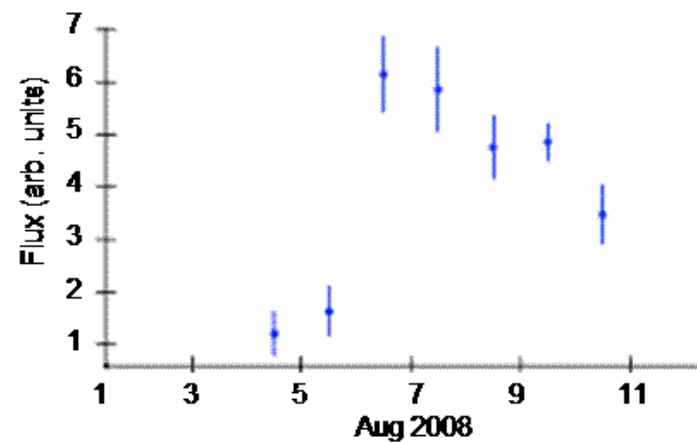
Fermi LAT 3 months sky



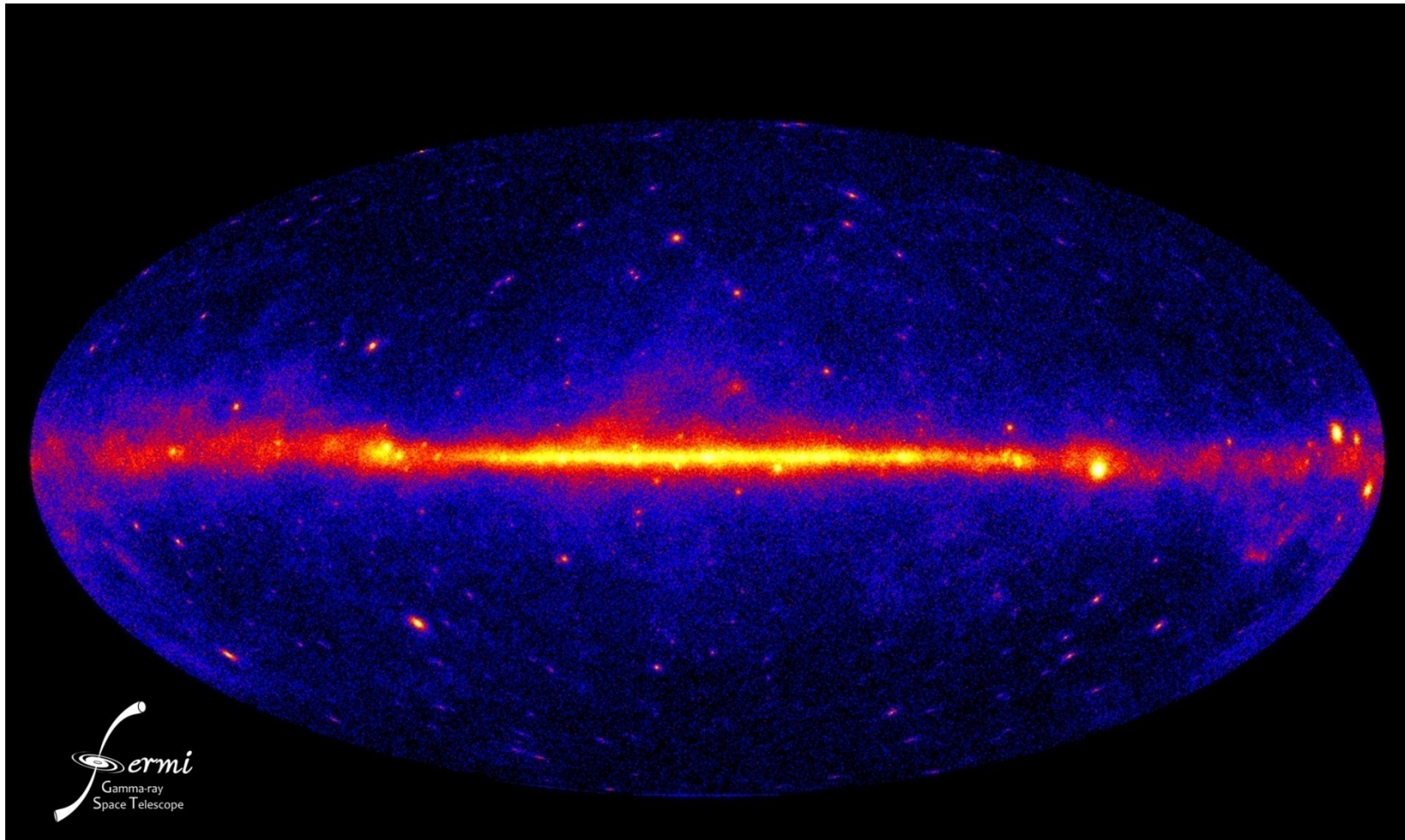
PKS 1502-106 and 3C454.3



- The sky is dynamic, Fermi is monitoring the sky, catching flaring sources over different time scales.
- Atel #1628 (3C454.3) and #1650 (PKS 1502-106) issued to announce these flares.



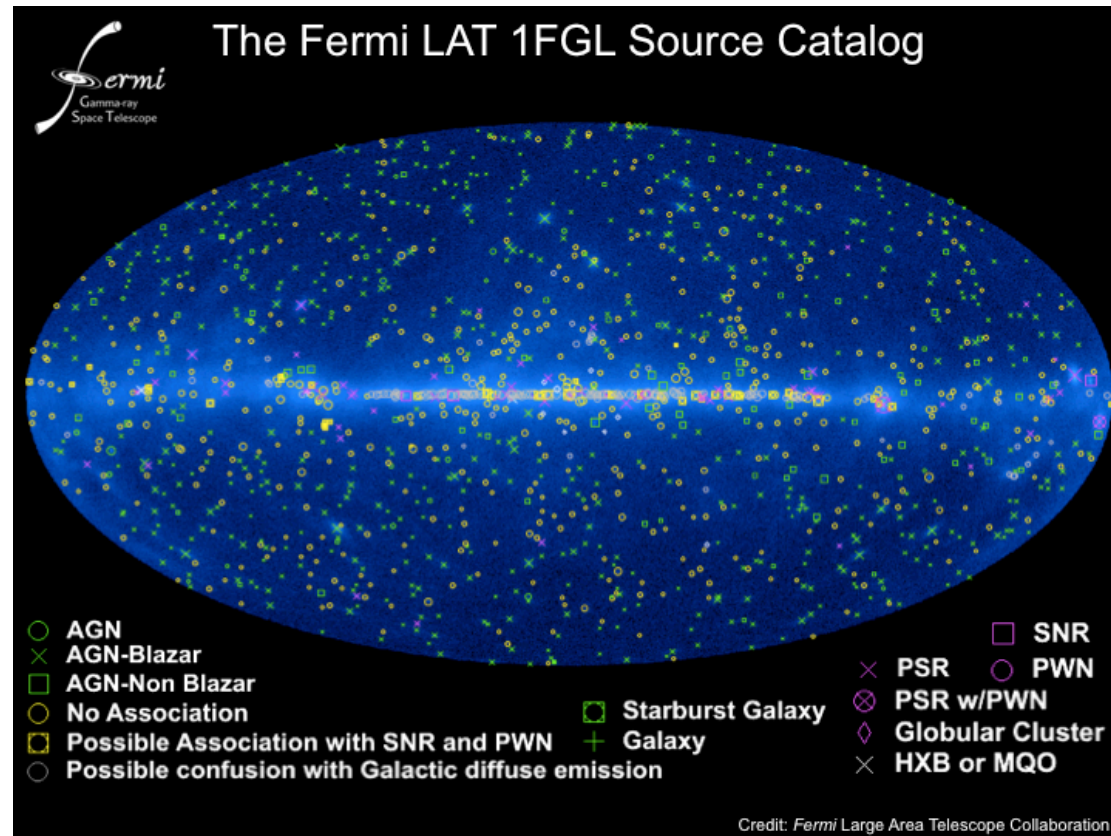
Fermi 1 yr sky



Fermi Year One Catalog

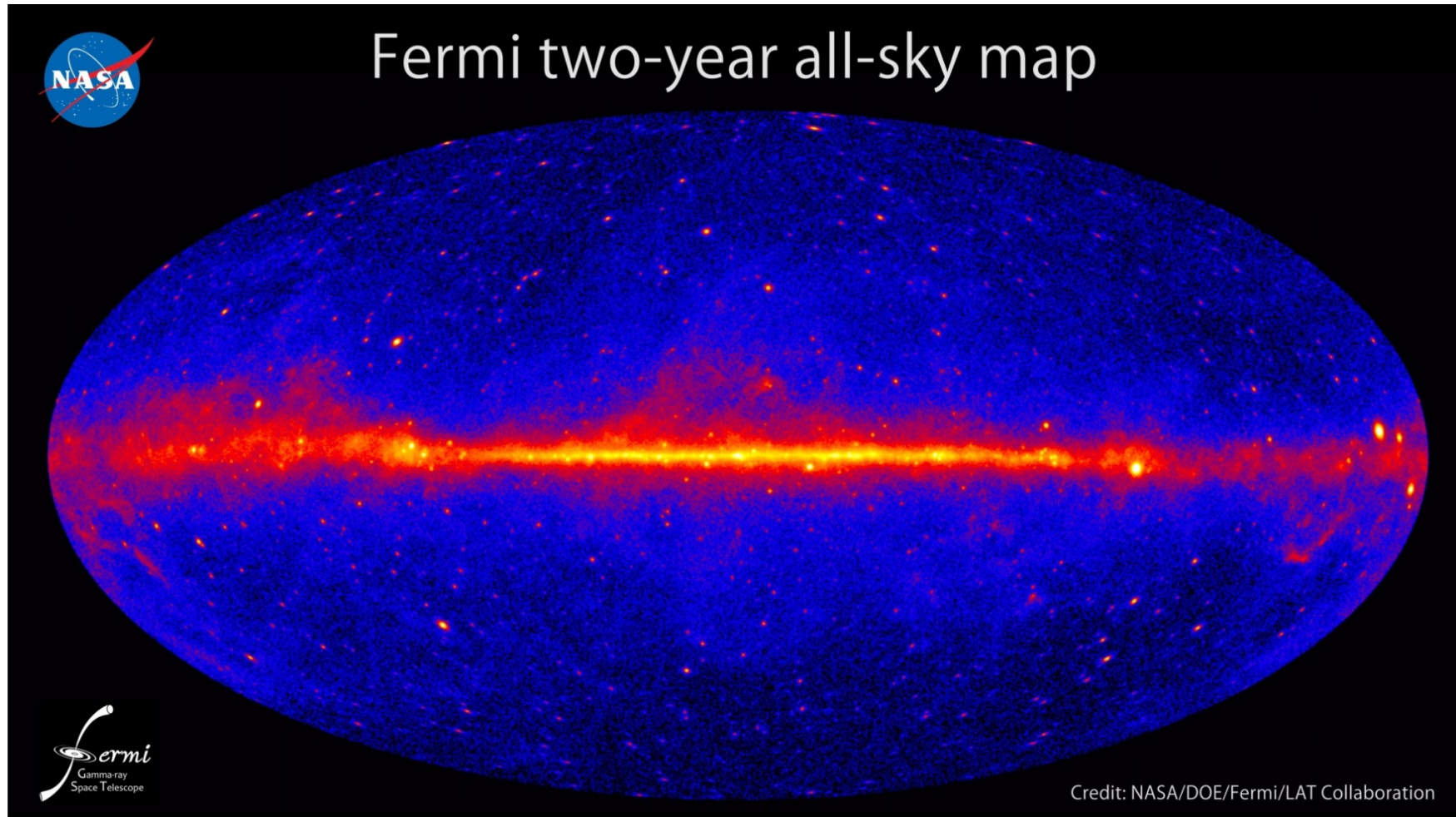
http://fermi.gsfc.nasa.gov/ssc/data/access/lat/1yr_catalog/

More than 1000 sources in year one catalog !



- About 250 sources show evidence of variability
- Half the sources are associated positionally, mostly blazars and PSRs
- Other classes of sources exist in small numbers (XRB, PWN, SNR, starbursts, globular clusters, radio galaxies, narrow-line Seyferts)
- Uncertainties due to the diffuse model, particularly in the Galactic ridge

2 year sky



2FGL Catalog

1,873 sources

○ AGN ⊗ AGN-Blazar

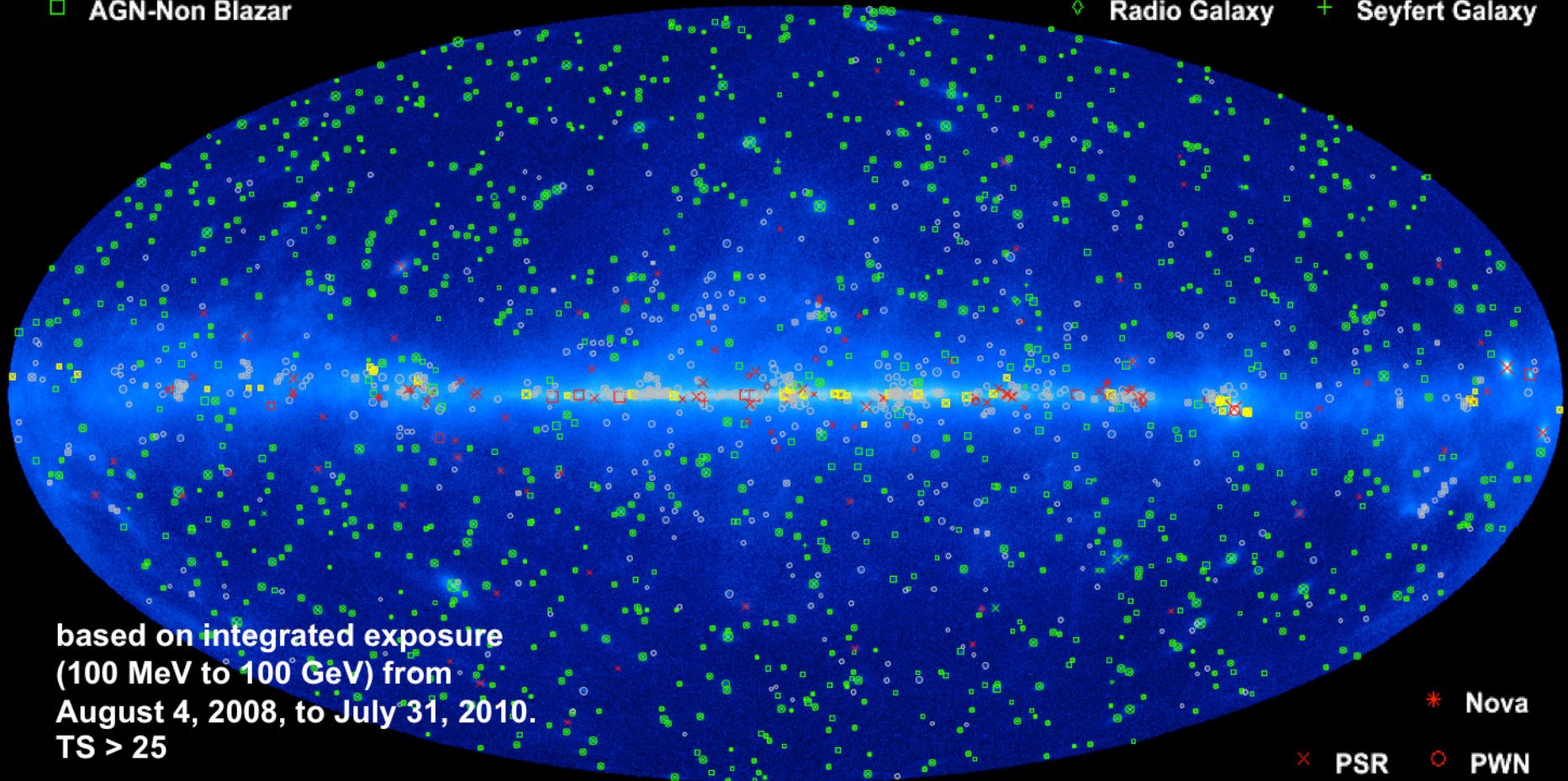
□ AGN-Non Blazar

× Galaxy

* Starburst Galaxy

◇ Radio Galaxy

+ Seyfert Galaxy



based on integrated exposure
(100 MeV to 100 GeV) from
August 4, 2008, to July 31, 2010.
TS > 25

○ Unassociated

□ Possible Association with SNR and PWN

* Nova

× PSR

○ PWN

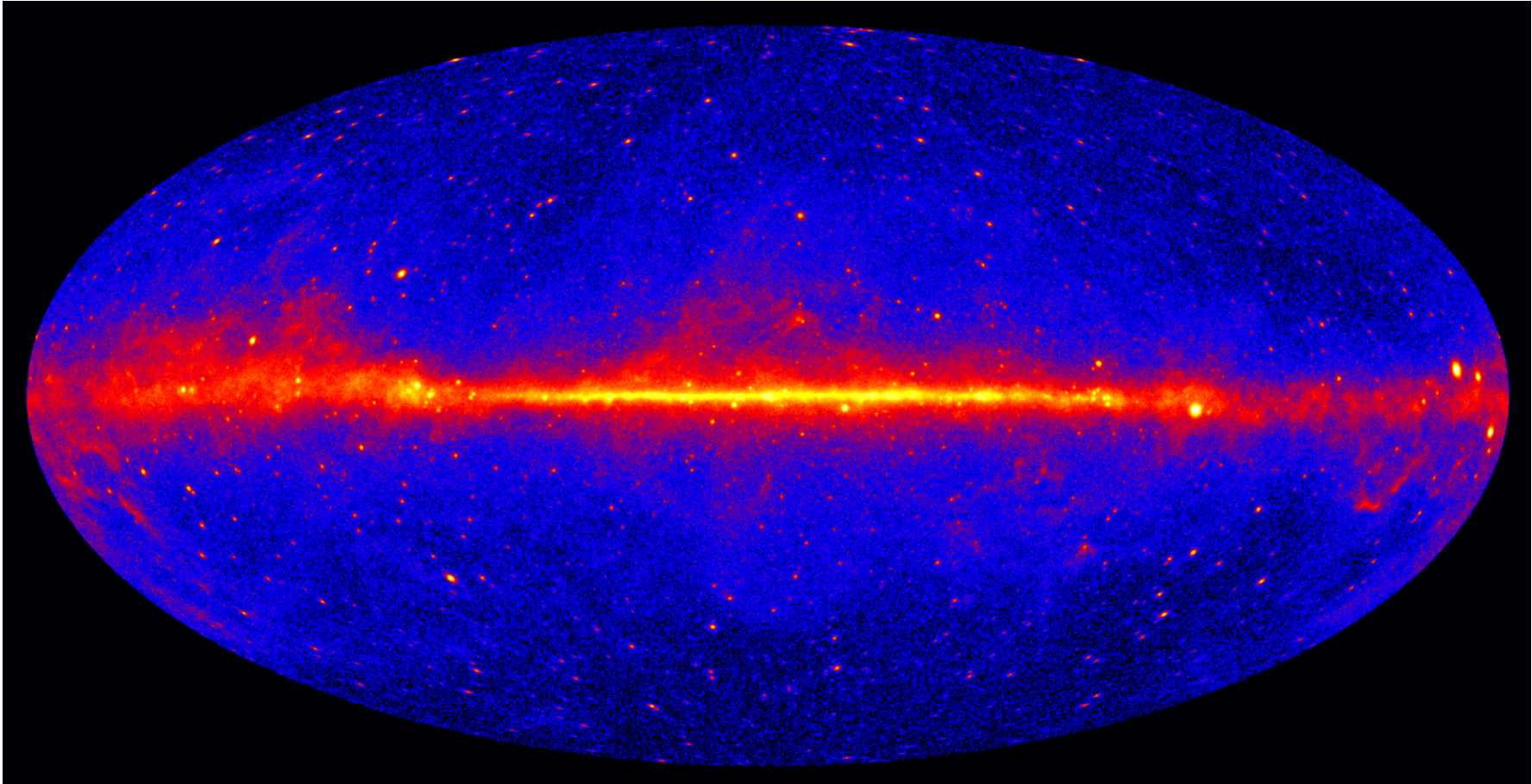
⊗ PSR w/PWN

□ SNR

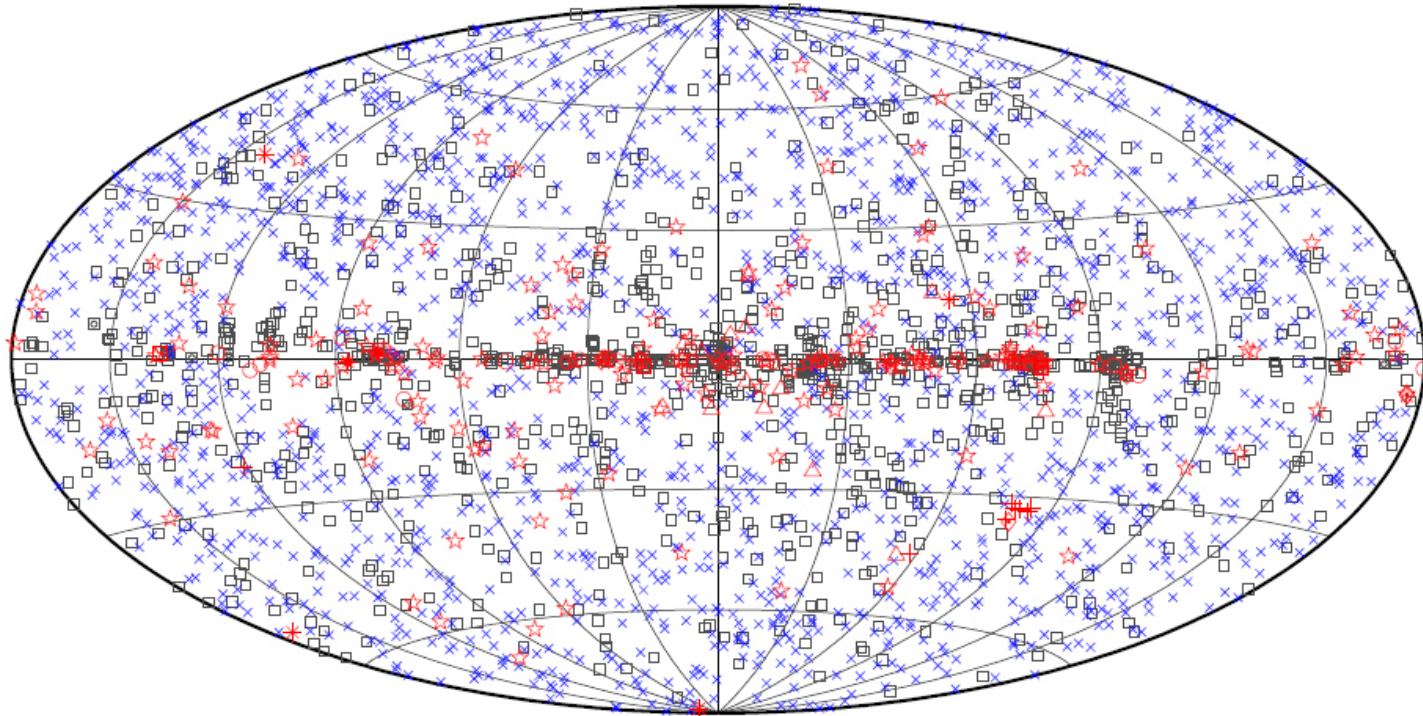
◇ Globular Cluster

+ HMB

4 years sky

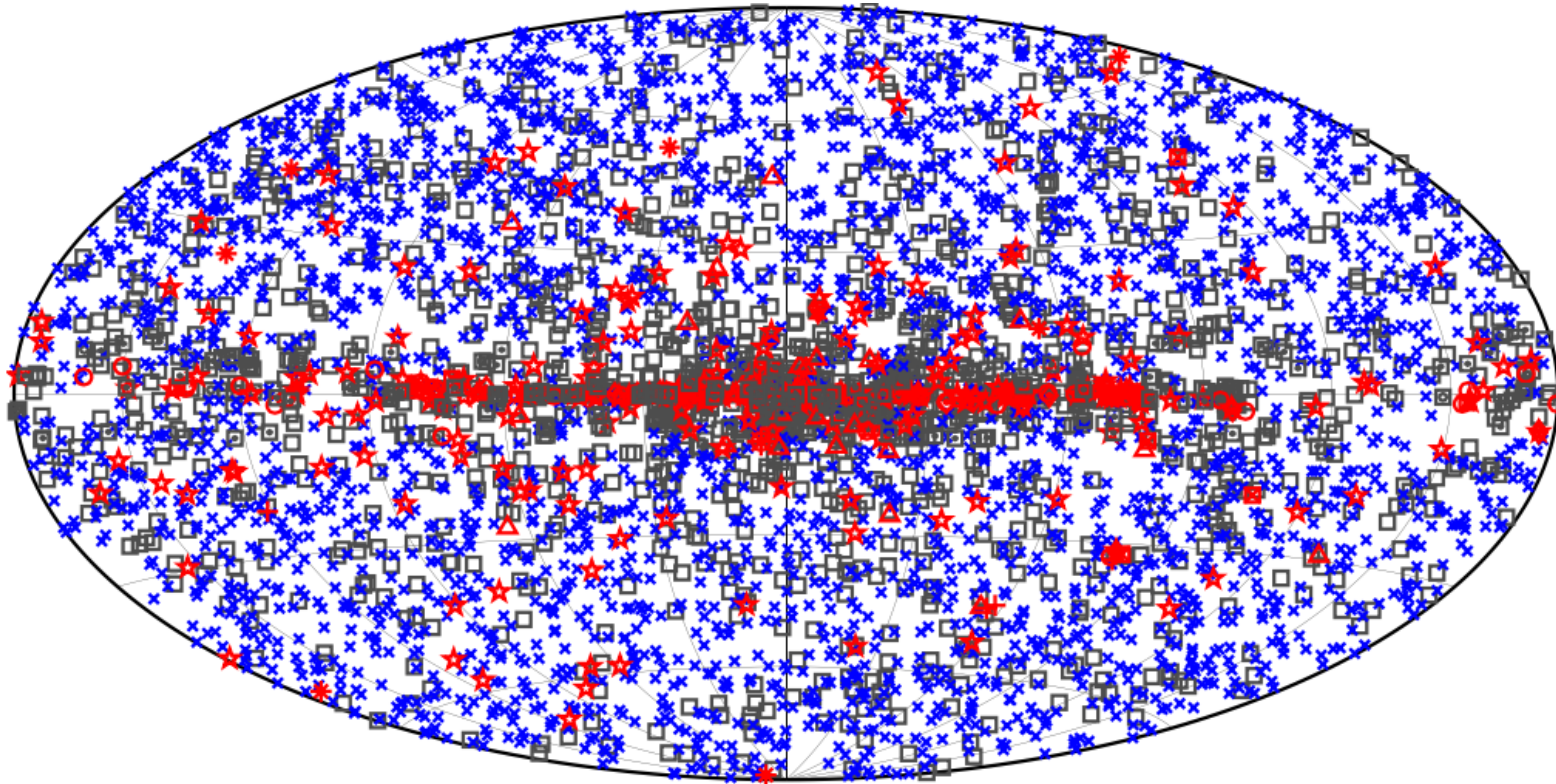


3FGL catalog – 3033 sources



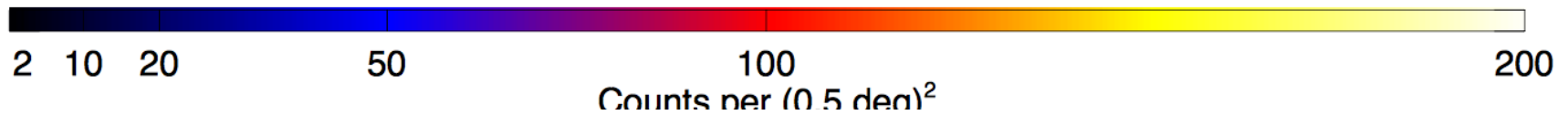
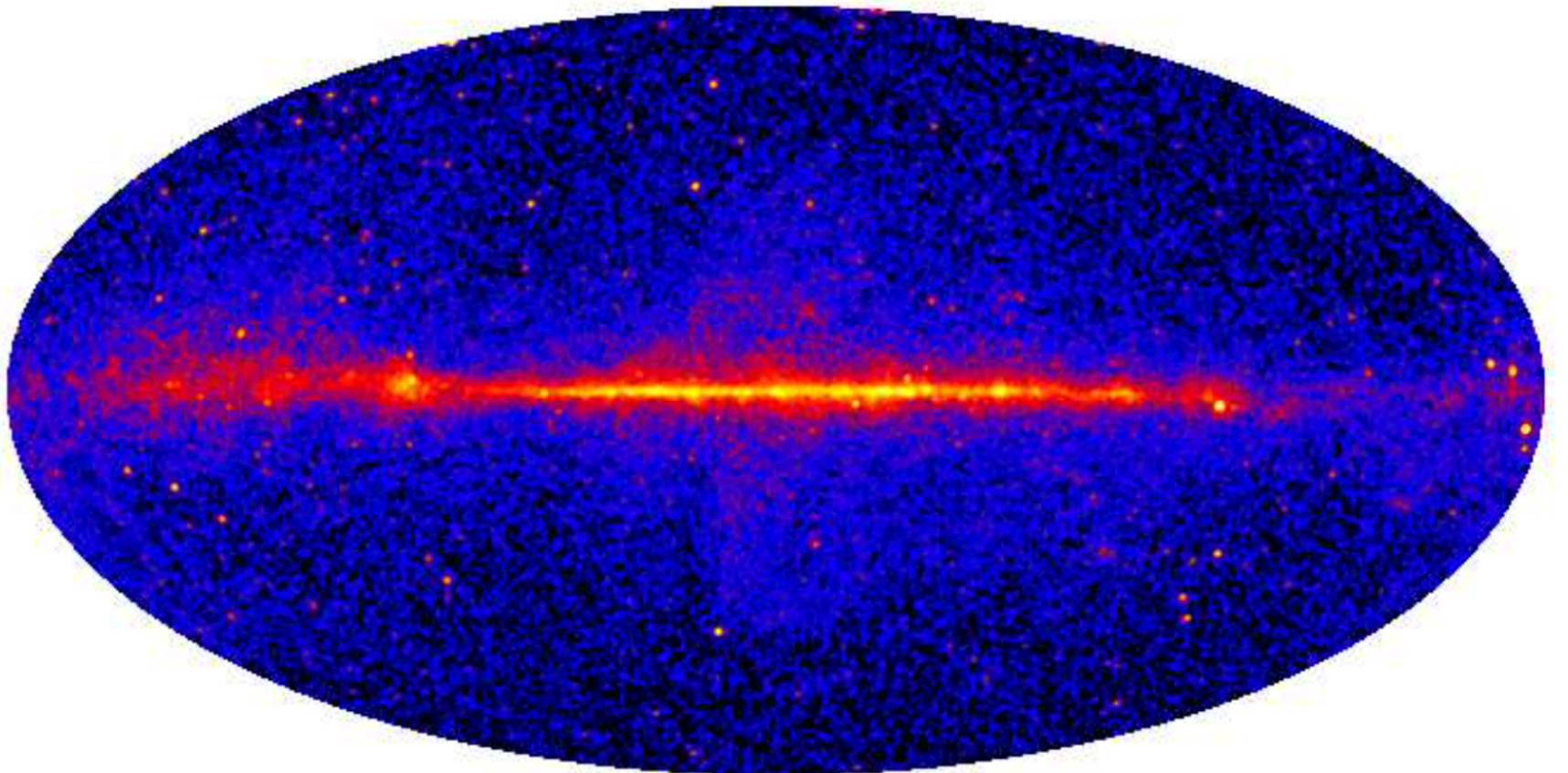
□ No association	□ Possible association with SNR or PWN	× AGN
☆ Pulsar	△ Globular cluster	☆ Starburst Galaxy
⊠ Binary	+ Galaxy	◇ PWN
★ Star-forming region	○ SNR	★ Nova

4FGL catalog

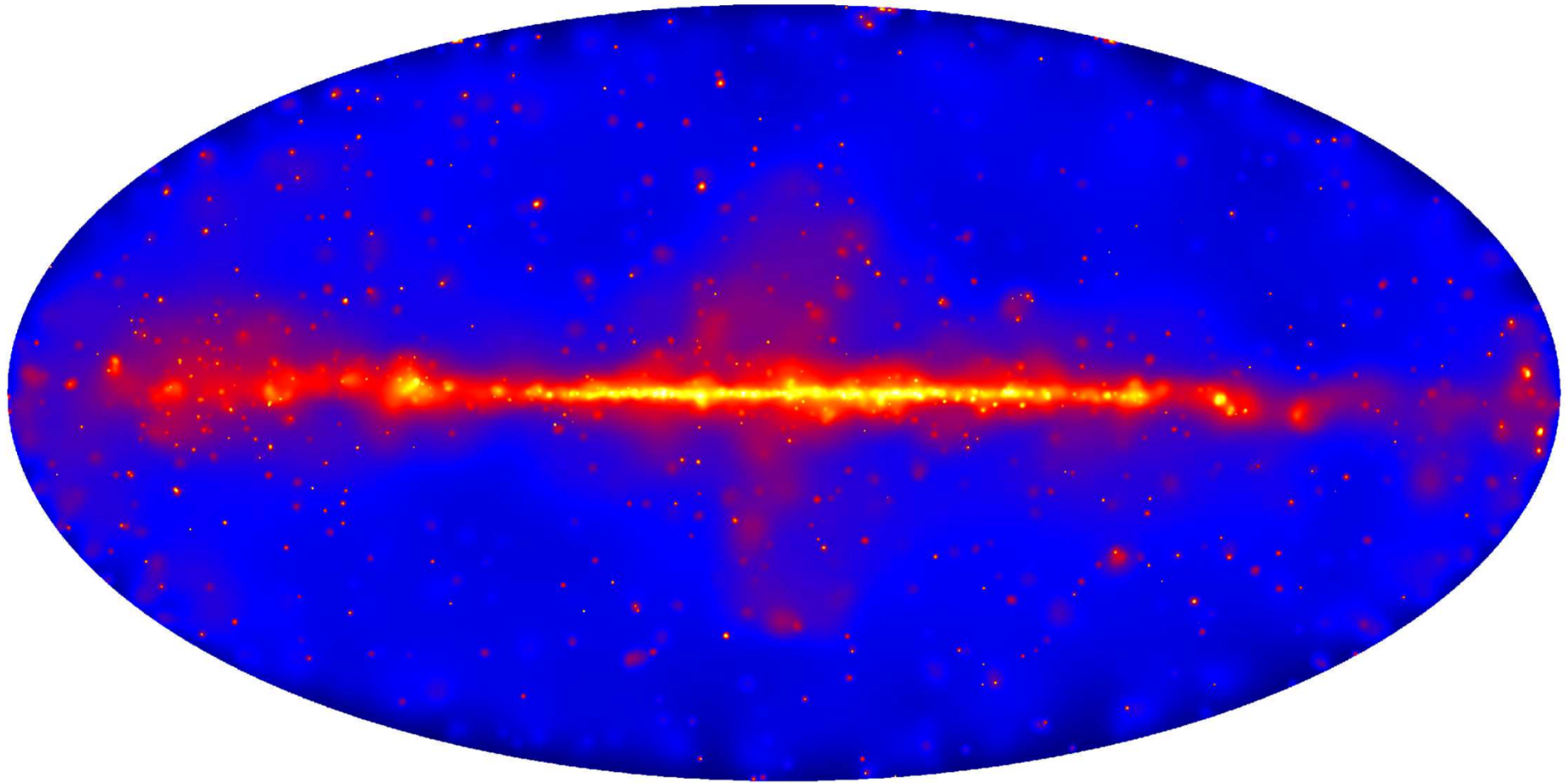


□ No association	■ Possible association with SNR or PWN	× AGN
★ Pulsar	△ Globular cluster	* Starburst Galaxy
▣ Binary	+ Galaxy	○ SNR
★ Star-forming region	□ Unclassified source	◆ PWN
		★ Nova

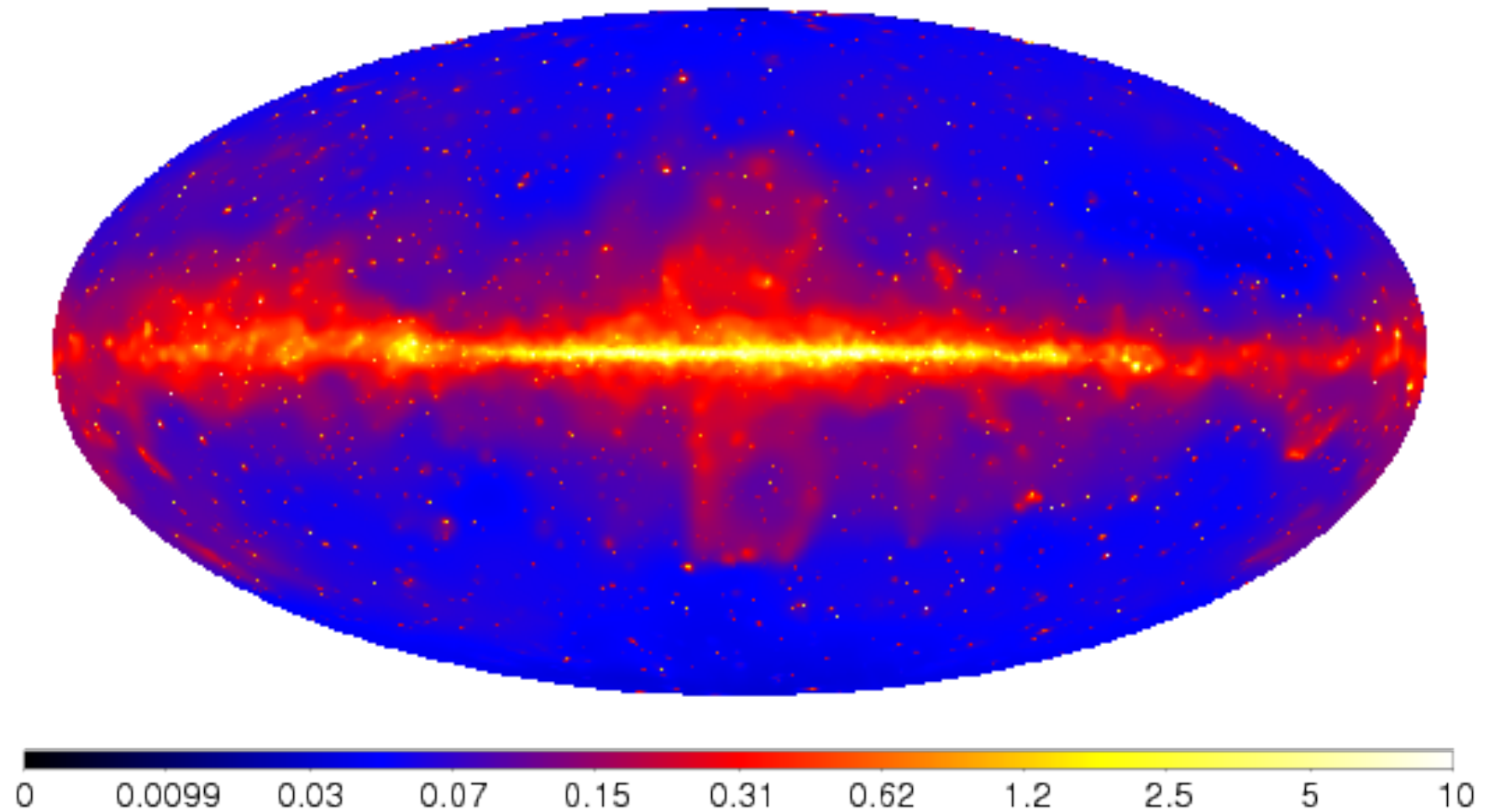
1 FHL (3 years, Pass7, E>10 GeV)



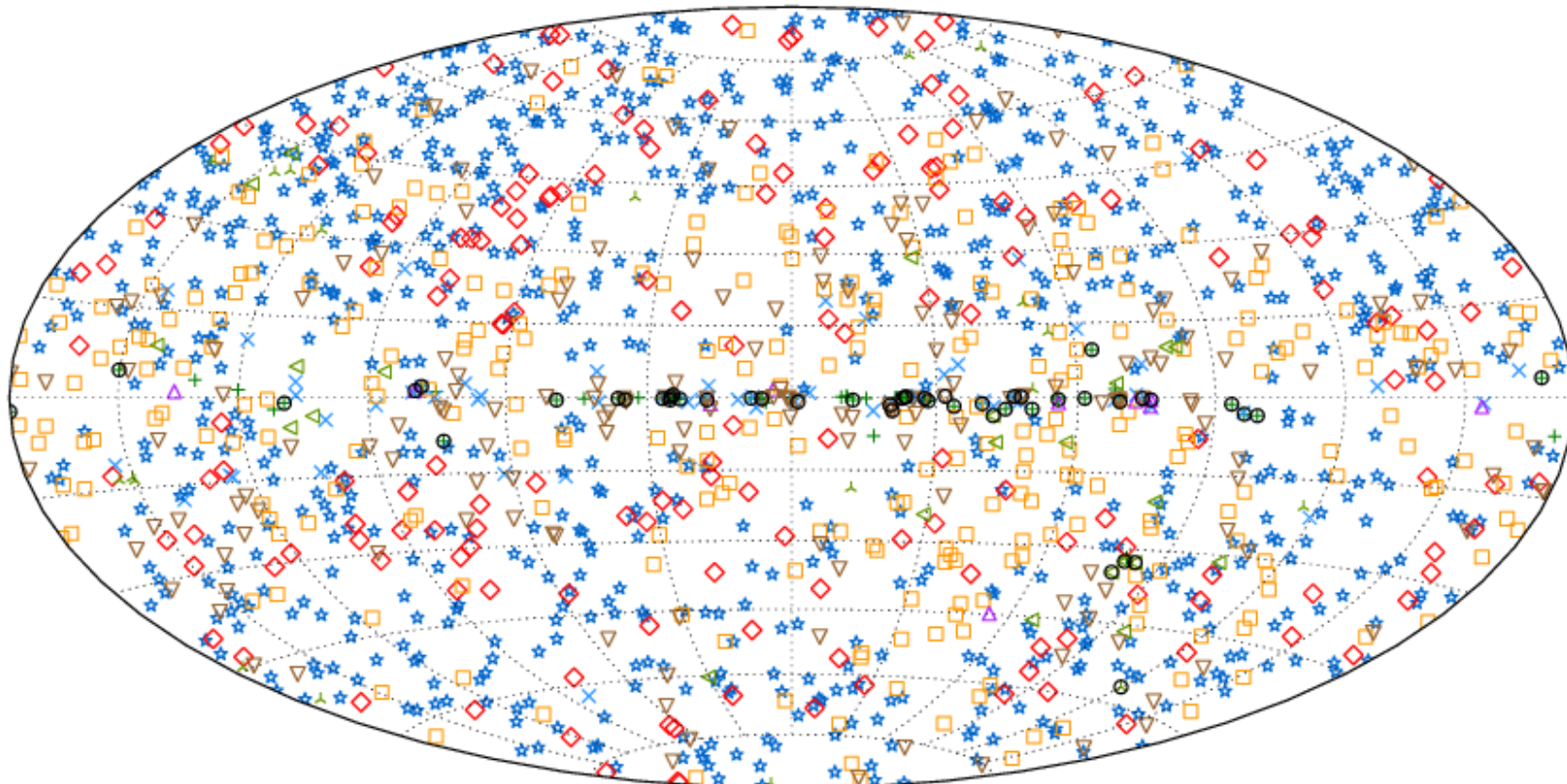
2FHL (P8 data >50 GeV) – 80 months



3FHL ($E > 10$ GeV – P8)



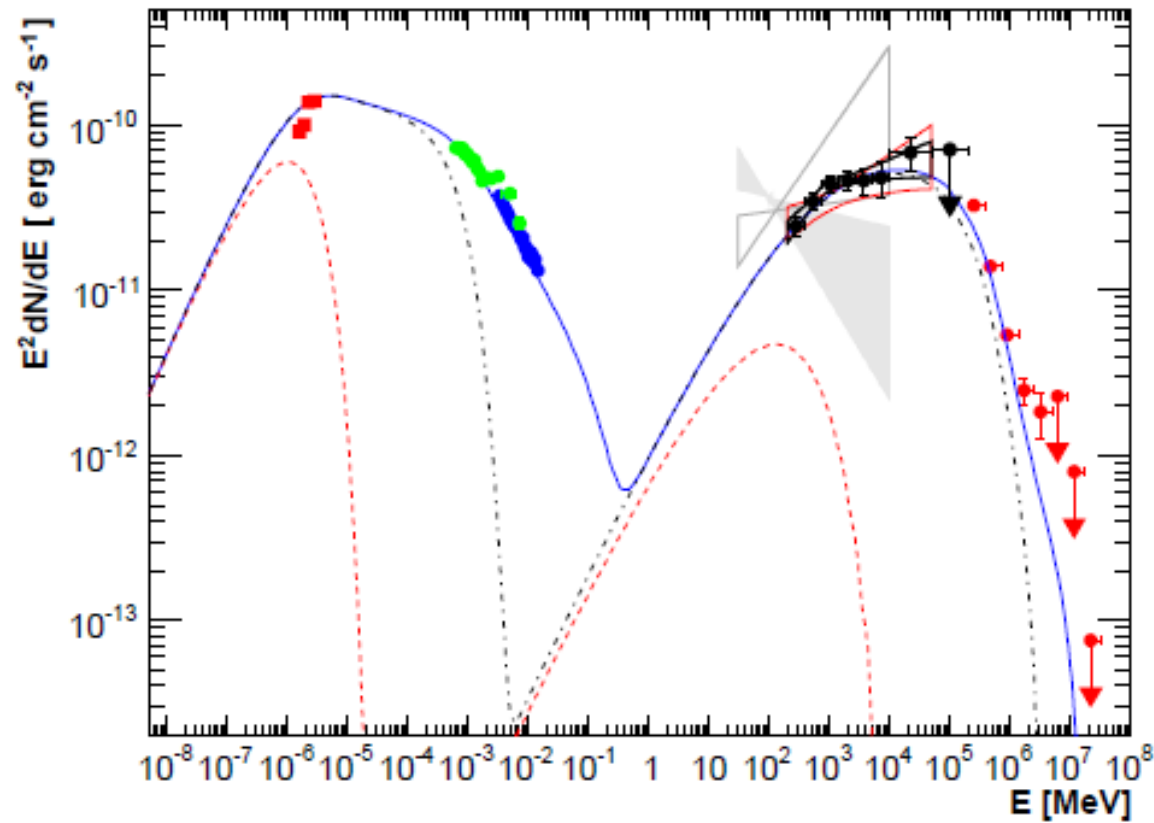
3 FHL



+	SNRs and PWNe	★	BL Lacs	◻	Unc. Blazars	▲	Other GAL	▽	Unassociated
×	Pulsars	◆	FSRQs	▲	Other EGAL	◀	Unknown	○	Extended

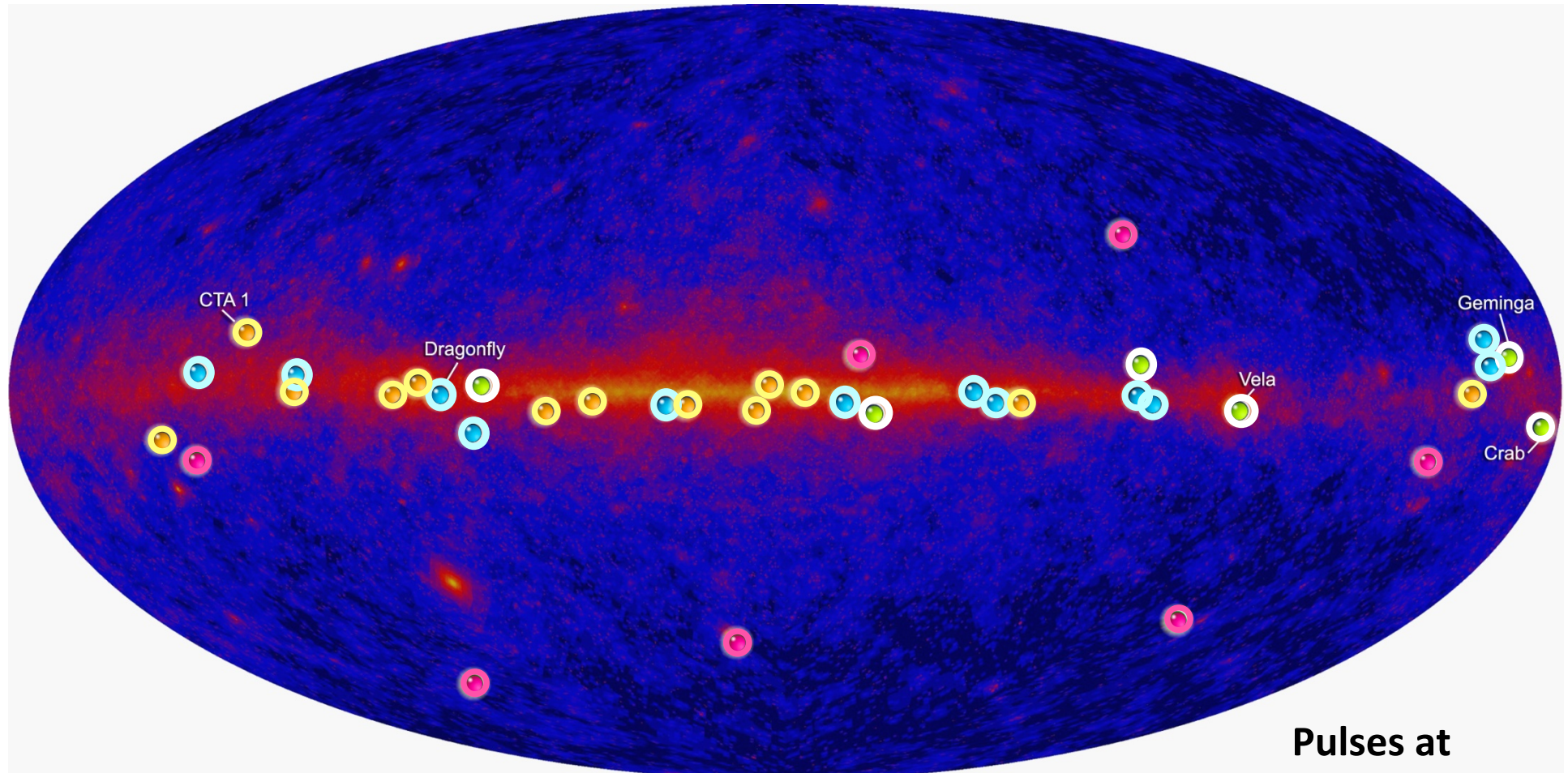
Challenge # 1 – AGN

Joint campaign on PKS 2155 with HESS



Aharonian et al. 2009

Challenge # 2 – Pulsars Blind Search



Fermi Pulsar Detections

Abdo et al..2010

- New pulsars discovered in a blind search
 - Millisecond radio pulsars
 - Young radio pulsars
 - Confirmed pulsars seen by Compton Observatory EGRET instrument
- Pulses at 1/10th true rate**

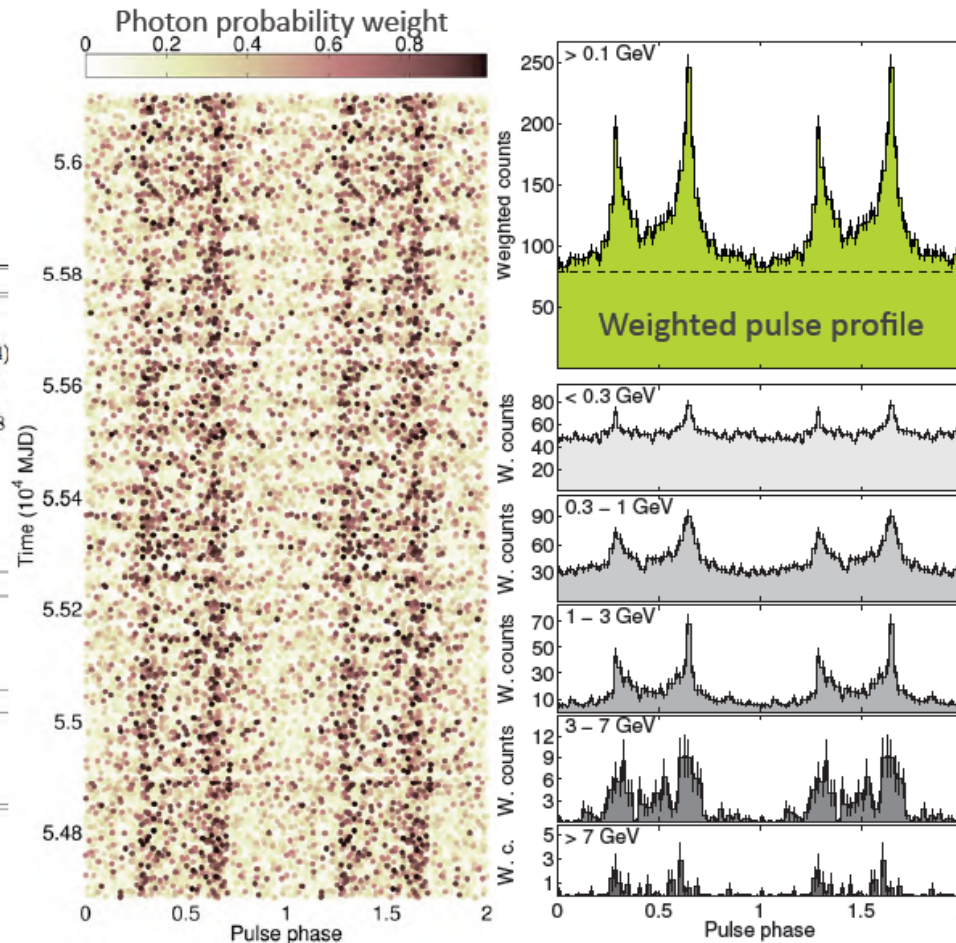
The first blind ms Pulsar

The PSR J1311-3430 system (1/2)

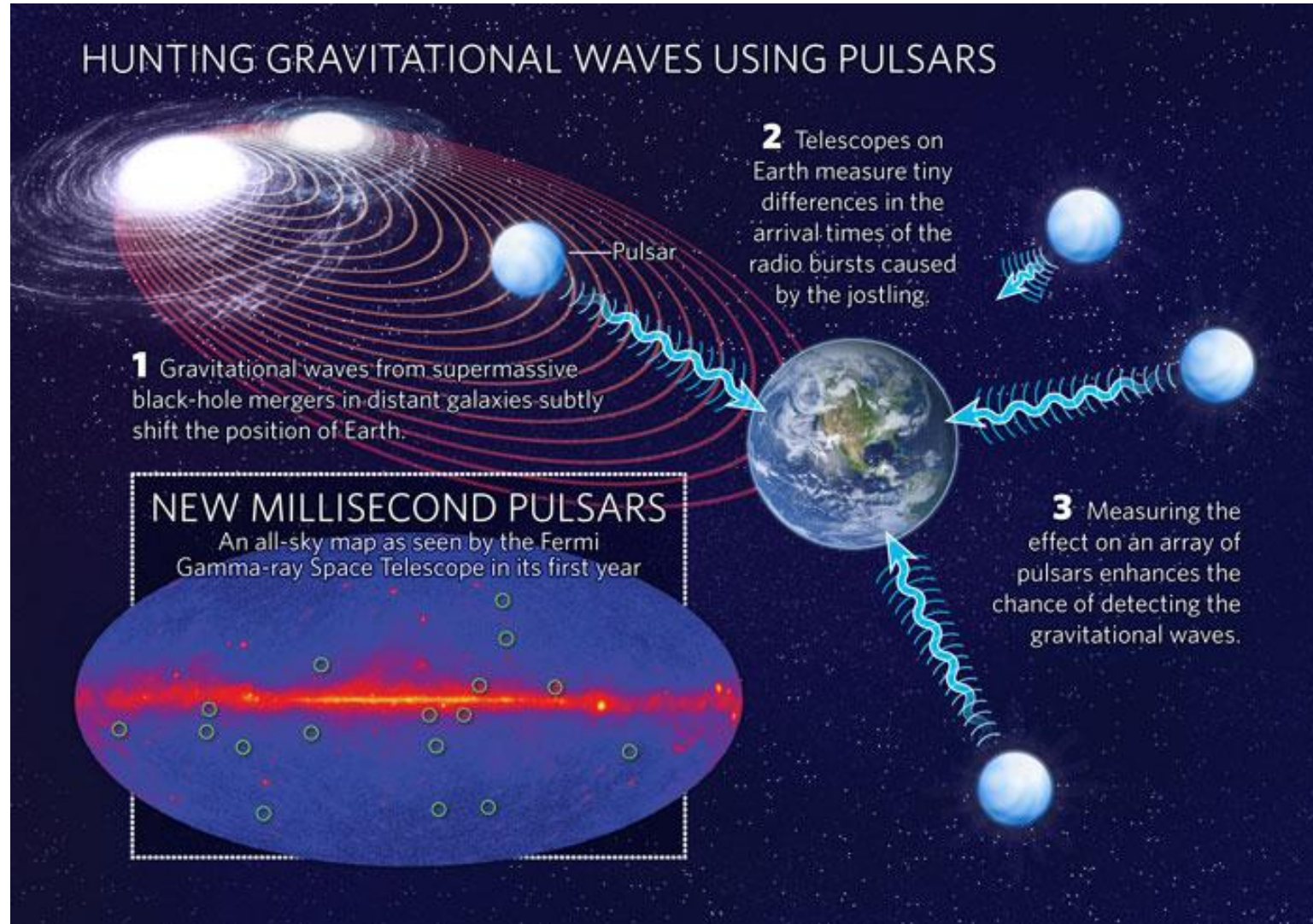


- Following the discovery:
→ pulsar timing to precisely measure the system parameters (■)

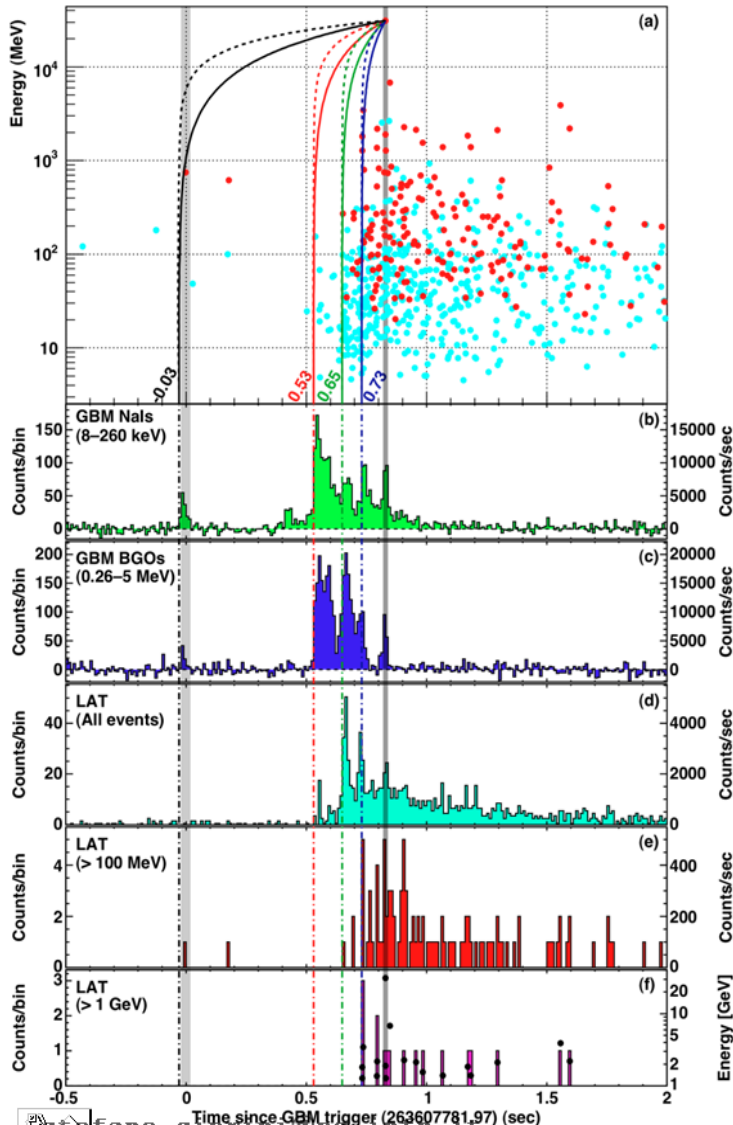
Parameter	Value
Right ascension (J2000.0) (hh:mm:ss)	13:11:45.7242(2)
Declination (J2000.0) (dd:mm:ss)	-34:30:30.350(4)
Spin frequency, f (Hz)	390.56839326407(4)
Frequency derivative, \dot{f} (Hz s ⁻¹)	-3.198(2) × 10 ⁻¹⁵
Reference time scale	TDB
Reference time (MJD)	55266.90789575858
Orbital period P_{orb} (d)	0.0651157335(7)
Projected pulsar semi-major axis x (lt-s)	0.010581(4)
Time of ascending node T_{asc} (MJD)	56009.129454(7)
Eccentricity e	< 0.001
Data span (MJD)	54682 - 56119
Weighted RMS residual (μ s)	17
Derived Quantities	
Companion mass m_c (M_\odot)	> 0.0082
Spin-down luminosity \dot{E} (erg s ⁻¹)	4.9 × 10 ³⁴
Characteristic age τ_c (yr)	1.9 × 10 ⁹
Surface magnetic field B_S (G)	2.3 × 10 ⁸
Gamma-Ray Spectral Parameters	
Photon index, Γ	1.8 ± 0.1
Cutoff energy, E_c (GeV)	3.2 ± 0.4
Photon flux above 0.1 GeV, F (10 ⁻⁸ photons cm ⁻² s ⁻¹)	9.2 ± 0.5
Energy flux above 0.1 GeV, G (10 ⁻¹¹ erg cm ⁻² s ⁻¹)	6.2 ± 0.2



New MSP and GW detection



Challenge # 3 – GRB



- ❑ This GRB is a perfect case for studying Lorentz Invariance Violation
 - ❑ $z = 0.9$ (5.381 Gyr)
 - ❑ Emission of 31 GeV photon after 859 ms since the trigger
- ❑ Only conservative assumption!
 - ❑ the HE photon is not emitted *before* the LE photons, at different events.

Table 2 | Limits on Lorentz Invariance Violation

#	$t_{\text{start}} - T_0$ (ms)	Limit on $ \Delta t $ (ms)	Reasoning for choice of t_{start} or limit on Δt or $ \Delta t/\Delta E $	E_1^\dagger (MeV)	Valid for s_n^*	Lower limit on $M_{\text{QG},1}/M_{\text{Planck}}$
(a)*	-30	< 859	start of any < 1 MeV emission	0.1	1	> 1.19
(b)*	530	< 299	start of main < 1 MeV emission	0.1	1	> 3.42
(c)*	648	< 181	start of main > 0.1 GeV emission	100	1	> 5.63
(d)*	730	< 99	start of > 1 GeV emission	1000	1	> 10.0
(e)*	—	< 10	association with < 1 MeV spike	0.1	± 1	> 102
(f)*	—	< 19	If 0.75 GeV ‡ γ -ray from 1 st spike	0.1	-1	> 1.33
(g)*	$ \Delta t/\Delta E < 30 \text{ ms/GeV}$	—	lag analysis of > 1 GeV spikes	—	± 1	> 1.22

[nature](#) > [letters](#) > article

[Published: 01 October 1998](#)

Tests of quantum gravity from observations of γ -ray bursts

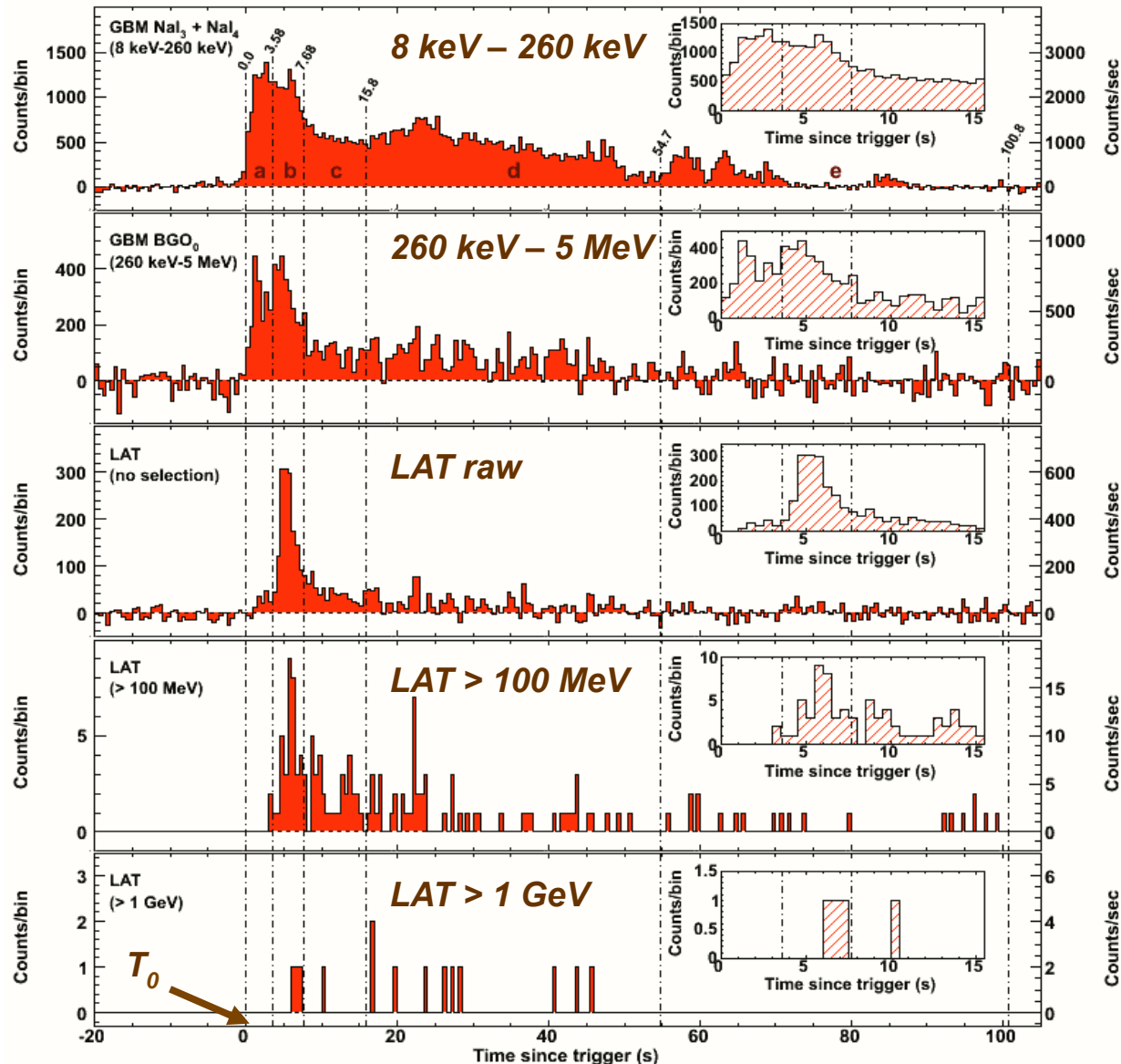
[G. Amelino-Camelia](#), [John Ellis](#), [N. E. Mavromatos](#), [D. V. Nanopoulos](#) & [Subir Sarkar](#)

[Nature](#) **395**, 525 (1998) | [Cite this article](#)

The recent confirmation that at least some γ -ray bursts originate at cosmological distances¹⁻⁴ suggests that the radiation from them could be used to probe some of the fundamental laws of physics. Here we show that γ -ray bursts will be sensitive to an energy dispersion predicted by some approaches to quantum gravity. Many of the bursts have structure on relatively rapid timescales⁵, which means that in principle it is possible to look for energy-dependent dispersion of the radiation, manifested in the arrival times of the photons, if several different energy bands are observed simultaneously. A simple estimate indicates that, because of their high energies and distant origin, observations of these bursts should be sensitive to a dispersion scale that is comparable to the Planck energy scale ($\sim 10^{19}$ GeV), which is sufficient to test theories of quantum gravity. Such observations are already possible using existing γ -ray burst detectors.

$$v = \frac{\partial E}{\partial p} \approx c \left(1 - \xi \frac{E}{E_{\text{QG}}} \right) \quad \Delta t \approx \xi \frac{E}{E_{\text{QG}}} \frac{L}{c}$$

GRB080916C - Multiple detector light curve



First 3 light curves are background subtracted

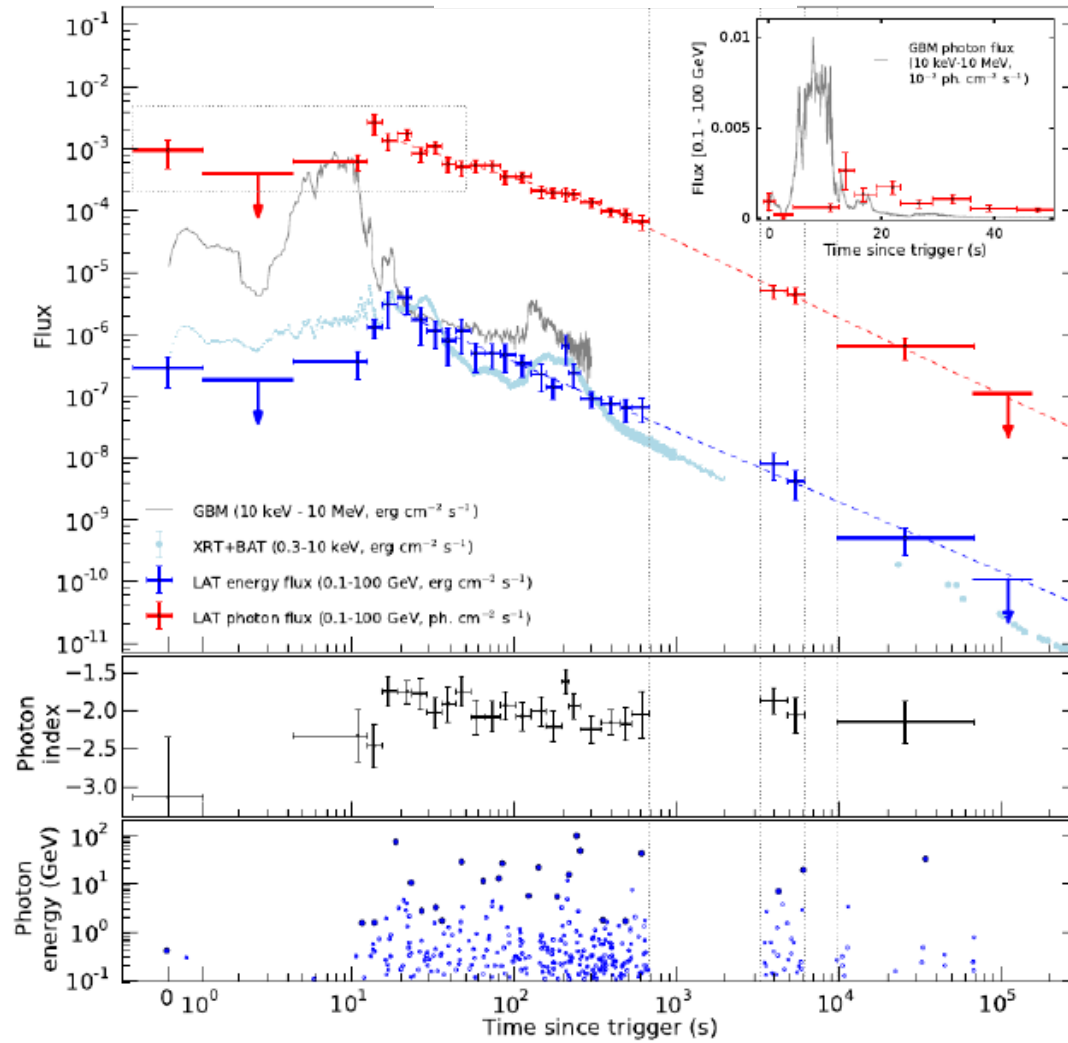
The LAT can be used as a **counter** to maximize the rate and to study time structures above tens of MeV

- The first low-energy peak is not observed at LAT energies

Spectroscopy needs LAT event selection (>100 MeV)

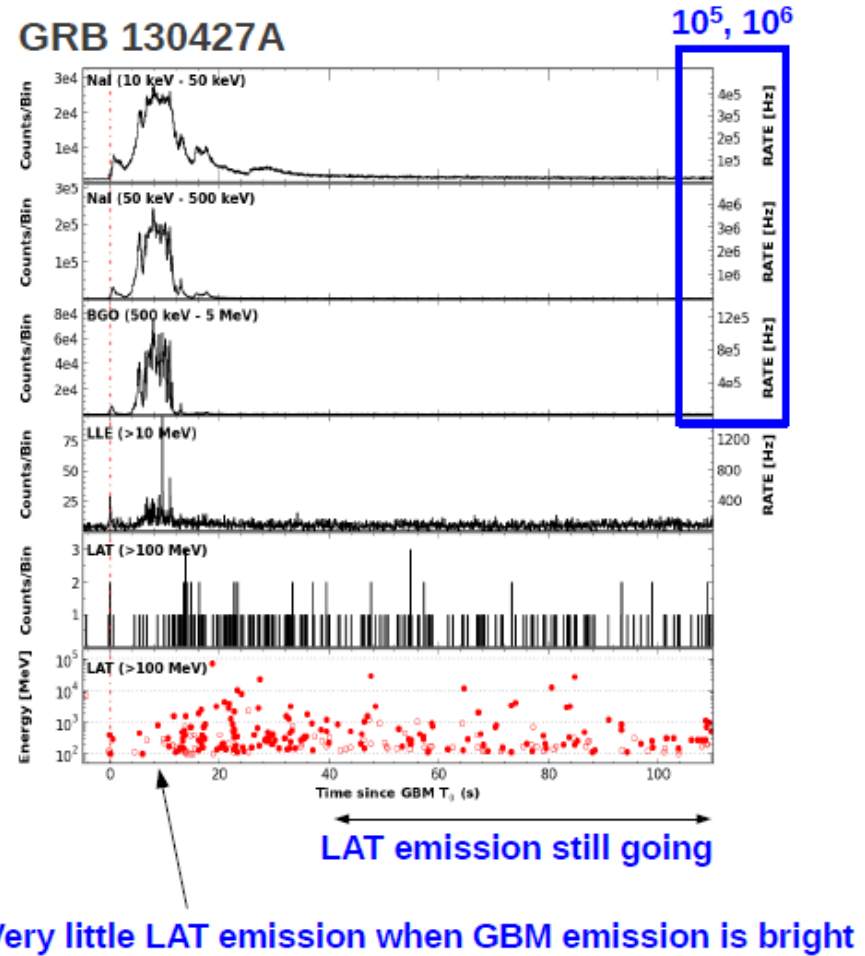
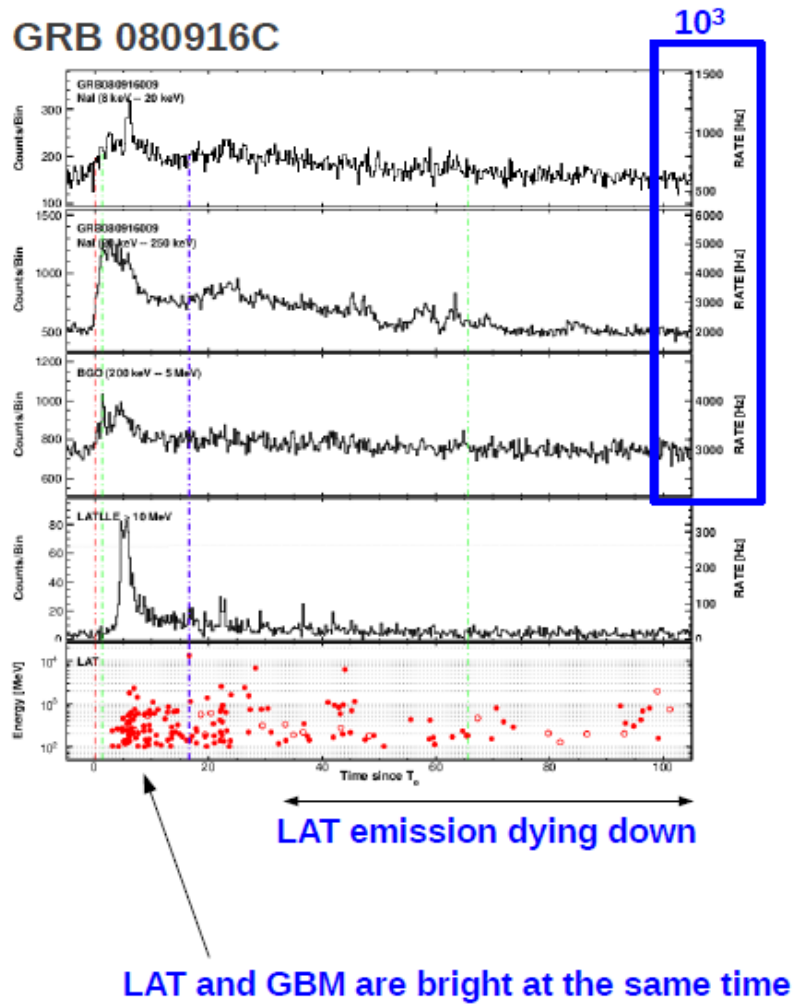
- 14 events above 1 GeV

GRB 130427A



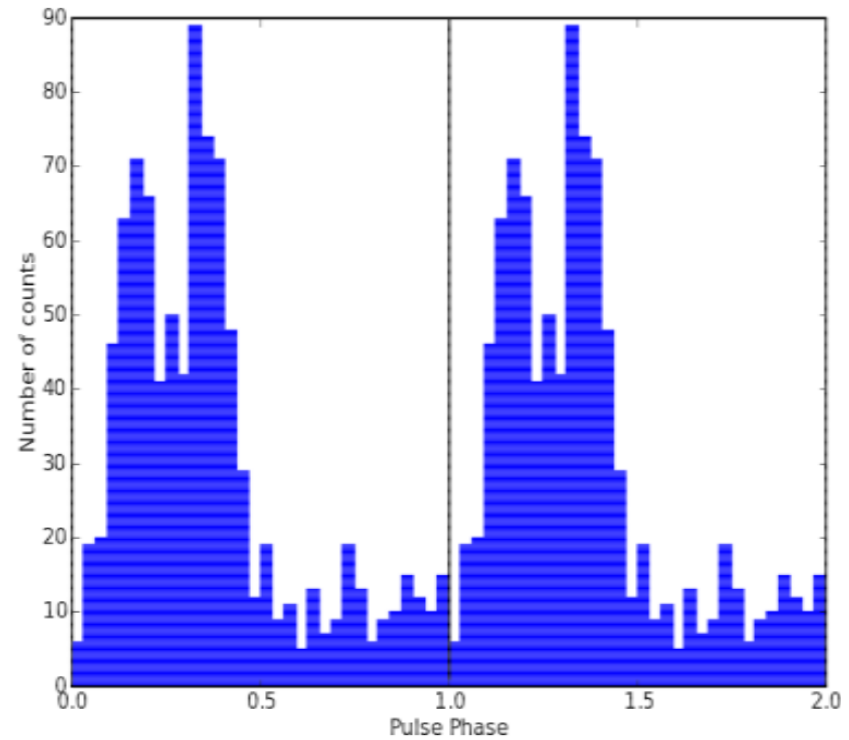
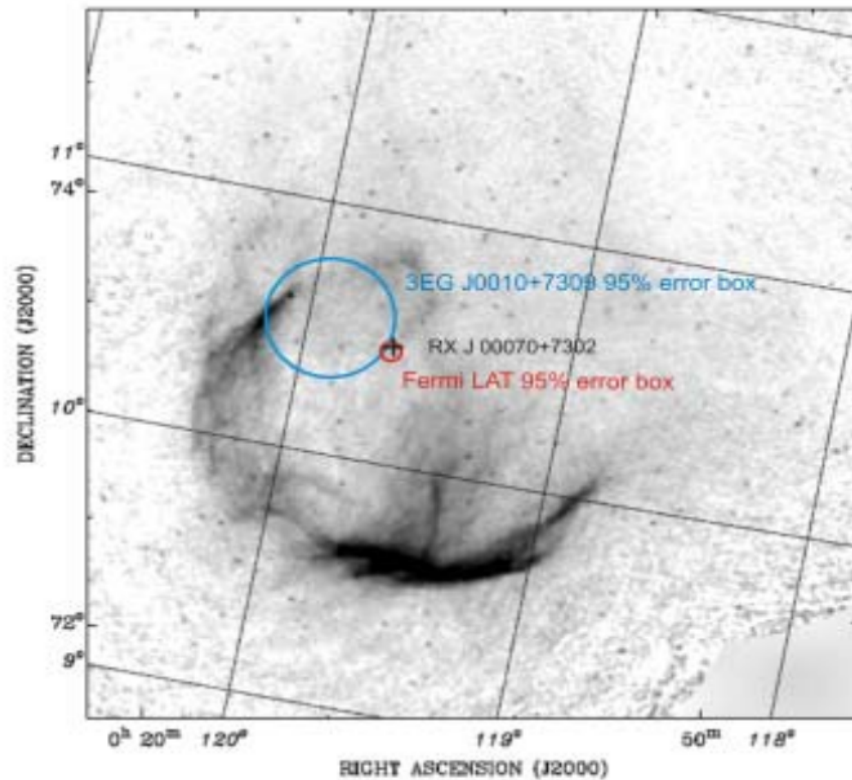
(Ackermann et al.,
Science, Vol. 343 no. 6166
pp. 42-47)

GRB 130427A



Challenge # 4 – Unidentified

CTA 1 Discovery

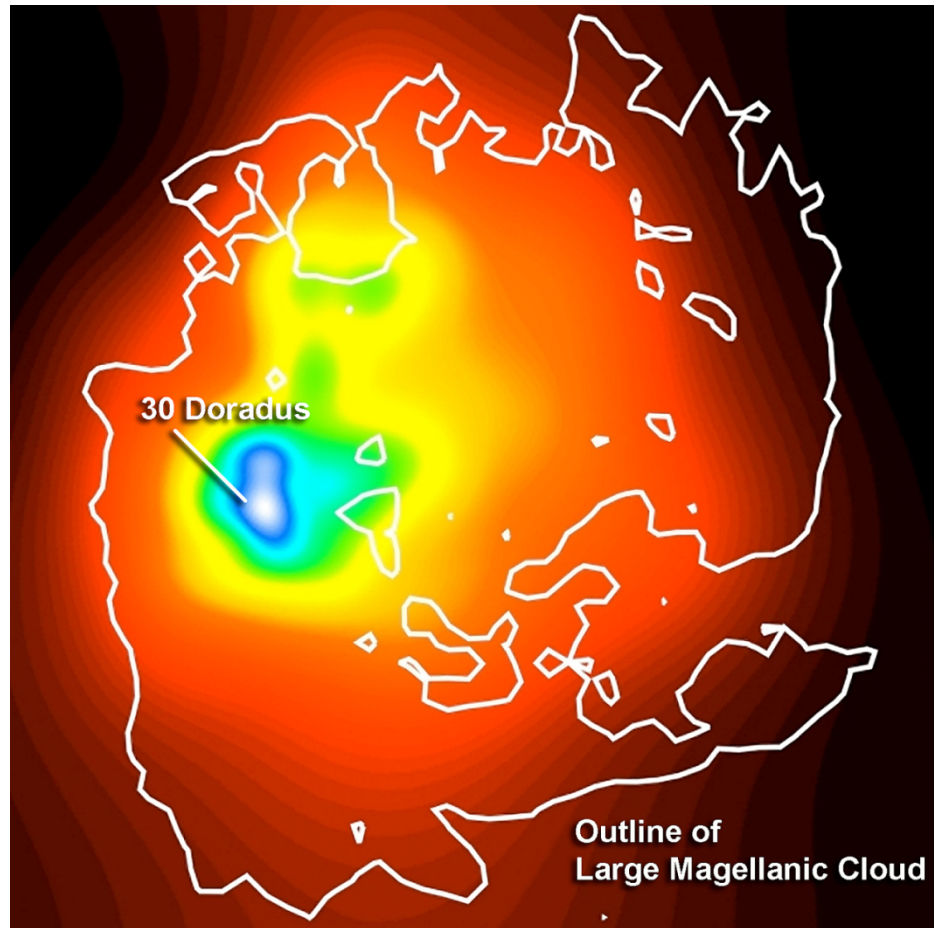


Abdo et al. 2008

Challenge # 4

Location of Gamma-ray emission

Observations of the Large Magellanic Cloud with *Fermi*

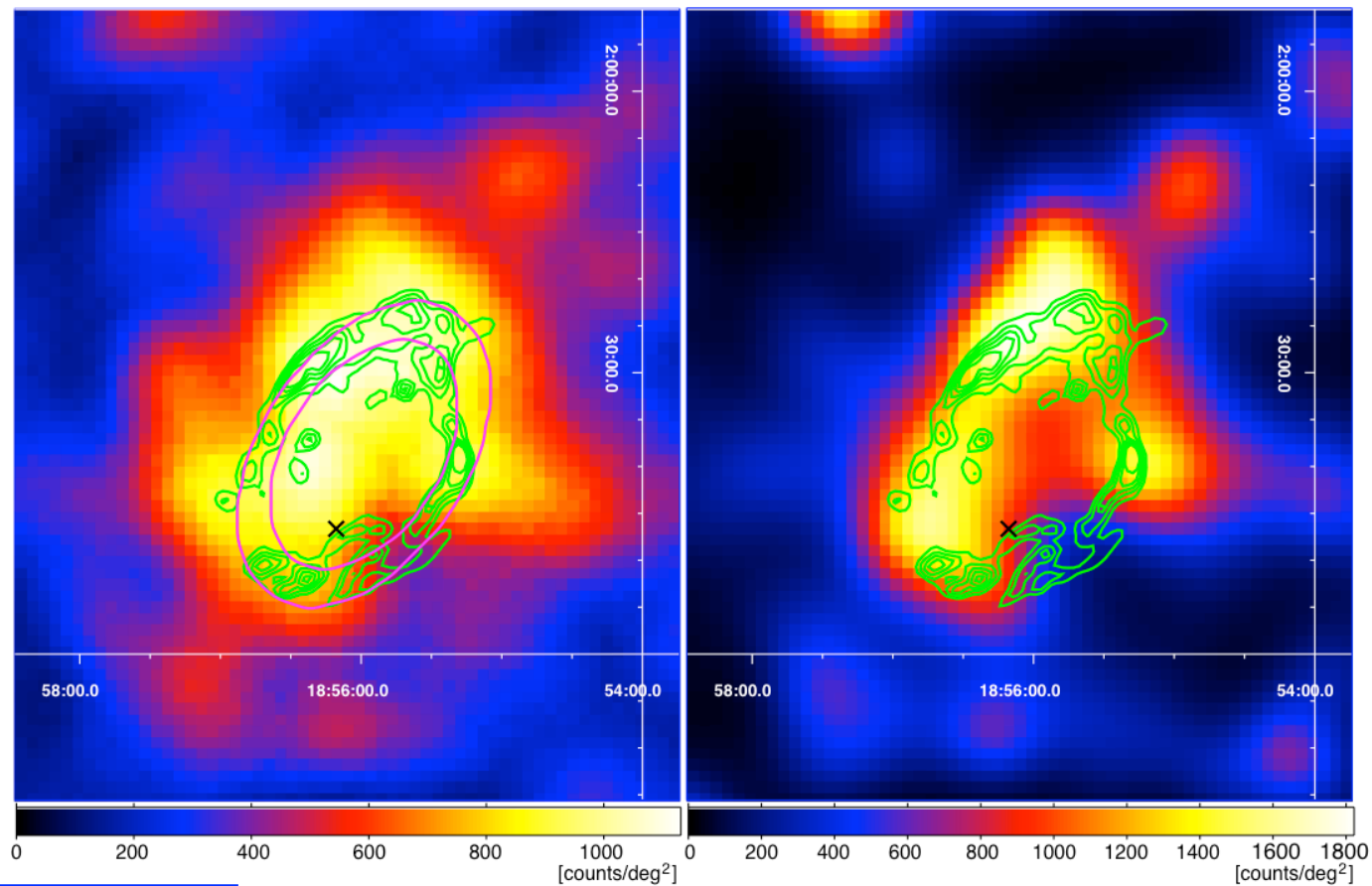


Abdo, A. A. et al. 2010

Challenge # 4

Location of Gamma-ray emission

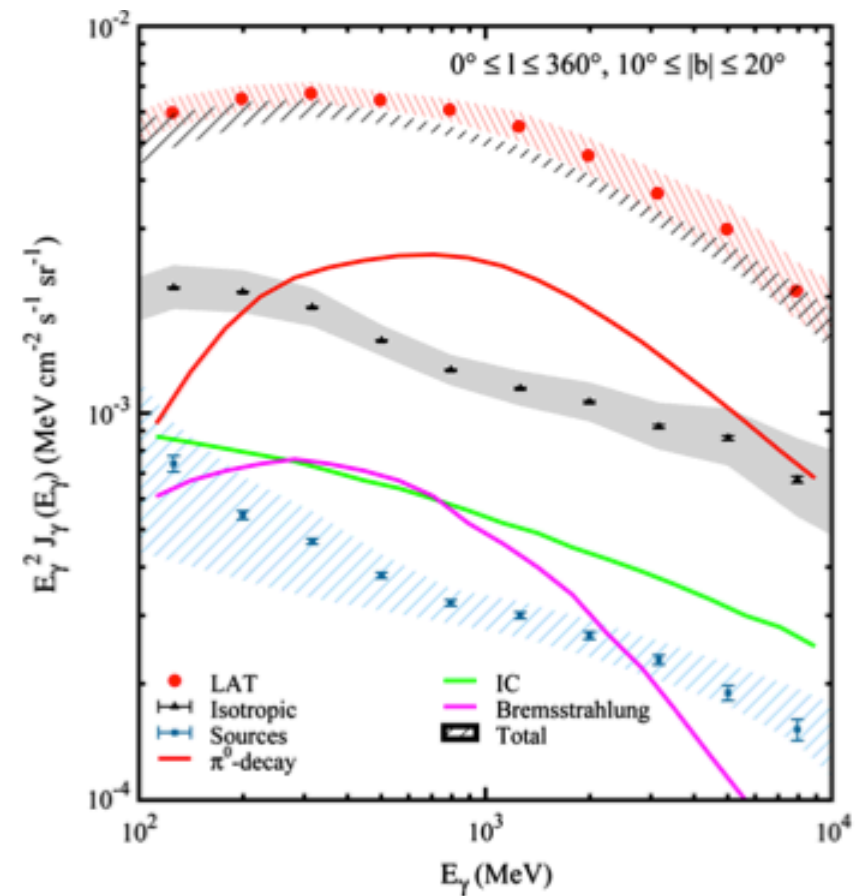
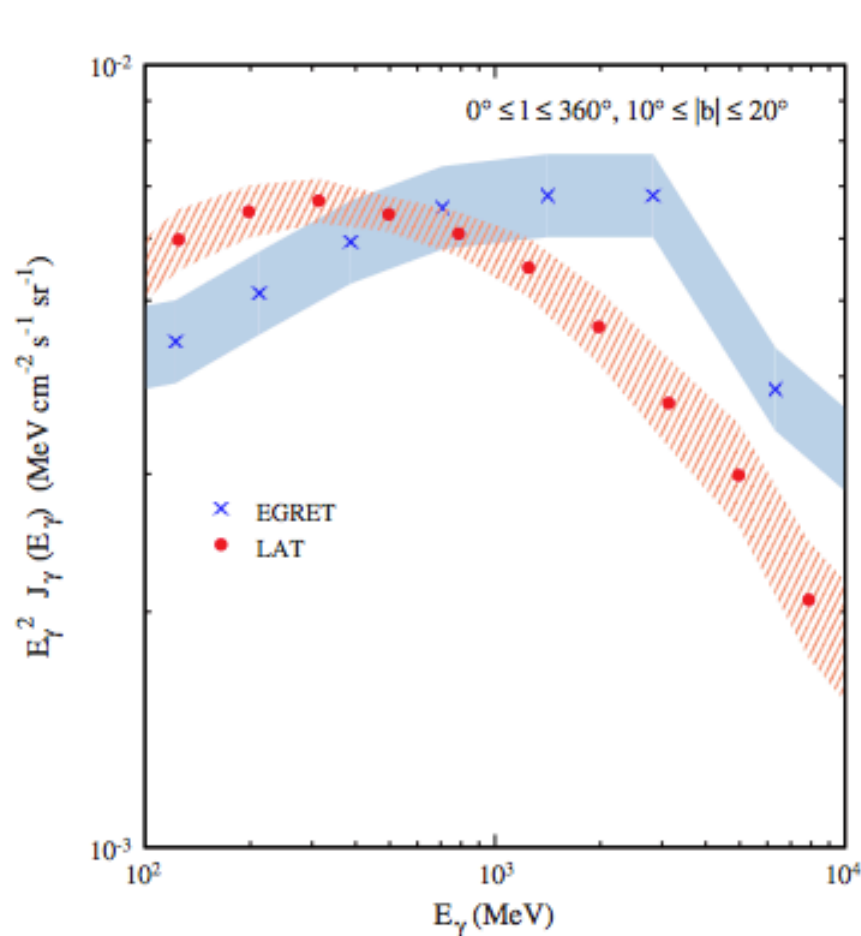
Gamma-Ray Emission from the Shell of Supernova Remnant W44 Revealed by the Fermi LAT



Abdo, A. A. et al. 2010

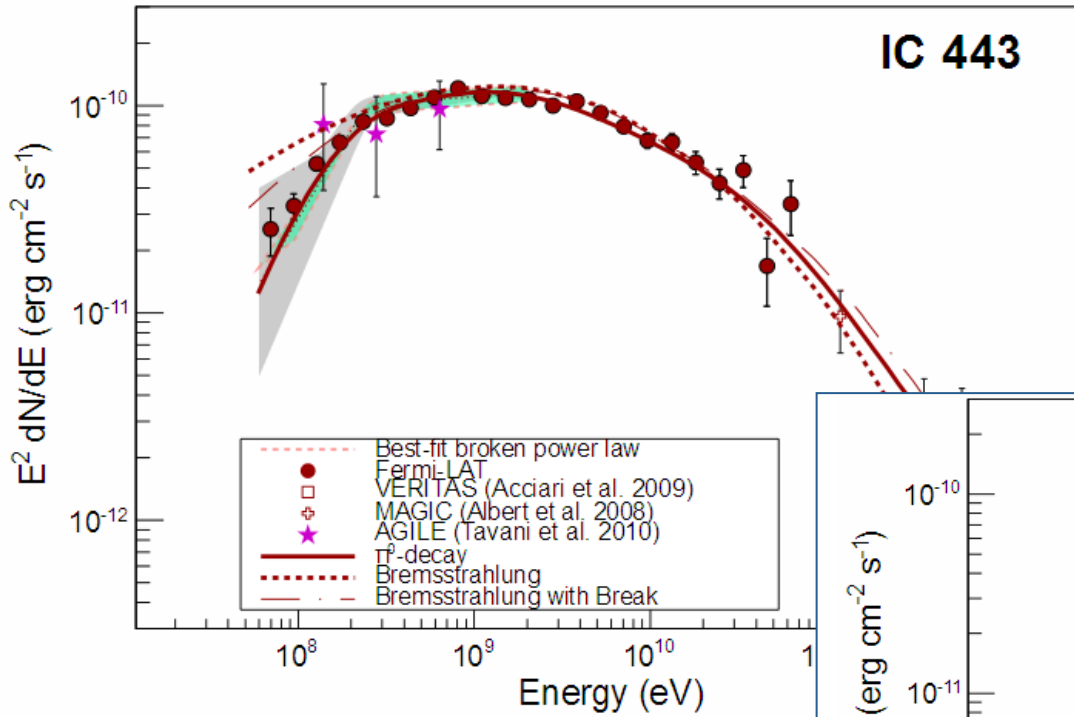
Challenge # 5 – Spectral Resolution

Fermi Large Area Telescope Measurements of the Diffuse Gamma-Ray Emission at Intermediate Galactic Latitudes

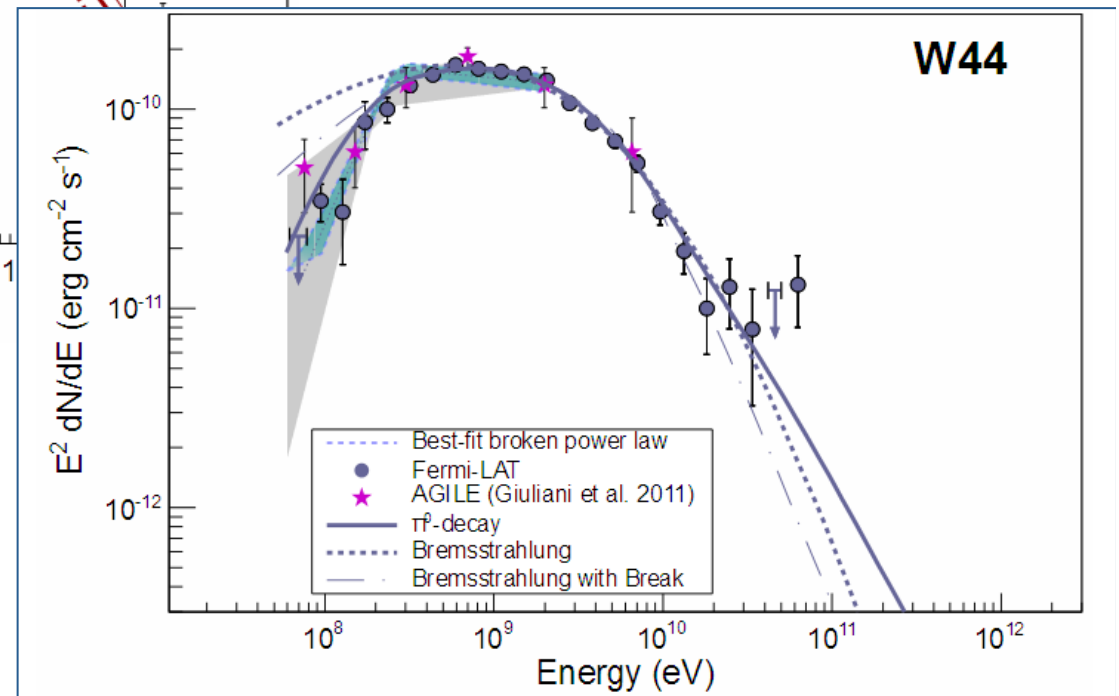


Abdo, A. A. et al. 2009

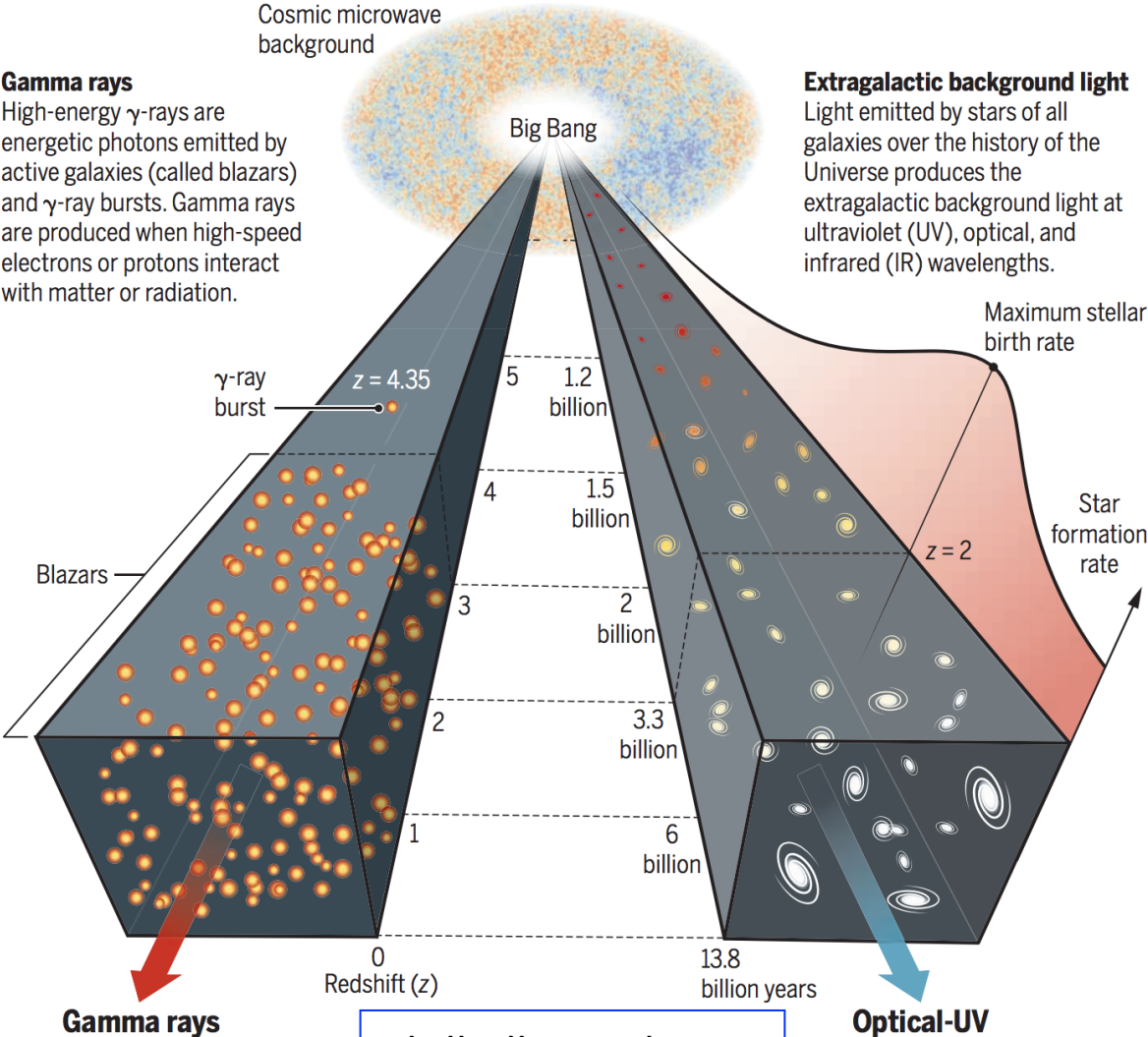
Supernova Remnants



Ackermann et al. 2013



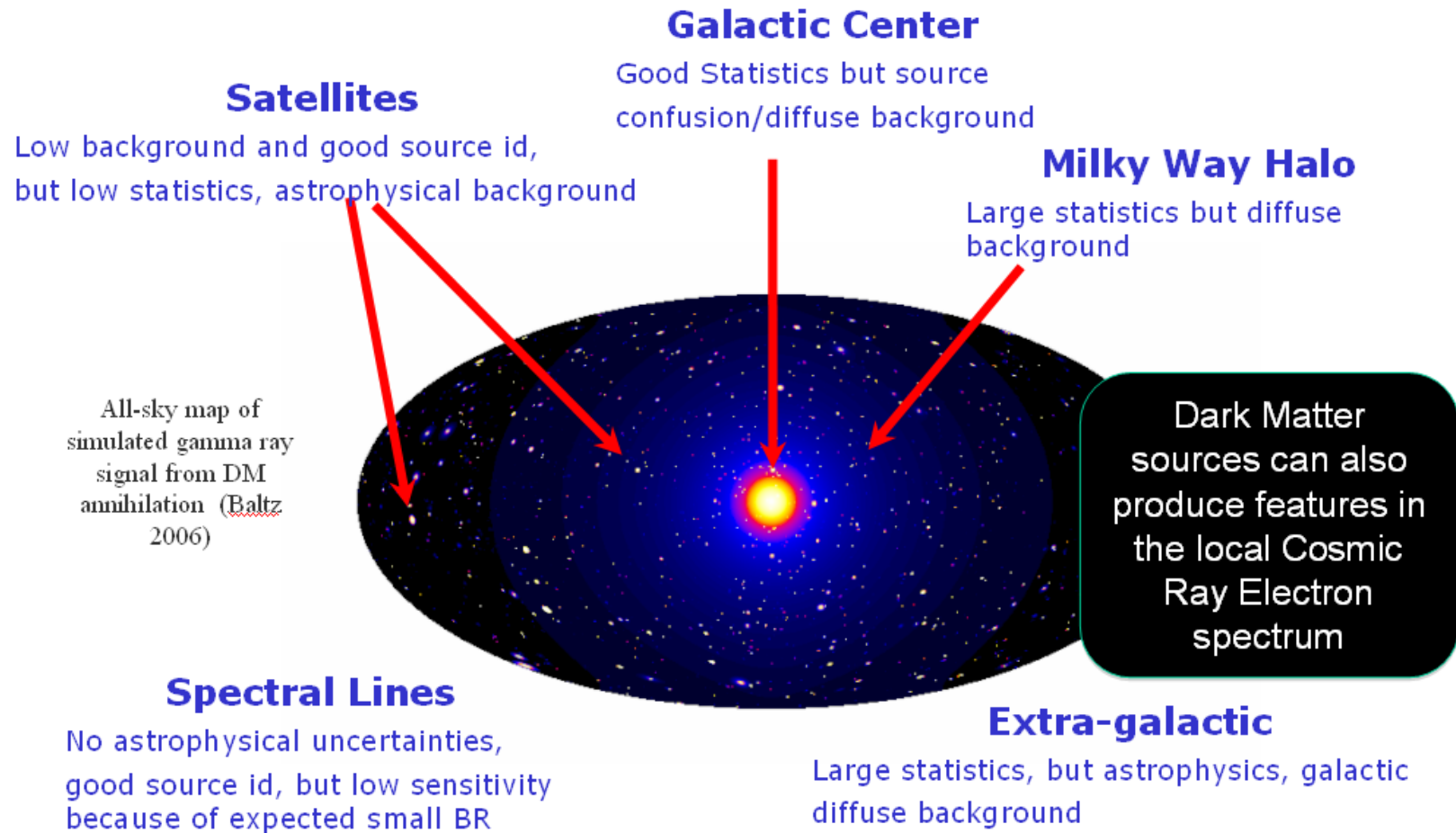
The EBL



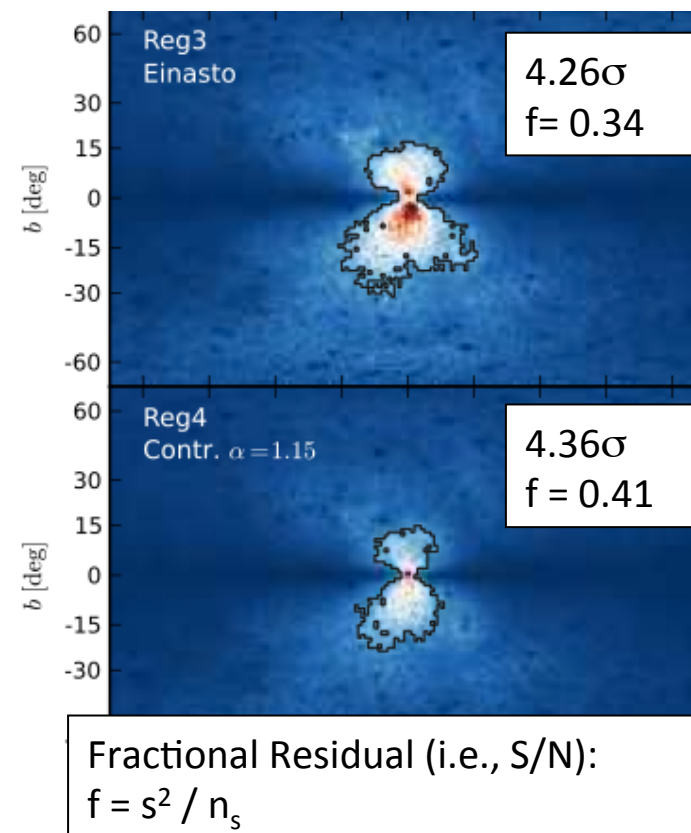
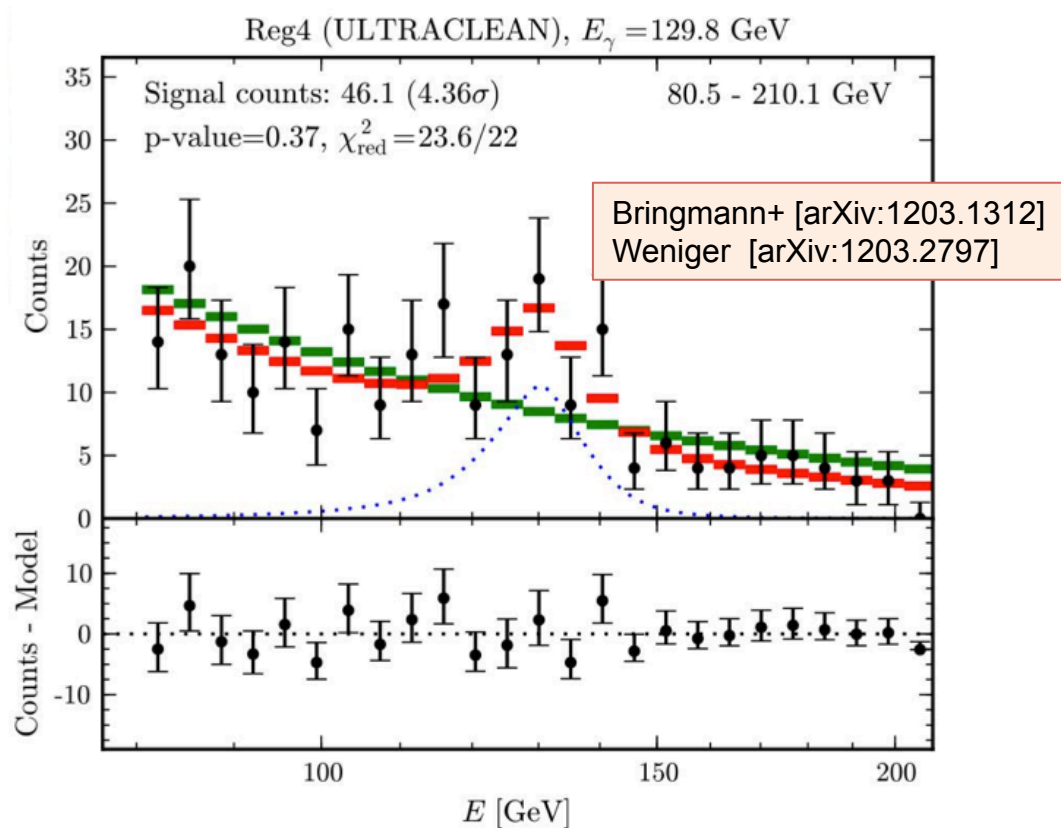
Abdollahi et al 2018

Dark Matter Searches

Gamma-ray indirect emission



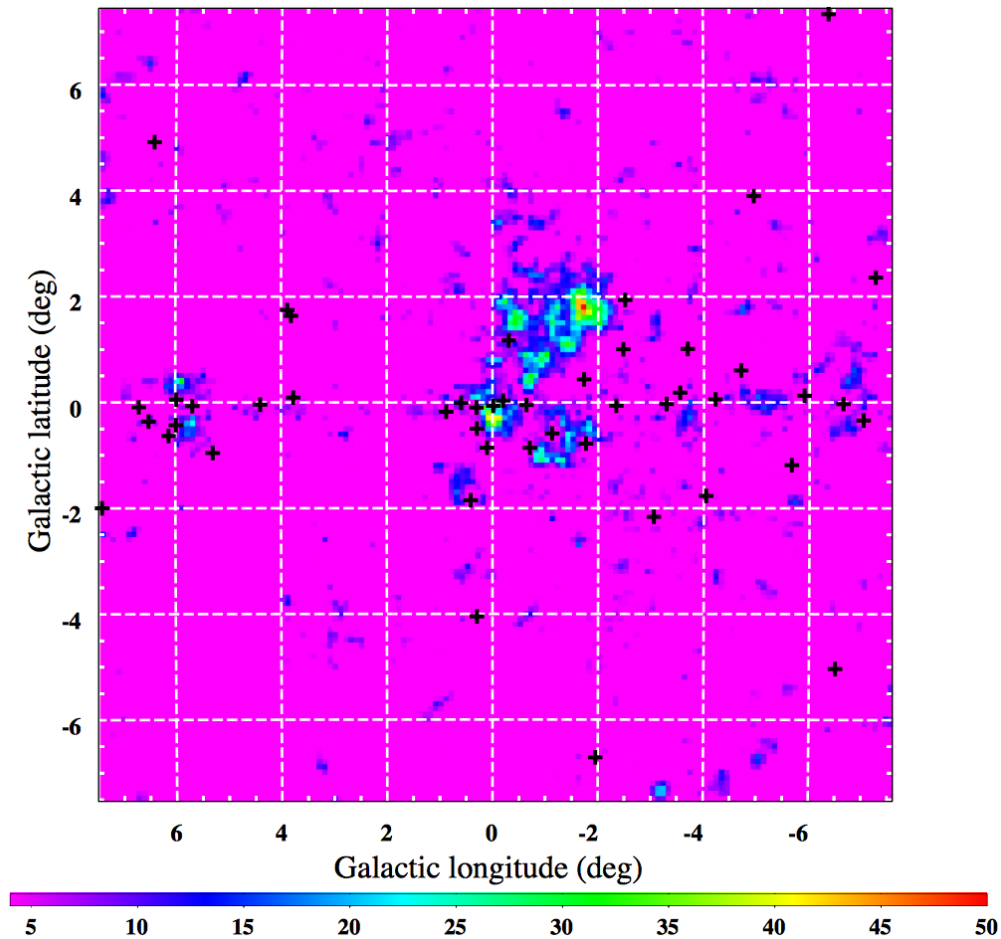
Narrow Spectral Feature at 130 GeV



Bringmann et al. and Weniger showed evidence for a narrow spectral feature near 130 GeV near the Galactic center (GC) in the LAT data.

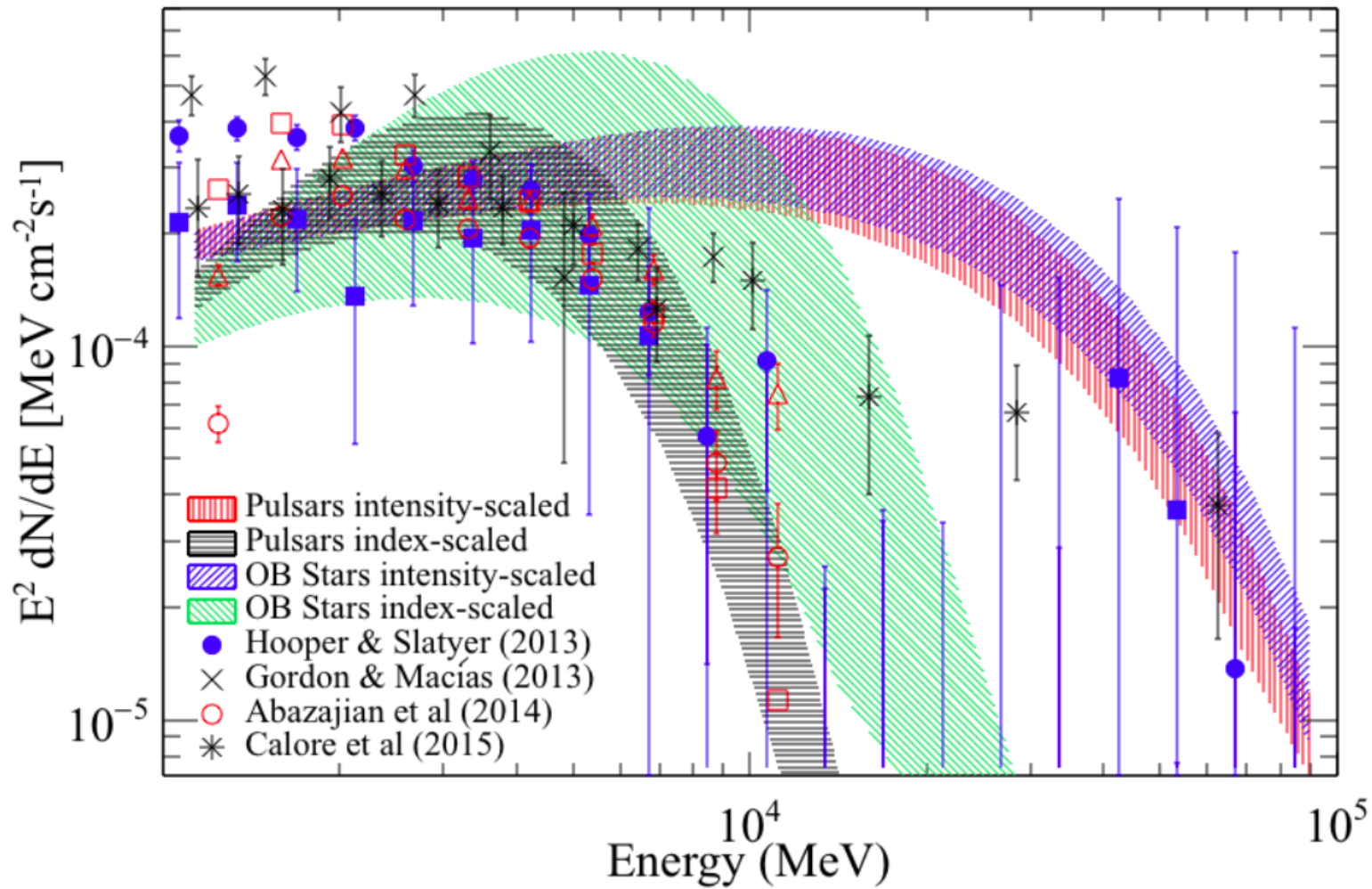
- Signal is particularly strong in 2 out of 5 test regions, shown above.
- Over 4σ local significance with $S/N > 30\%$, up to $\sim 60\%$ in optimized ROI.
- Some indication of double line (111 & 130 GeV).

Dark Matter searches – Galactic Center



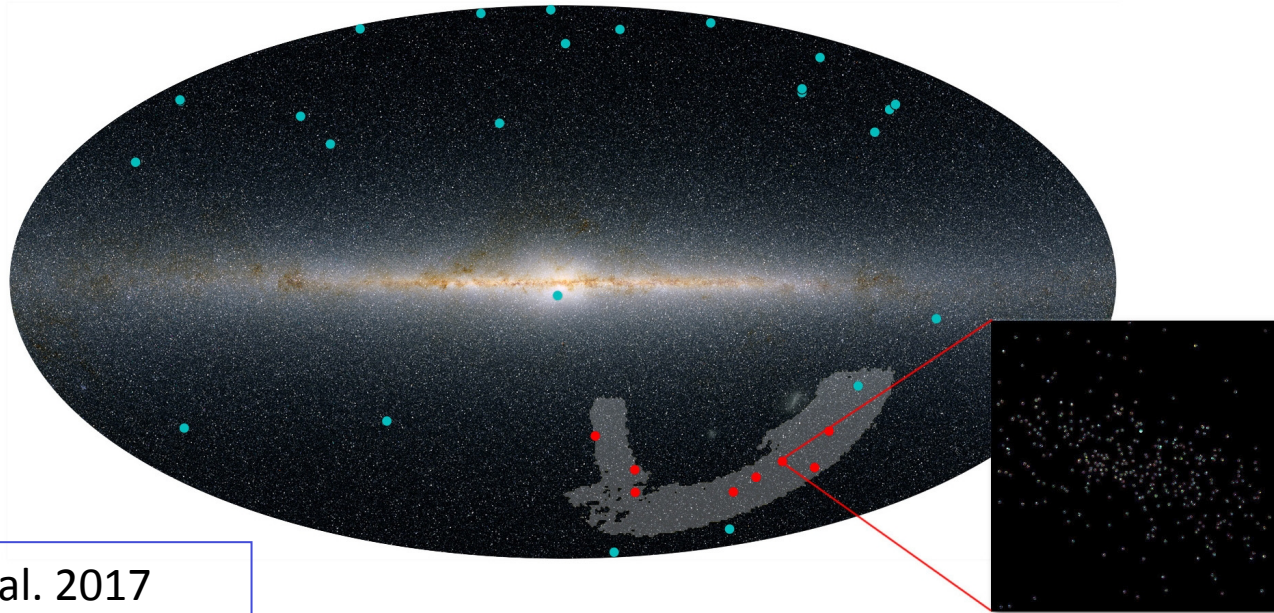
Ackermann, M. et al. 2017

Dark Matter searches – GC

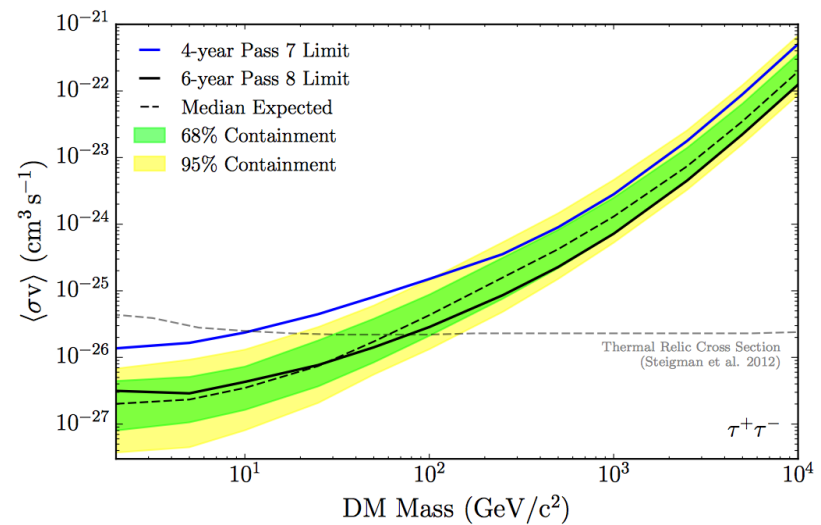
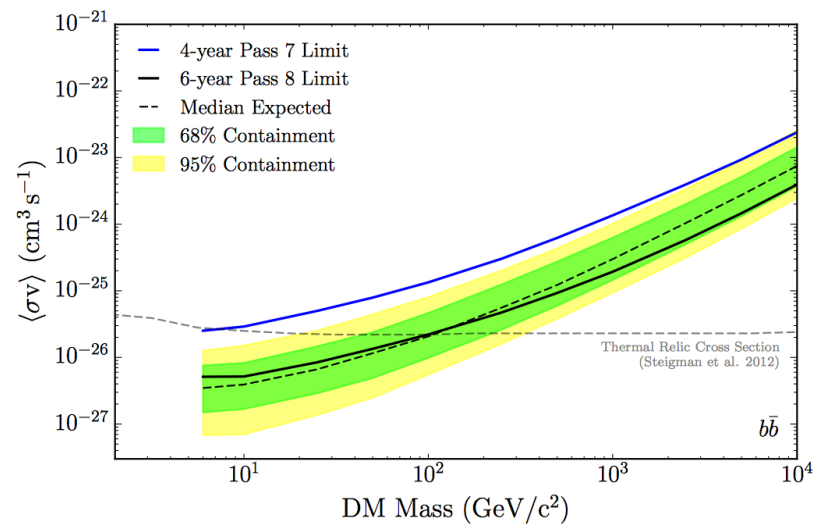


Ackermann, M. et al. 2017

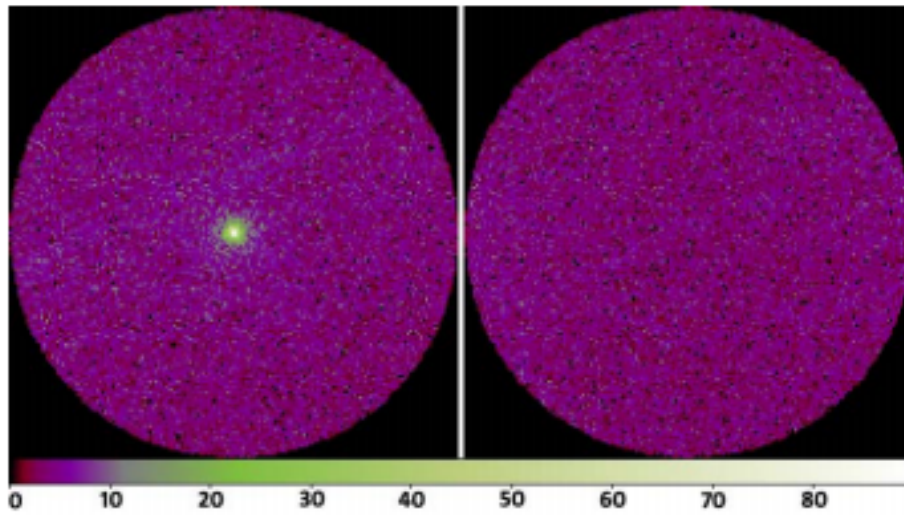
Dark Matter searches – Dwarfs Galaxies



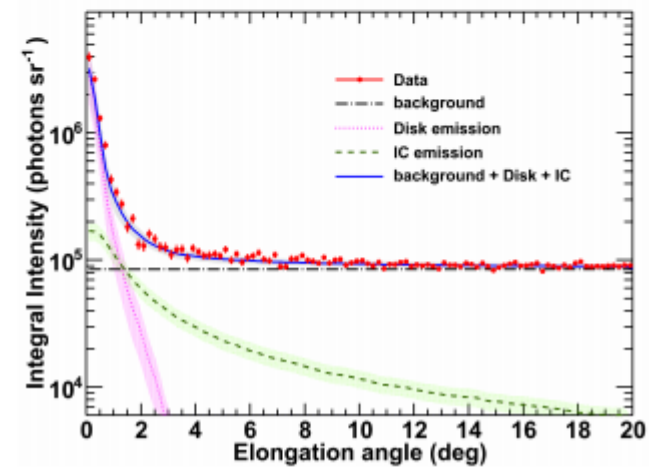
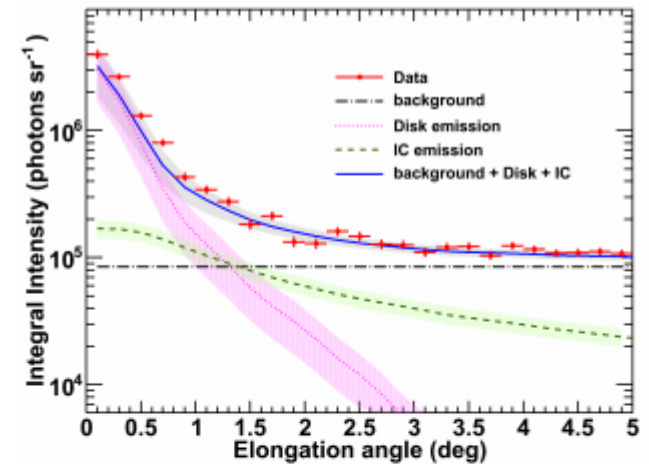
Albert, A. et al. 2017



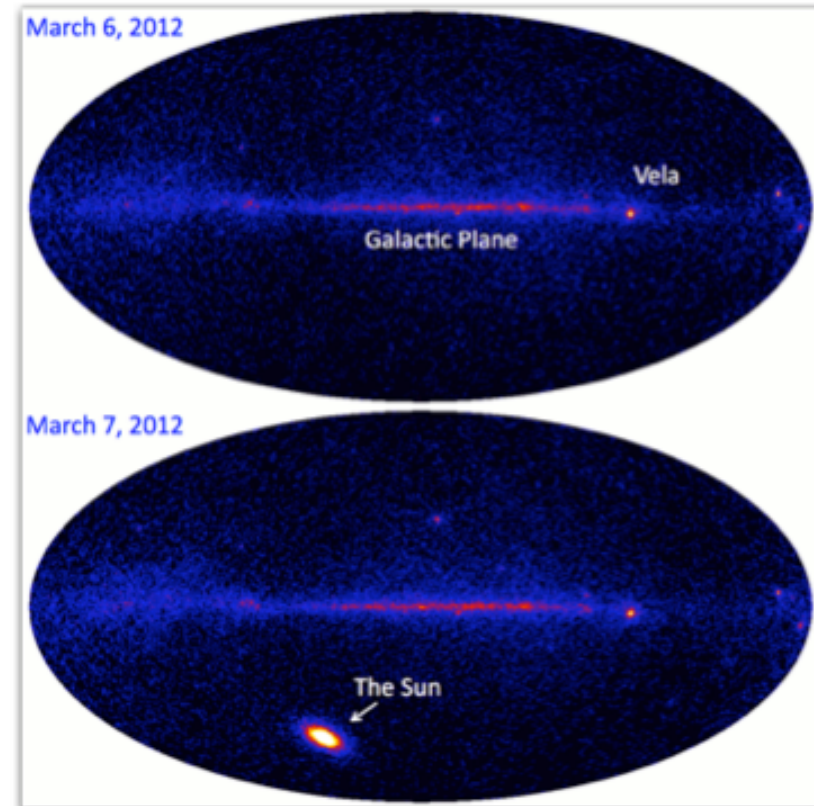
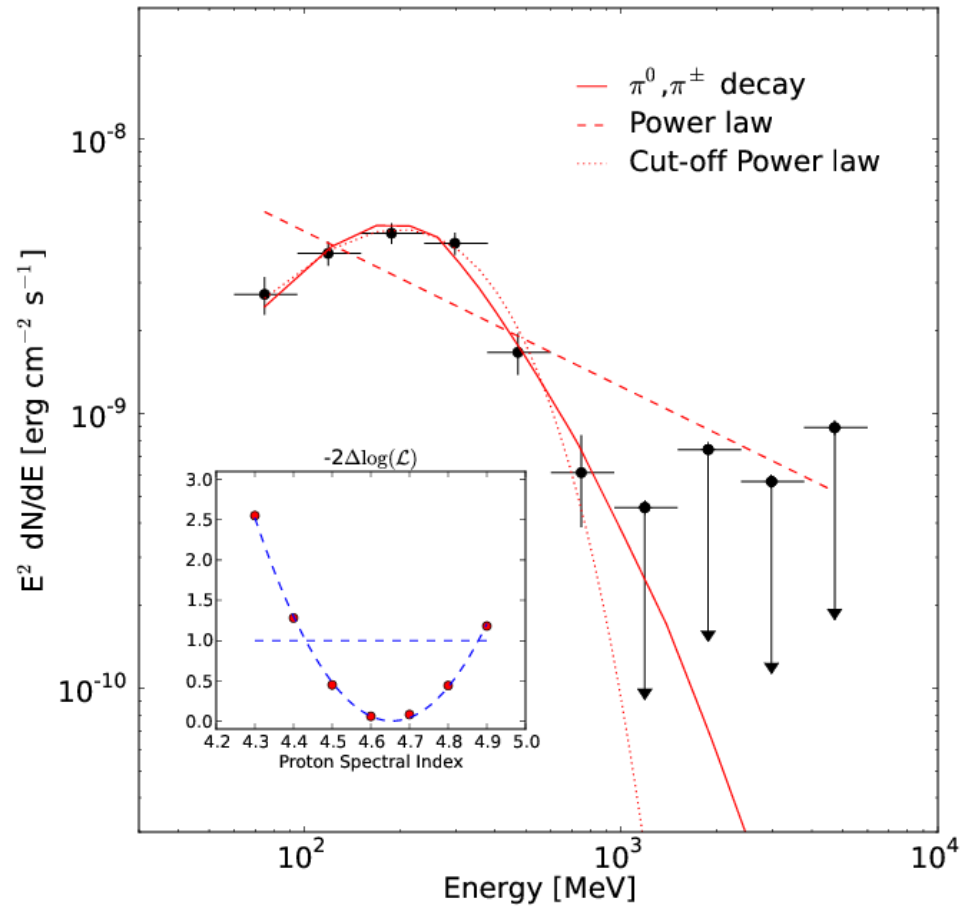
The Quiet Sun



Abdo, A. A. et al. 2011

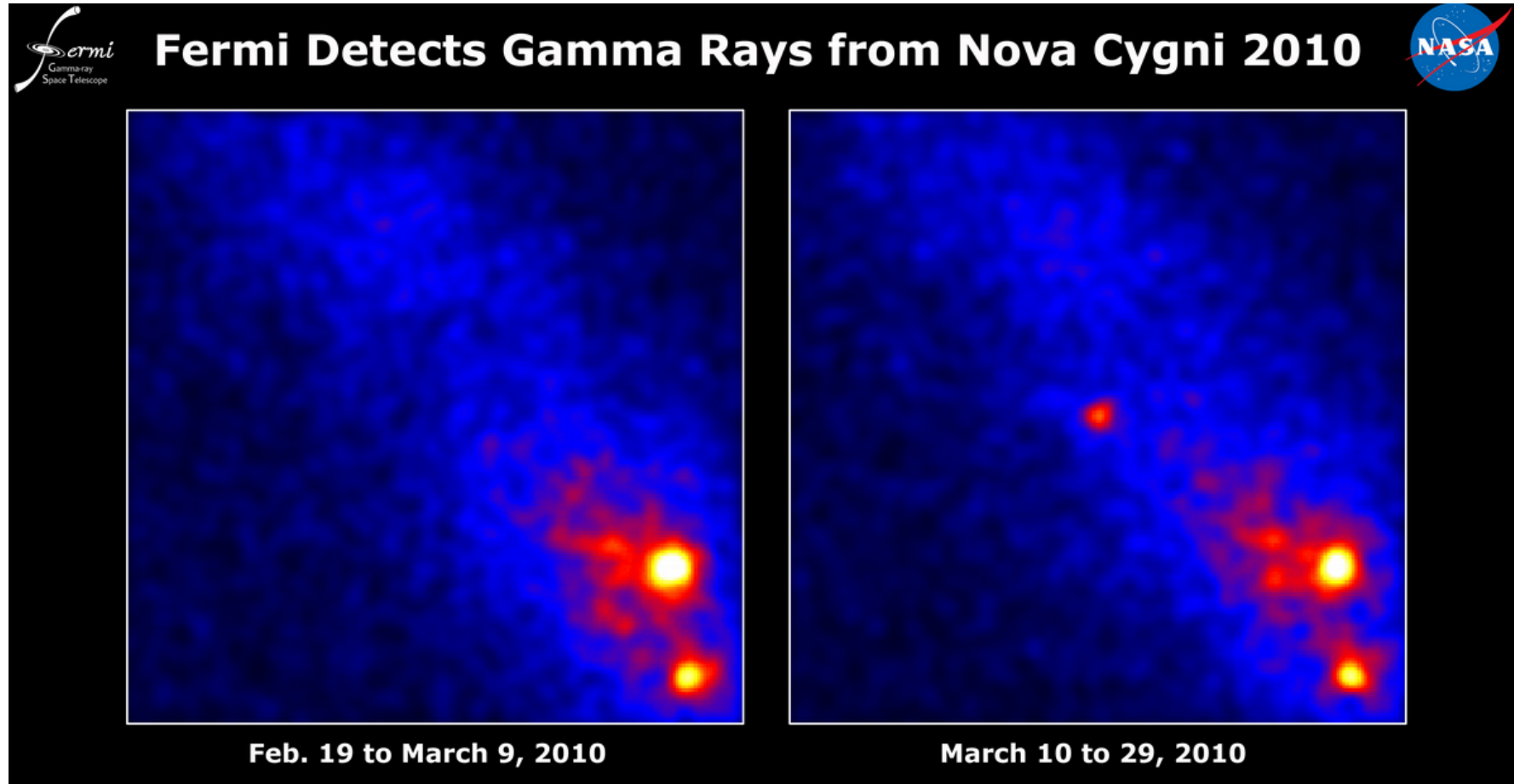


Solar Flares



Ajello, M. et al. 2014

Surprise! Nova emitting in Gamma Rays!



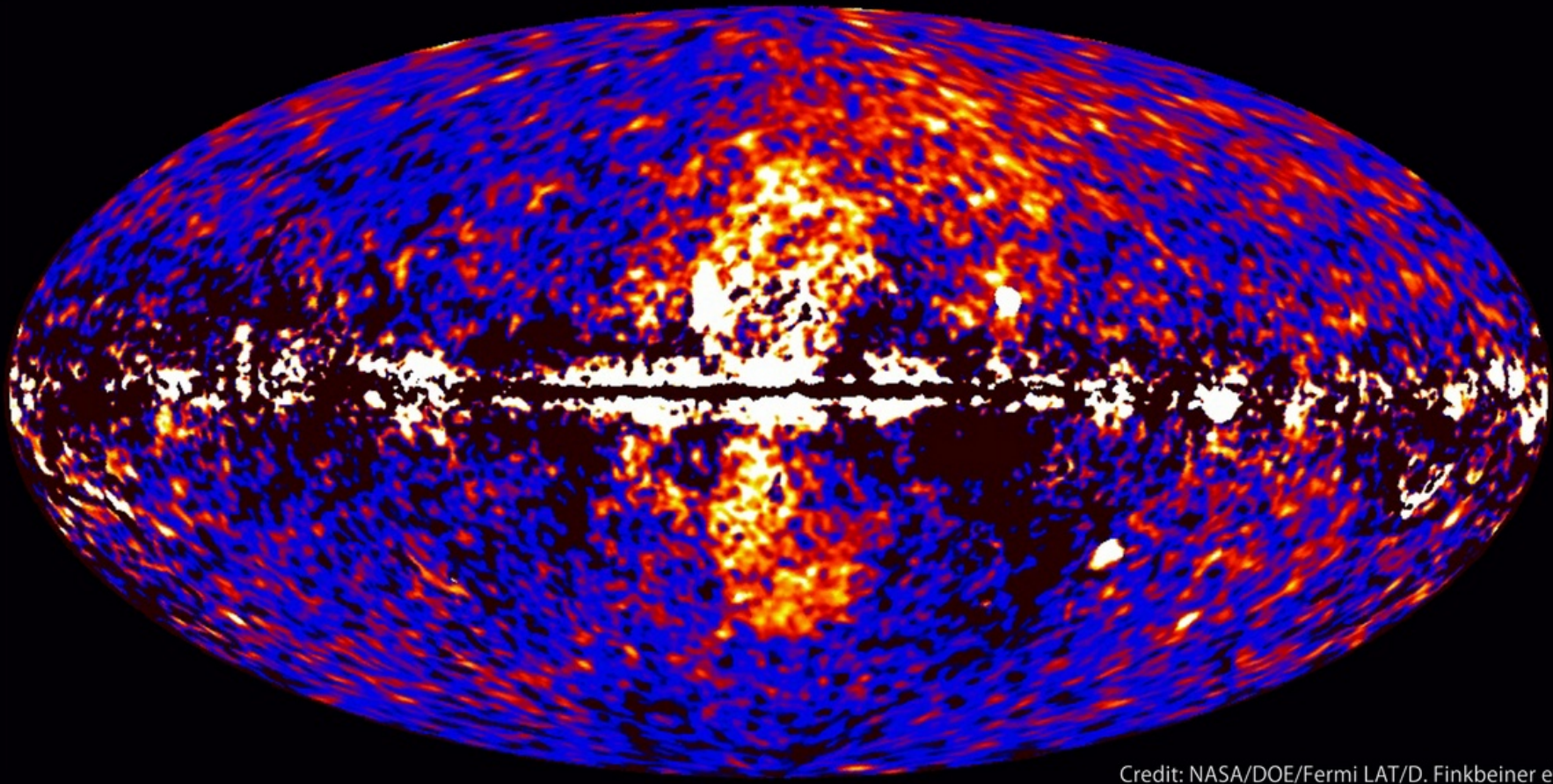
Abdo, A. A. et al. 2010

Gamma Ray Novae



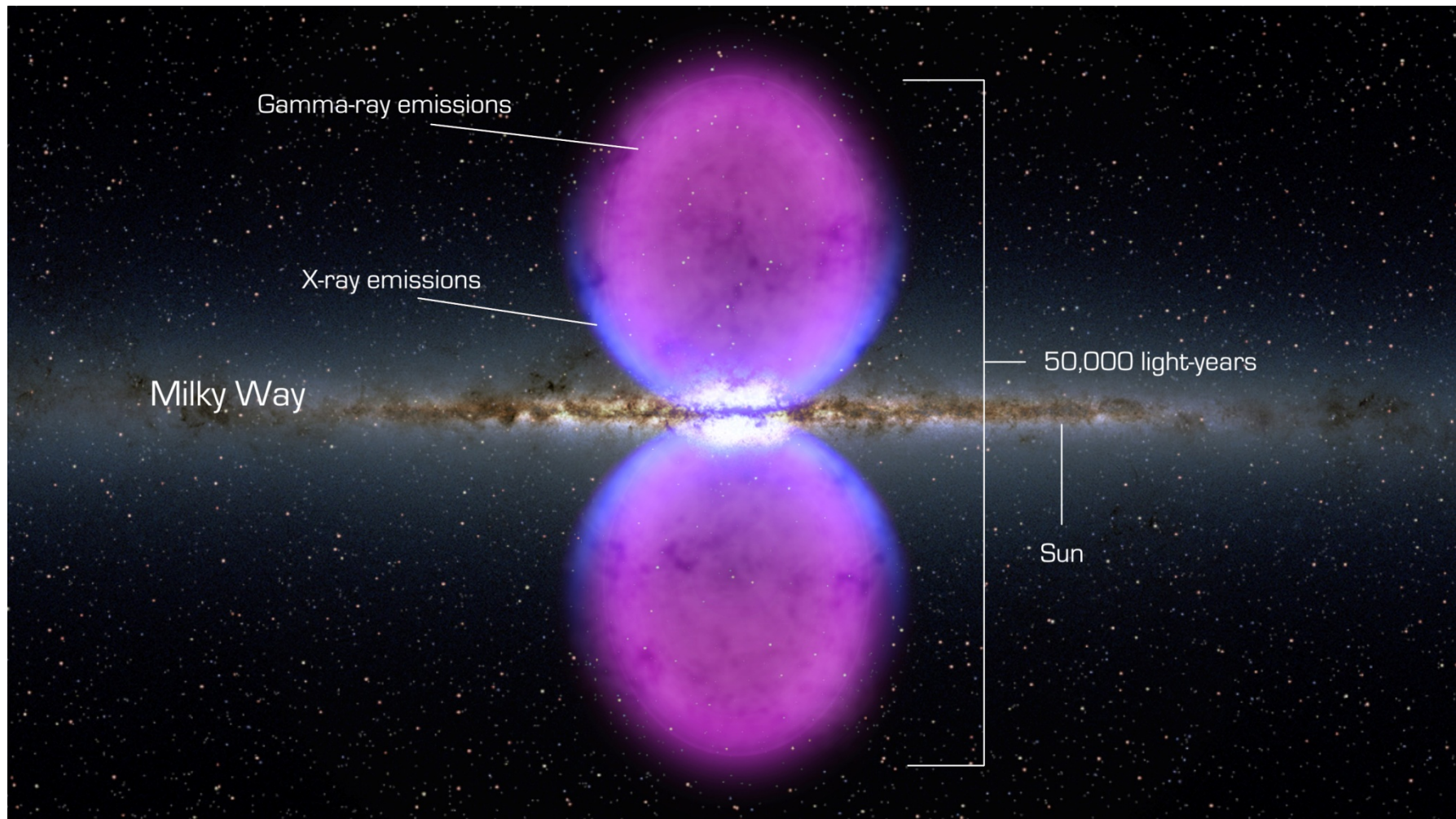
Surprise! The Fermi Bubbles

Fermi data reveal giant gamma-ray bubbles



Credit: NASA/DOE/Fermi LAT/D. Finkbeiner et al.

Fermi bubbles



LAT team analysis: Ackermann, M. et al. 2017

Scientific Highlights of the LAT

National Aeronautics and Space Administration



Fermi's Decade of Gamma-ray Discoveries

Fermi 10-year Sky Map

This all-sky view, centered on our Milky Way galaxy, is the deepest and best-resolved portrait of the gamma-ray sky to date. It incorporates observations by NASA's Fermi Gamma-ray Space Telescope from August 2008 to August 2018 at energies greater than 1 billion electron volts (GeV). For comparison, the energy of visible light falls between 2 and 3 electron volts. Lighter shades indicate stronger emission.

NASA/DOE/Fermi LAT Collaboration

GRB 130427A

On April 27, 2013, a blast of light from a distant galaxy became the focus of astronomers around the world. The explosion, known as a gamma-ray burst, and designated GRB 130427A, was detected by Fermi for about 20 hours. The burst included a 95 GeV gamma ray, the most energetic light yet detected from a GRB.

NASA/DOE/Fermi LAT Collaboration

Solar Flare

Although our Sun is not usually a bright gamma-ray source, solar flares can briefly outshine everything else in the gamma-ray sky. On March 7, 2012, Fermi detected flares erupting on the side of the Sun not visible to the spacecraft. The flares produced accelerated particles that fell onto the side of the Sun-facing Earth, resulting in gamma rays Fermi could detect.

NASA/DOE

PSR J1744-7619

Discovered by Einstein@Home, a distributed computing project that analyzes Fermi data using home computers, PSR J1744-7619 is the first gamma-ray millisecond pulsar that has no detectable radio emission.

NASA/DOE/Fermi LAT Collaboration/SSU/A. Siemsen et al.

ASASSN-16ma

Fermi has discovered several novas, outbursts powered by thermonuclear explosions on white dwarf stars. This was a surprise because novas weren't expected to be powerful enough to produce gamma rays. One event, dubbed ASASSN 16ma, shows that both gamma rays and visible light seem to be produced by the same physical process.

NASA/DOE/Fermi LAT Collaboration

GRB 170817A

This landmark event represents the first time light was seen from a source that produced gravitational waves. Fermi's detection of GRB 170817A coincided with a signal from merging neutron stars detected by the LIGO and Virgo gravitational-wave observatories.

ASTRO2017/DOE/SSU/AM. Simons et al.

TXS 0506+056

Among the nearly 2,000 active galaxies Fermi monitors, TXS 0506+056 stands out as the first one known to have produced a high-energy neutrino. Neutrinos are tiny, ghost-like particles that barely interact with matter and are thought to be produced in the same extreme physical environments as gamma rays. In July 2018, Fermi linked this galaxy to a detection by the IceCube Neutrino Observatory at the South Pole.

NASA/DOE/Fermi LAT Collaboration



Fermi Bubbles

Fermi data revealed vast gamma-ray bubbles extending tens of thousands of light years from the Milky Way's plane. The Fermi Bubbles may be related to past activity of the supermassive black hole at our galaxy's heart.

NASA/DOE

Galactic Center

The central region of the Milky Way is brighter in gamma rays than expected. Whether this excess is a collection of undiscovered millisecond pulsars or possibly evidence of annihilation of dark matter particles remains a mystery and will be part of Fermi's ongoing studies.

NASA/DOE/Fermi LAT Collaboration/DOE/SSU/AM. Siemsen et al.

IC 443, the Jellyfish Nebula

The shock waves of supernova remnants like the Jellyfish Nebula can accelerate protons to near the speed of light. When they slam into nearby gas clouds, gamma rays are produced. Fermi detects this emission, confirming that supernova remnants accelerate high-energy cosmic rays.

NASA/DOE/Fermi LAT Collaboration/DOE/SSU/AM. Siemsen et al.

Crab Nebula

The Crab Nebula, a young supernova remnant surrounding a pulsar, surprised Fermi astronomers with gamma-ray flares driven by the most energetic particles ever traced to a specific astronomical object. To account for the flares, scientists say electrons near the pulsar must be accelerated to energies a thousand trillion (10¹⁴) times greater than visible light.

NASA/CXC/NASA/MSU. Heiter et al.

